Determining the Critical Degree of Saturation of Brick Using Frost Dilatometry

by

Peter Mensinga

A thesis
presented to the University of Waterloo
in fulfillment of the
thesis requirement for the degree of
Master of Applied Science
in
Civil Engineering

Waterloo, Ontario, Canada, 2009

AUTHOR'S DECLARATION

I hereby declare that I am the sole author of this thesis. This is a true copy of the thesis, including any required final revisions, as accepted by my examiners.

I understand that my thesis may be made electronically available to the public.

Abstract

Improving the energy efficiency of the existing building stock is beneficial in terms of reducing both operational cost and environmental impact. Solid, load bearing masonry buildings comprise an appreciable part of the existing building stock, are valued for their durability and are often of historical significance, however their thermal performance is often poor. Thermal upgrades with interior insulation are usually considered risky as this lowers the drying potential of the wall enclosure which increases the moisture content of the masonry, possibly to damaging levels during freeze-thaw cycles.

The current approach to assessing the suitability of brick for exterior use is based on acceptance criteria or a severe freeze-thaw test as prescribed by ASTM and CSA. The first method is based on an incomplete understanding of freeze-thaw physics. The second method subjects the bricks to a set of conditions that cannot encompass the highly variable range of in-service exposures.

Past research indicates that rigid porous materials, such as brick and concrete, experience frost damage only if saturated beyond a fixed, critical degree of saturation. A more useful approach to assessing the risk of damage due to freeze-thaw would be to determine the critical degree of saturation of a material and then compare that to anticipated moisture loads under service conditions using computer modelling software such as WUFI.

A test method was developed to determine the critical degree of saturation of a material requiring less than two weeks of testing by means of frost dilatometry. Representative brick were first sliced into 10 mm thick specimens. Material properties of the brick specimens were determined, including dry weight, dry density, porosity (determined by either boiling or vacuum saturation), water uptake coefficient (A-value), and initial length, to allow for computer modeling and analysis of results. The specimens were wetted to various degrees of saturation (based on either boil or vacuum saturation), sealed in a manner to ensure minimal moisture loss, and then subjected to at least six freeze-thaw cycles. The change in length of the specimens following freeze thaw testing was measured and the expansion, which in this study was expressed in terms of microstrain, plotted against degree of saturation. Any specimen that experienced expansion greater than that attributable to instrument error was considered damaged by frost.

Determining the total open porosity of a material, necessary for measuring degree of saturation, is difficult due to close voids and trapped air in dead end pores. Boiling saturation and vacuum saturation are two methods commonly used to determine open porosity. For the size of specimens used in the test, almost all

water absorption when using the boil method occurred during the first hour of boiling and first hour of soaking. The repeatability of boiling to determine total open porosity is low, with approximately 10% variability experienced over three rounds of boiling. Specimens absorbed a greater or equal amount of moisture using the vacuum saturation method than the boiling saturation method, indicating that vacuum saturation is more effective at determining total open porosity. The repeatability of vacuum saturation is good with very little variability observed over 3 rounds. The benefit of boiling saturation is that its equipment requirements and procedure are simpler than that of vacuum saturation.

Freeze-thaw cycling was carried out by immersing the sealed specimens in a liquid bath. The change in length was determined by measuring pins attached to the specimens with an outside digital micrometer with a ratchet stop.

A combination of experimentation and computer modeling showed that the samples could be wetted to target moisture contents with excellent accuracy and that moisture redistributed evenly in less than 24 hours for most samples. The minimum required temperature of the freeze cycle was chosen to be less than -12°C, in order to freeze all water contained in pores with a radius of 10nm and greater. It was determined, for the small specimen sizes used, that the cooling and warming phases should be at least one hour in duration to ensure that the specimens entirely freeze and thaw.

Three sets of brick were subjected to the test to determine their critical degree of saturation: modern extruded brick, pressed brick from the 1950s, and historic brick dating to the 1870s. The older bricks experienced frost dilatation above 0.25 and 0.30 vacuum saturation respectively, with no damage evident below these thresholds. The modern extruded brick only experienced damage at 0.87 of vacuum saturation and greater.

Knowledge of the critical degree of saturation of a brick allows architects and engineers to pursue retrofit strategies that increase thermal performance without jeopardizing the durability of the material by creating the conditions that allow the moisture content to increase to dangerous levels.

Acknowledgements

I would like to thank my supervisor, Dr. John Straube, for nurturing the interest to pursue studies in building science while still an undergraduate and then providing the opportunity to do so through a Masters degree at UW. Dr. Straube's knowledge and guidance throughout my work on this thesis was indispensible, and his ability to cut through the details and refocus one's attention to the broader issues was appreciated.

A big thank you goes out to the staff of BSC for their material help with the lab work that was carried out for this thesis, particularly, Chris Schumacher whose interest in my topic and helpful suggestions were incredibly useful, and Aaron Grin who spent a great deal of time and effort in assembling the vacuum saturation apparatus.

The collegial atmosphere and friendship with my fellow graduate students in the Building Engineering Group – Rachel Smith, Ivan Lee, Brittany Hannam, Nick Bronsema, and Matthew Charbaneau – will be missed.

Lastly, I have to thank my wife, Erin, for her assistance with some of the more mundane and repetitive lab work, for her willingness to be a sounding board, and most importantly, for her love, patience and support throughout this process.

For Dad

It is not only flesh and blood but the heart which makes us father and son.

Table of Contents

List of Figures

List of Tables

Chapter 1
Introduction

Masonry buildings have a reputation of withstanding the ravages of time as evidenced by the continued existence of stone and masonry monuments hundreds and even thousands of years old. For instance, the use of fired clay brick in construction was revived in England in the early 1400s after falling into disuse with the fall of Roman civilization in Britain. Many of the castles, churches, and estate houses from this era have survived to the present day in relatively sound condition [Wight 1972]. This longevity of masonry is highly dependent on the method of construction, material properties, and climate.

In a review of literature, the two predominant causes of deterioration in masonry appear to be salt attack and freeze-thaw damage. In brief, salt attack occurs when dissolved salt ions, transported by water, re-crystallize in masonry thereby exerting an expansive force greater than the inherent strength of masonry can withstand. Over time, the masonry loses mass as small bits flake or powder off initially disfiguring the finish and eventually reducing its structural capacity [Watt 1999]. Salt attack is the primary mode of deterioration in climates where temperatures mostly stay above freezing.

Most research into freeze-thaw damage is published in North American and Scandinavian countries, indicating that frost damage is the primary cause of masonry failure in cooler climates, such as Canada's. The physics of freeze-thaw damage will be more closely examined in subsequent chapters, but in essence, masonry when frozen with high moisture levels will sustain damage, due in part to the 9% volume expansion of water as it changes phase from liquid to solid.

So why do some masonry buildings survive virtually unscathed for centuries while others fail within a few years? Regular maintenance and repairs certainly play an important part in

extending the life of a building, but there have been major changes over the past century in the use of masonry.

The greatest change has been the transition from multi-wythe masonry enclosures to single-wythe veneers [Sissons 1998]. Multi-wythe enclosures have a large moisture storage capacity which allows the enclosure to absorb moisture during rain events and then dry out later as conditions permit. Single-wythe veneers do not have inner wythes in which to redistribute moisture after substantial moisture loading events and therefore tend to have elevated moisture contents during freeze-thaw cycles.

The selection of glazed finishes for aesthetic reasons or the improper selection and use of face sealers has increased the frequency of surface spalling. Glazed finishes and face sealers trap moisture that has entered the façade by some other means such as rising dampness from the foundation, leaks through the enclosure, internal condensation due to air leakage, or outward vapour diffusion. The result is that moisture collects just behind the impermeable surface which during freezing cycles leads to spalling [Anderson 1999].

Lastly, to improve energy efficiency and occupant comfort, interior insulation is frequently added to solid masonry buildings. The addition of interior insulation lowers the temperature of the masonry enclosure, decreasing its drying potential which leads to a higher moisture content. This could potentially increase the moisture content of the masonry to a value at which freeze-thaw damage occurs.

Currently there are few tools available to evaluate the effect of interior insulation retrofits on the durability of masonry buildings. A review of literature revealed that there appears to be a critical degree of saturation below which no frost damage occurs regardless of the number of freeze-thaw cycles the material is exposed to [Fagerlund 1977]. Computer models of the insulated masonry envelop could be used to predict the expected moisture contents during freezing events and compared to the critical degree of saturation to determine the likelihood of frost damage.

1.1 Objective

The objective of the research is to evaluate the feasibility that frost dilatometry can be used to determine the critical degree of saturation of clay fired brick. This thesis reviews moisture storage and transport, and current theories of frost damage in porous, brittle materials.

1.2 Scope

The scope of this thesis was to demonstrate proof of concept for determining the critical degree of saturation of brick. Three sets of brick were selected from three distinct eras of brick manufacture: modern brick was represented by brick manufactured by Canada Brick in the late 1990s, sample brick taken from Upper Canada College and Montreal represent historic brick from the 1950s and 1880s respectively. Various methods of saturating the brick were carried out and their effectiveness was analysed. The ability of the brick to redistribute and retain moisture is quantified by computer modelling and measurements of mass over time respectively. Furthermore, specimens taken from the sample bricks were subjected to freeze-thaw cycles over a range of degrees of saturation and the resultant strain, if any, was recorded.

1.3 Approach

Initially, moisture storage and transport of water held in the pore space of brittle porous building materials such as brick, concrete and tile is reviewed. Following this, frost damage is discussed with respect to several leading theories of the damage mechanism, methods for detecting frost damage, and an overview of factors known to influence the severity of frost damage. The discussion continues with a critique of the existing methods used to determine durability in clay fired brick as regulated in North America by ASTM and CSA. An alternative approach is presented utilizing frost dilatometry to determine the critical degree of saturation, S_{crit}, of brick to be part of a larger risk assessment strategy for mitigating freeze-thaw damage. The remainder of the thesis provides proof of concept for the frost dilatometric method of determining S_{crit}. Chapter 5 investigates the effectiveness of boiling and vacuum saturation of brick and compares the two methods. Chapter 6 demonstrates how to wet the brick specimens to precise moisture contents and uses the WUFI computer model to predict moisture redistribution times after initial wetting. Chapter 7 presents the results strain measurements on of specimens taken from all three

sets of brick after being exposed to six freeze-thaw cycles at various degrees of saturation. Chapter 8 presents the conclusions of this thesis and recommendations for continued research.

Chapter 2

Moisture Storage & Transport in Masonry

Brick may appear to be both solid and water-shedding but in actuality it is a hydrophilic porous material. It is porous in that there are voids, or pores, within the solid matrix of the material and is hydrophilic in that water is readily absorbed into the void spaces. The size, shape, interconnectivity and spacing of the pores within the material is known as the pore structure. Figure 2-1 displays a microscopic view of the pore structure of a clay-fired brick.

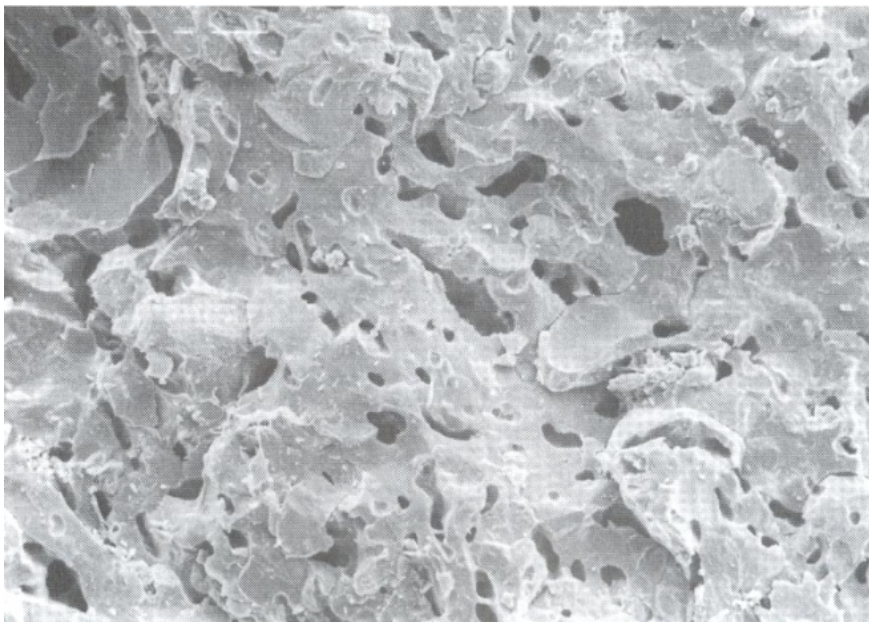

Figure 2-1 Fired clay brick porosity at 160 x 110 μm [Hall 2002]

The water content of a material such as brick can be expressed in any number of ways [Bear 1972]. In this study, water content will be expressed in one of two ways: moisture content or degree of saturation. Moisture content is defined as the ratio of mass of water held in the material, whether in adsorbed, liquid, or solid state, to the dry mass of material:

$$MoistureContent, MC = \frac{M_{wet} - M_{dry}}{M_{dry}} \times 100\% \quad (2\text{-}1)$$

where

M_{wet} = mass of a wetted material [g]
M_{dry} = mass of the material in a dry state [g]

Moisture content of a material when the entire pore space is filled with liquid is termed the saturated moisture content and is calculated as:

$$SaturatedMoistureContent, MC_{sat} = \frac{M_{sat} - M_{dry}}{M_{dry}} \times 100\% \quad (2\text{-}2)$$

where

M_{sat} = mass of the water saturated material [g]

and other terms are as defined previously. The degree of saturation of a material is defined as the ratio of water held in the material to the amount of water held in the material when it is in a saturated state:

$$DegreeofSaturation = \frac{M_{wet} - M_{dry}}{M_{sat} - M_{dry}} \quad (2\text{-}3)$$

The material is in a dry state when water is not contained in its void spaces in either adsorbed, liquid, or solid phases. In practice, the dry mass of a material is determined by placing it in a oven to drive out moisture and until the change in mass of the material, weighed at regular intervals, is less than a predetermined limit.

2.1 Moisture Storage

The moisture level of a porous material can range from completely dry, at which moisture content and relative humidity are equal to 0%, to supersaturated, where the entire open pore space is filled with water. There are three predominant modes of moisture storage. At low moisture contents, water vapour molecules cling to pore walls in a process known as adsorption. The quantity of adsorbed moisture held by a material is a function of relative humidity. The hygroscopic regime refers to the range of moisture contents where adsorption is the dominant form of moisture storage. As relative humidity rises above 95%, water starts to fill capillaries and is held by capillary suction, this referred to as the capillary or super-hygroscopic zone. Lastly, a porous material is described as super-saturated when its moisture content is greater than what can be held by capillary suction alone [Pazera 2007]. Figure 2-2 plots a typical sorption isotherm, relating moisture content to relative humidity.

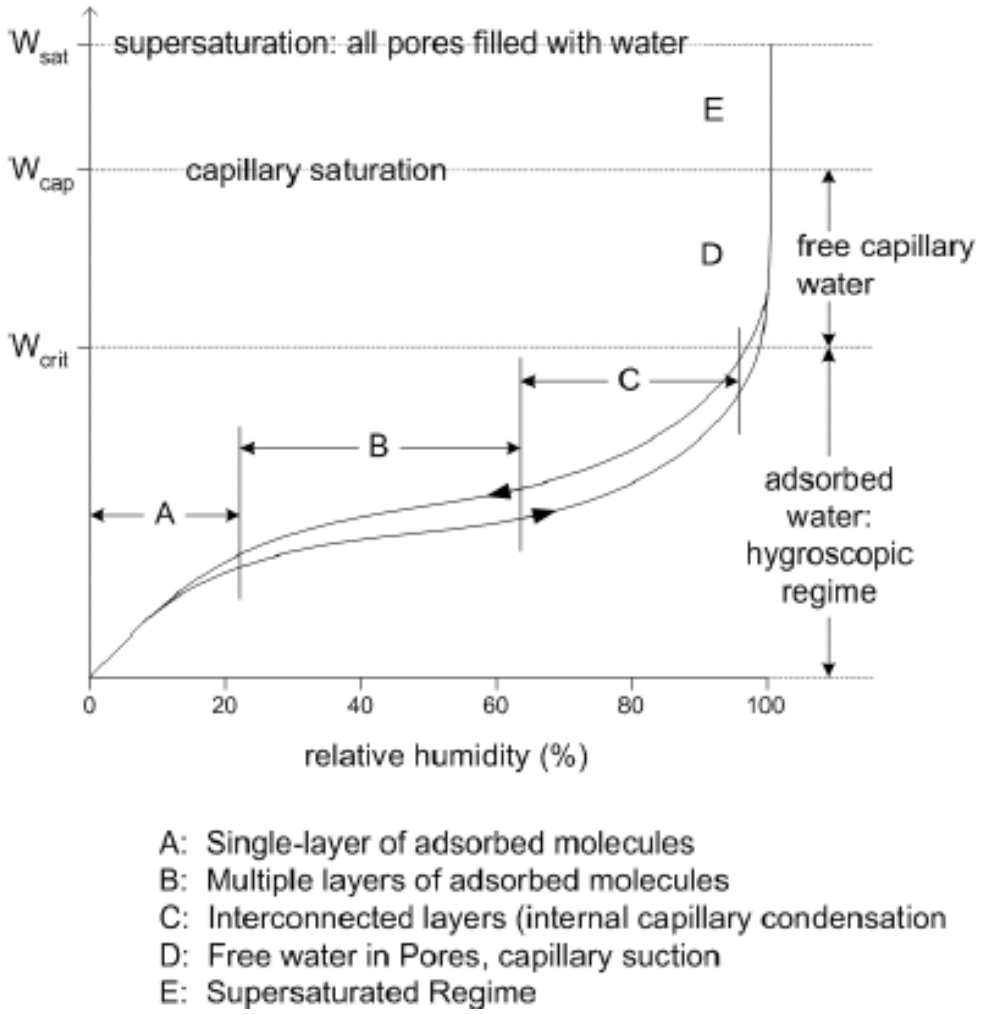

Figure 2-2 Moisture storage of a hygroscopic material [Straube and Burnett 2005]

2.1.1 Hygroscopic Regime

Moisture content in the hygroscopic regime is directly related to relative humidity and can be further subdivided into three phases. In the first phase, assuming a material is in a perfectly dry condition, as relative humidity increases from 0% vapour molecules adsorb to pore walls until a single layer of molecules covers the entire internal surface area of the material. The upper limit of the first phase is demarcated by the relative humidity level required for a single continuous layer of adsorbed moisture to cover pore walls with a single layer of water molecules. Moisture content rises fairly quickly due to the strong bond between the pore wall and vapour molecules.

As relative humidity continues to rise, vapour will continue to be deposited on the internal surface area of the material several layers of molecules deep. The bond between these layers of adsorbed water is weaker than the direct bond between the pore wall and the first layer of water molecules. Since these outer layers of adsorbed water molecules are not bonded as strongly, they are less firmly held in place. This is why moisture content rises more slowly as a function of relative humidity following the initial more rapid deposition of vapour molecules.

In the final phase of the hygroscopic regime, multiple layers of water molecules build up thick enough to fill the cross-sectional area of a pore, resulting in capillary condensation. The bond between water molecules in this regime is stronger than the multi-layer adsorbed regime and so moisture content rises steeply as relative humidity approaches 100%. The amount of moisture held by capillary condensation at close to 100% relative humidity is referred to as the critical moisture content, w_{crit}.

The sorption isotherm in Figure 2-2 exhibits hysteresis as the material is being dried due to the "ink-bottle" effect (see Figure 2-3). In completely filled, irregularly shaped pores the surface tension at narrow bottle-necks is strong enough to resist initial desorption. This causes the moisture content to be greater while drying than while wetting at any specific value of relative humidity in the hygroscopic regime.

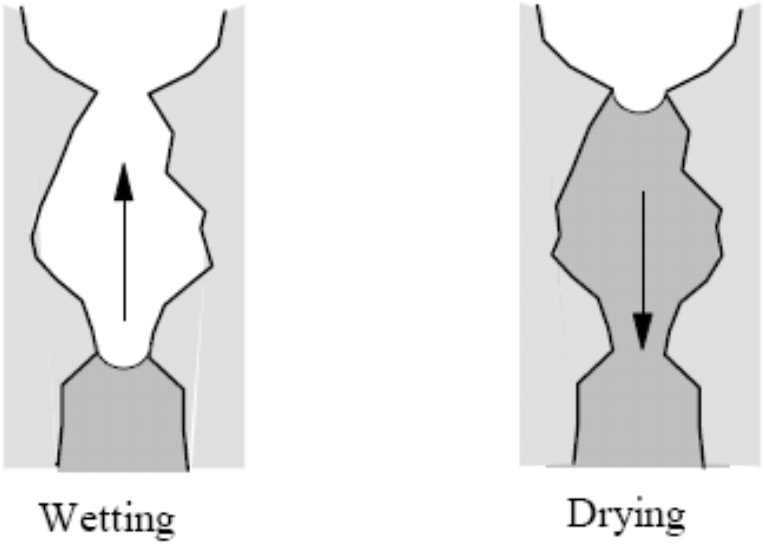

Figure 2-3 Moisture storage hysteresis due to ink bottle effect [Straube and Burnett 2005]

2.1.2 Capillary Regime

In the capillary regime, liquid moisture is held in pores by suction pressure. By idealizing a pore as a cylinder, the suction stress can be estimated as [Künzel 1995]:

$$P = \frac{2\sigma \cdot \cos\theta}{r} \tag{2-4}$$

where

P = suction stress [Pa]
σ = surface tension of water [N/m]
θ = contact angle [°]
r = capillary radius [m]

Thus, if a porous material is put in contact with liquid water, the capillaries will draw water. When all of the capillaries are saturated, the moisture content is denoted as w_{cap}.

2.1.3 Super-saturated Regime

Super-saturated storage occurs when liquid is deposited in pores that are too large to be completely filled due to adsorption and capillary suction. Relative humidity in the super-saturated regime is always at or above 100%. Moisture is deposited by condensation in whatever

unfilled pore space remains by vapour diffusion across a temperature gradient. The upper limit of the super-saturated range is reached when all the pores in the material are completely filled.

2.2 Moisture Transport

Moisture transport in a hygroscopic porous material primarily occurs by three processes: vapour diffusion, surface diffusion and capillary conduction. Each mode of transport is driven by a different gradient or force. Vapour diffusion is driven by differences in vapour pressure, surface diffusion is driven by gradients in relative humidity and capillary conduction moves liquid by suction forces.

2.2.1 Vapour Diffusion

Diffusion is the process by which molecules disperse from a volume with a high concentration to that of a lower concentration by random movement. Vapour diffusion refers specifically to the diffusion of water molecules in gaseous form. Mass flow of vapour can be expressed by Fick's Law [Petković 2005]:

$$g_v = -\delta_a \cdot \nabla P_w \tag{2-5}$$

where

g_v = diffusion flow [kg/m^{2}s]
δ_a = water vapour permeability of air [kg/m·s·Pa]
P_w = water vapour pressure [Pa]

This is valid for an environment with close to uniform temperature and total pressure. The negative sign is included to represent flow from high to low concentrations. The water vapour permeability of air can be determined based on the absolute temperature and total air pressure by the following equation:

$$\delta_a = 2.0 \times 10^{-7} \cdot T^{0.81} / P_{air} \tag{2-5}$$

where

T = absolute temperature [K]
P_{air} = total air pressure [Pa]

In small pores, 5 nm and less, at low vapour pressures, collisions between the pore walls, rather than with other gaseous molecules, dominate the rate of diffusion. This is referred to as Knudsen diffusion. The driving force behind both types of diffusion is vapour pressure. For most building physics applications, Knudsen diffusion can be ignored as Fickian diffusion predominates.

2.2.2 Surface Diffusion

When relative humidity gradients form across a porous material, the adsorbed layer will be thicker where the relative humidity is greater. The bond between water molecules in the multi-layer adsorbed phase is relatively weak and so some adsorbed water molecules will break free. If located adjacent to a thinner adsorbed layer some of these molecules will resettle there. This movement from thick to thin multi-layer adsorbed layers is known as surface diffusion [Straube 2005].

2.2.3 Capillary Conduction

Moisture transport in the capillary storage regime is dominated by conduction. Capillary conduction starts to operate in small pores that have been filled by capillary condensation, allowing both surface diffusion and capillary conduction to occur simultaneously, as illustrated in Figure 2-4.

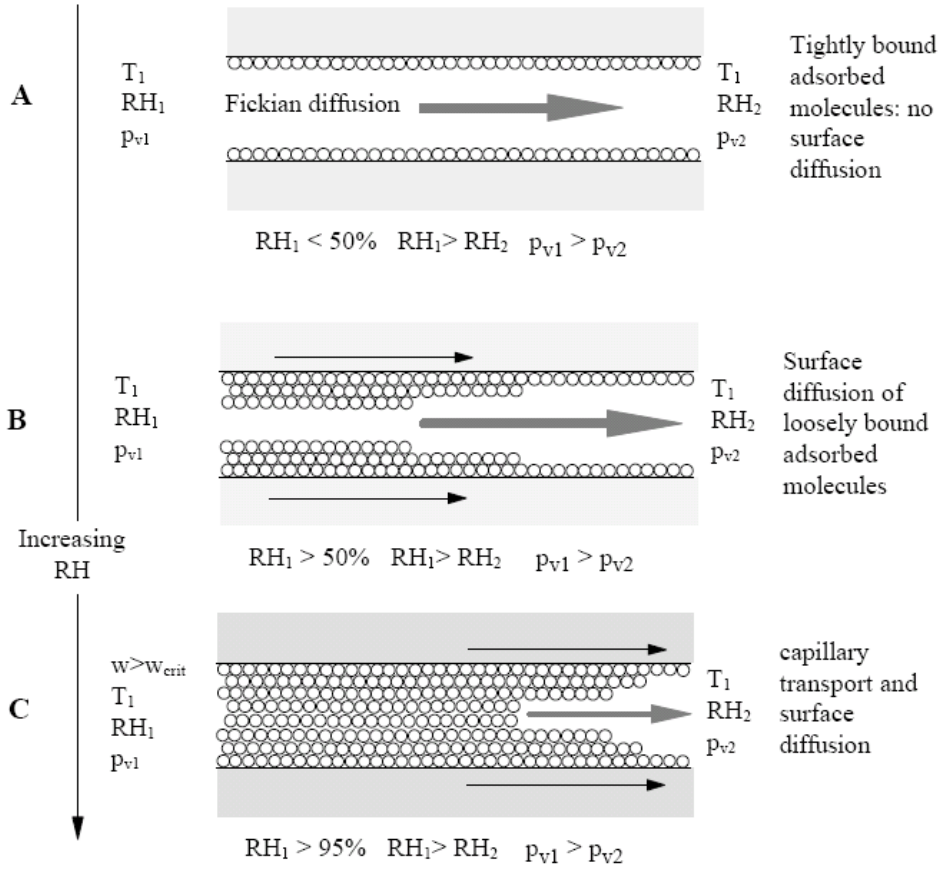

Figure 2-4 Moisture transport mechanisms [Straube and Burnett 2005]

The capillary uptake of a porous material when put in contact with a moisture source can be approximated using a diffusion equation, developed by Krischer [1978]:

$$g_w = -D_w(u)\frac{du}{dx} \qquad (2\text{-}6)$$

where

g_w = liquid transport flow density [kg/m^2·s]
$D_w(u)$ = liquid transport coefficient [m^2/s]
u = water content [% volume]

When a moisture source is removed prior to all capillaries being filled, redistribution of the moisture between capillaries will take place. Small pores have a greater suction stress but a lower rate of uptake than larger pores and will therefore suck moisture from the larger fuller pores through cross-connections until equilibrium is reached [Krus 1999].

It follows that the equilibrium moisture content of an assembly, such as masonry, when in contact with liquid water (for example, from a rainstorm) will differ based on the average capillary size of the constituent materials. Supposing brick and block have a coarser pore structure than mortar, initially it will absorb and hold more moisture than the mortar. However, after the moisture source is removed (the rainstorm comes to an end) water will redistribute from the brick to the mortar as it has a higher capillary pressure.

In the super saturated regime there is little to no internal liquid transport as capillary suction stresses are at equilibrium, and there are no open, interconnected pores to allow vapour and surface diffusion. This has been determined experimentally by Künzel [1995] where two super saturated materials with differing moisture contents were placed in contact, sealed, and essentially no moisture transfer was observed.

2.3 Summary

Brick is a brittle, porous material. The pore space of brick allows it to store moisture due to adsorption, capillary absorption and in a super-saturated state. Moisture stored in brick is constantly being redistributed in the pore space by vapour diffusion driven by vapour pressure, surface diffusion driven by relative humidity and capillary conduction driven by capillary suction pressures. The concepts reviewed in this chapter are a necessary precursor for understanding the causes of frost damage and how to prevent or ameliorate it.

Chapter 3
Frost Damage in Porous Solids

The physics of frost damage in building materials such as brick and concrete is still incompletely understood with several theories being advanced. Determining if a material has been damaged by freeze-thaw action is possible by visual inspection, dilatometry and changes in the material's elastic modulus. This has allowed several factors affecting the severity of frost damage to be identified, the most importance of which is the moisture content of the material during freezing, but also includes rate of freezing and material properties.

3.1 Theory

A number of theories have been developed to explain the mechanism of freeze-thaw damage however, the relative importance of each in contributing to frost damage is still uncertain.

3.1.1 Closed Container

As liquid water freezes to a solid, the molecules arrange themselves into a six-sided crystal. In this configuration the energy state is lower than any other configuration, however, the crystal occupies 9% more volume, and is subsequently less dense, than water in a liquid state. Liquid water held in a closed container (or pore) will exert a pressure on the container wall if prevented from freezing, which can be calculated by the Clapeyron Equation [Lindmark 1998]:

$$\frac{\Delta P}{\Delta T} = \frac{\Delta_{fus} H}{T \Delta_{fus} V} = \frac{6010 J/mol}{273.15K \times -1.64 \cdot 10^{-6} m^3/mol} = -13.4 MPa/K \qquad (3\text{-}1)$$

where

$\Delta P/\Delta T$ = change in pressure per degree Kelvin [MPa/K]
$\Delta_{fus}H$ = change in molar enthalpy [6010 J/mol]
$\Delta_{fus}V$ = change in molar volume [-1.64×10^{-6} m^3/mol]
T = temperature of fusion [273.15K]

For every degree below the freezing point of bulk water, a pressure of 13.4MPa is required to prevent freezing. The tensile strength of brick ranges from 0.10 to 0.32 of the compressive

strength [Drysdale 1994] and the minimum allowable compressive strength of exterior grade brick is 17.2MPa [CSA 2006]. Thus the tensile strength of exterior brick can be in the range of 1.7MPa to 10MPa, far less than the pressure required to contain water at even 1°C below freezing.

3.1.2 Ice Lensing

The adequacy of the closed container model in explaining of freeze-thaw damage has been questioned as early as 1930. A geological engineer, Taber, found that a column of clay saturated with liquid nitro-benzene, which does not expand upon freezing, and subjected to a temperature gradient, experienced frost heave consistent with that of soil saturated with water. He developed the ice lensing theory to explain this phenomenon [Wessman 1997]. This experiment was later repeated with far greater precision and control by Litvan [1972] in Canada which lead him to develop the disequilibrium theory as described later in section 3.1.4.

Ice lensing can be explained with reference to Figure 3-1. In this scenario, a unidirectional temperature gradient is imposed on a column of soil, with colder, sub-zero temperatures at the top and warmer temperatures at the bottom. The upper reservoir is filled with ice and is connected to the lower reservoir containing liquid water by capillaries. The chemical potential of ice, μ_{ice}, is less than that of water, μ_{water}, at temperatures just below zero, causing water to migrate from the liquid reservoir through capillaries to the ice face where it crystallizes, displacing the loose soil. As the process continues, an ice lens forms perpendicular to the direction of heat flow. When the pressure created by the formation of the ice lens exceeds that imposed by the mass of the overburden, frost heave occurs [Hall 2002].

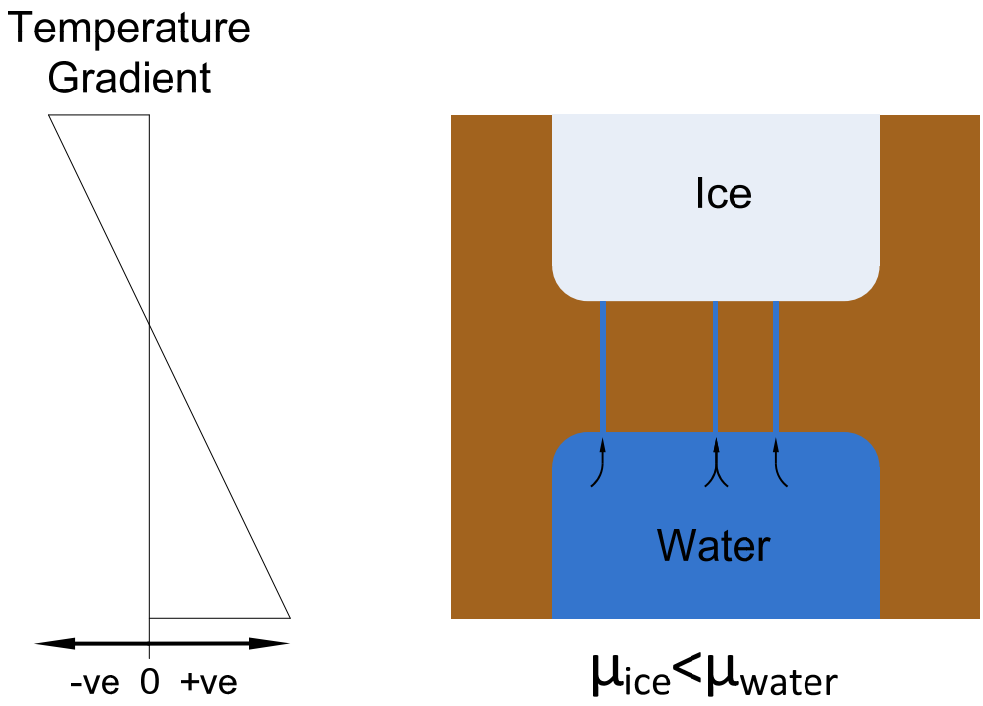

Figure 3-1 Ice lensing in soil

This process operates slightly differently in building materials in two regards. First, the water source comes from small capillaries that contain super-cooled liquid water. The freezing point of liquid water decreases as a function of pore size, which can be found by rearranging the Kelvin equation [Wessman 1997]:

$$T = T_0 \cdot e^{\left(\frac{-2\sigma \cdot M_w}{\rho_w \cdot \Delta H \cdot (r_\theta - t_a)}\right)} \tag{3-2}$$

where

T	=	pore freezing temperature (K)
T_0	=	freezing temperature of bulk water [K]
r_θ	=	pore radius of a cylindrical pore [m]
t_a	=	thickness of the adsorbed unfrozen water layer [m]
σ	=	surface tension water-air [N/m]
M_w	=	molecular weight of water [18.0153×10^{-3} kg/mole]
ρ_w	=	density of bulk water [kg/m^3]
ΔH	=	molar heat of fusion of water [6010 J/mole]

Although surface tension and density vary slightly with temperature, for ease of calculation they can be assumed constant at 75.6×10^{-3} N/m and 1000 kg/m^3 respectively. Furthermore, the thickness of the adsorbed frozen layer can be ignored in all but the smallest pores. Figure 3-2 plots freezing point depression as a function of pore radius.

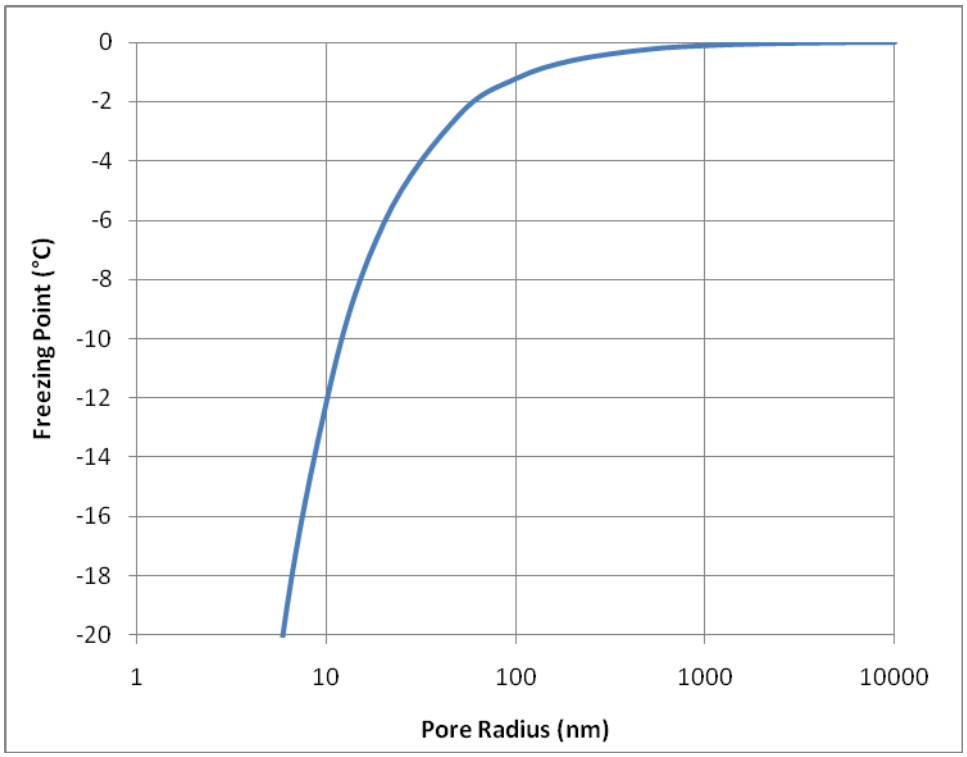

Figure 3-2 Depression of freezing point based on pore size

So at sub-zero temperatures, water contained in large pores will freeze while water in smaller pores will remain in a liquid state. As long as the energy level in the ice is lower than the free energy of the super-cooled water, water will migrate from the small capillaries to the ice in the coarser pores [Wessman 1997].

Building materials also differ from the soils in that they are a closed system. In the soils model, it is assumed that water travalling through the capillaries to the ice lens can continue indefinitely as water will be drawn from adjacent reservoirs. With building materials, the only source of liquid water is that held in the small capillaries. These small capillaries will dry as the super-cooled water leaves the capillary and enters larger adjacent pores, which in turn lowers the free

energy in the capillary. Once the energy in a desicated capillary is equal to that of the ice in the pore, the flow of water and subsequent growth of the ice crystal stops [Lindmark 1998]. It is important to note that if the pore is only partly filled with ice, the growth of the ice crystal will not cause damage. Only when there is no remaining space in the pore to accomodate ice crystal growth will the solid matrix be damaged.

3.1.3 Hydraulic Pressure

Hydraulic pressure theory builds on the closed container model, in that damage is dependent on the volumetric expansion of water as it freezes. As ice formation displaces liquid water, it either forces the liquid water to flow through capillaries ahead of the freezing front or it exerts pressure on water trapped in small capillaries between ice bodies in adjacent pores. This differs from the closed container model in that the damaging pressures are transferred from the ice via super-cooled liquid water in adjacent capillaries to the solid matrix as opposed to direct pressure from enclosed ice-liquid on the restraining solid matrix.

In the first scenario, as ice forms in large pores at close to saturation it will displace liquid water which is forced to flow into smaller adjacent capillaries ahead of the freezing front. Pressure is related to mass flow according to the Darcy equation [Wessman 1997]:

$$q = \frac{K_p}{\eta} \cdot \frac{dp}{dx} \tag{3-3}$$

where

P	=	pressure (Pa)
η	=	coefficient of dynamic viscosity of fluid [Pa·s]
q	=	flow [kg/m^{2}s]
K_p	=	permeability [kg/m]
x	=	distance of flow [m]

As the rate of ice formation increases, the rate of flow in adjacent capillaries rises, this in turn raises pressure in the capillary. If the capillary pressure is raised above the tensile strength of the solid matrix, damage will occur.

Several other factors can act to increase damage due to hydraulic pressure. Increased viscosity, inversely related to temperature, amplifies hydraulic pressure as illustrated in Figure 3-3 [data from Bear 1988]. Additionally, as the freezing front advances ahead of the capillary, the permeablity of the material decreases due to the formation of ice ahead of the direction of flow in the pore, which has the effect of lengthening the distance of flow. Both serve to further increase hydraulic pressure related to flow in small capillaries, increasing the probability and severity of damage.

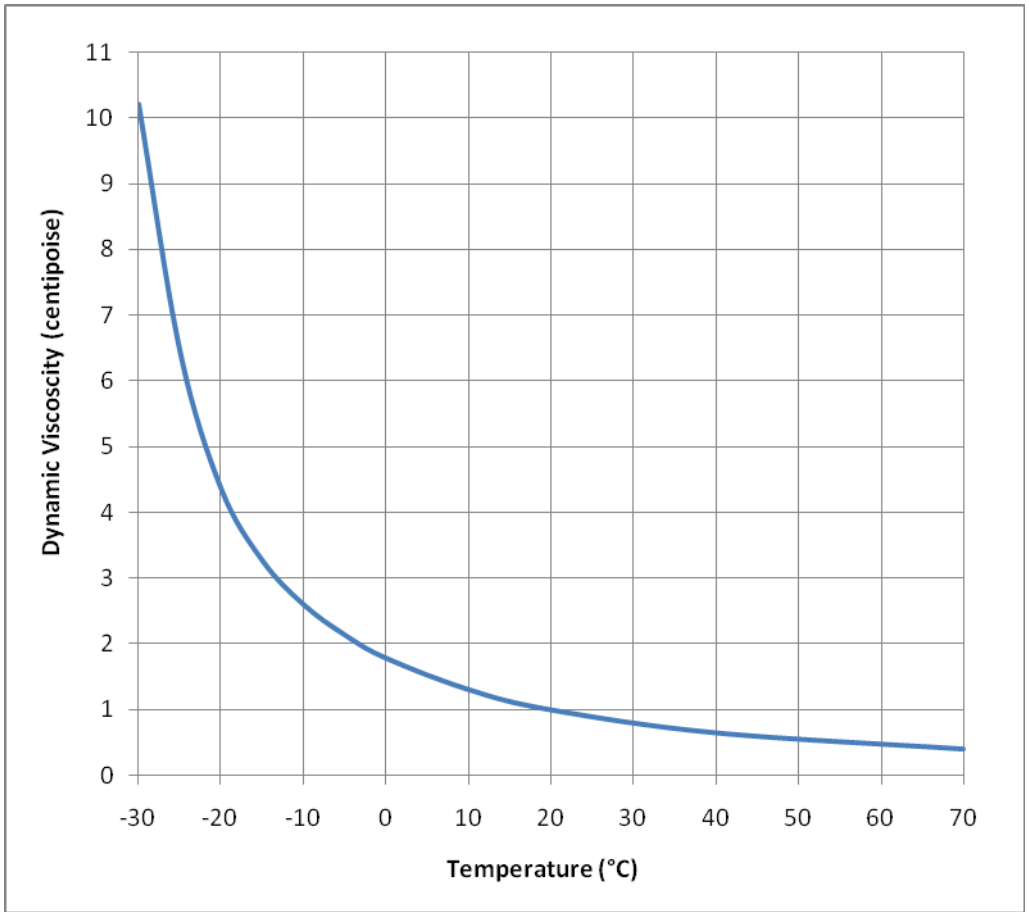

Figure 3-3 Dynamic viscosity of water

The second scenario occurs when water is trapped in capillaries between two or more ice filled pores. As water in the large pores freezes, liquid is displaced into the capillary raising the capillary pressure, until it surpasses the tensile strength of brick and causes damage.

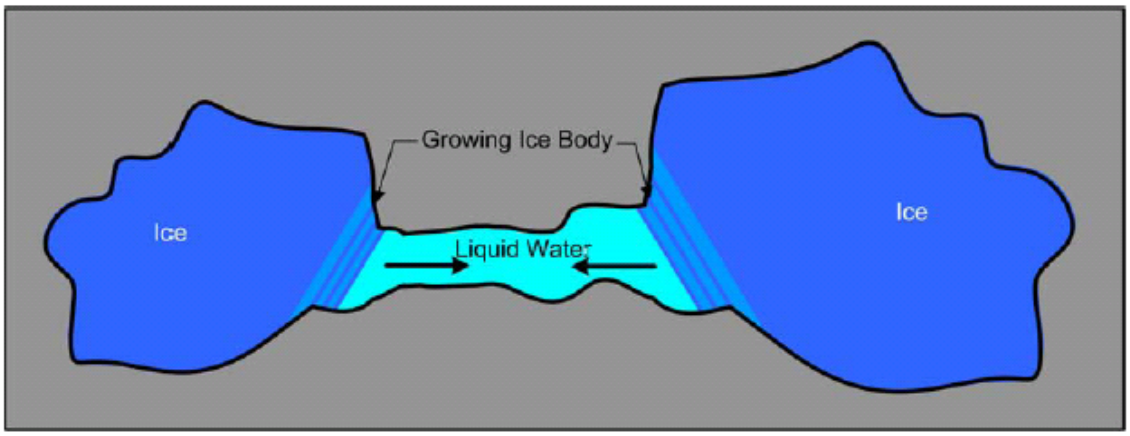

Figure 3-4 Increasing hydraulic pressure in a capillary connected to large pores [Roppel 2003]

In situations of omni-directional cooling, freezing fronts advance from multiple directions, displacing water to the interior of the material. As these freezing fronts converge, liquid water will be trapped in the centre of the material, again raising the hydraulic pressure to damaging levels [Hall 2002].

3.1.4 Disequilibrium Theory

The disequilibrium theory combines elements of both hydraulic pressure and ice lensing theories. The disequilibrium mechanism is driven by an imbalance in vapour pressure over super-cooled liquid in capillaries and over ice in large pores for partly saturated materials. The ratio of vapour pressure over super-cooled water to vapour pressure over ice can be calculated according to the following equation [Litvan 1973]:

$$\log\left|\frac{P_{water}}{P_{ice}}\right| = -\frac{1.1489T}{273.1+T} - 1.330\times10^{-5}\cdot T^{2} + 9.084\times10^{-8}\cdot T^{3} \qquad (3\text{-}4)$$

where

P_{water} = vapour pressure over super-cooled water [Pa]
P_{ice} = vapour pressure over ice [Pa]

T = temperature [°C]

The ratio of P_{water} to P_{ice} and the difference between P_{water} and P_{ice} are plotted in Figures 3-5 and 3-6 respectively.

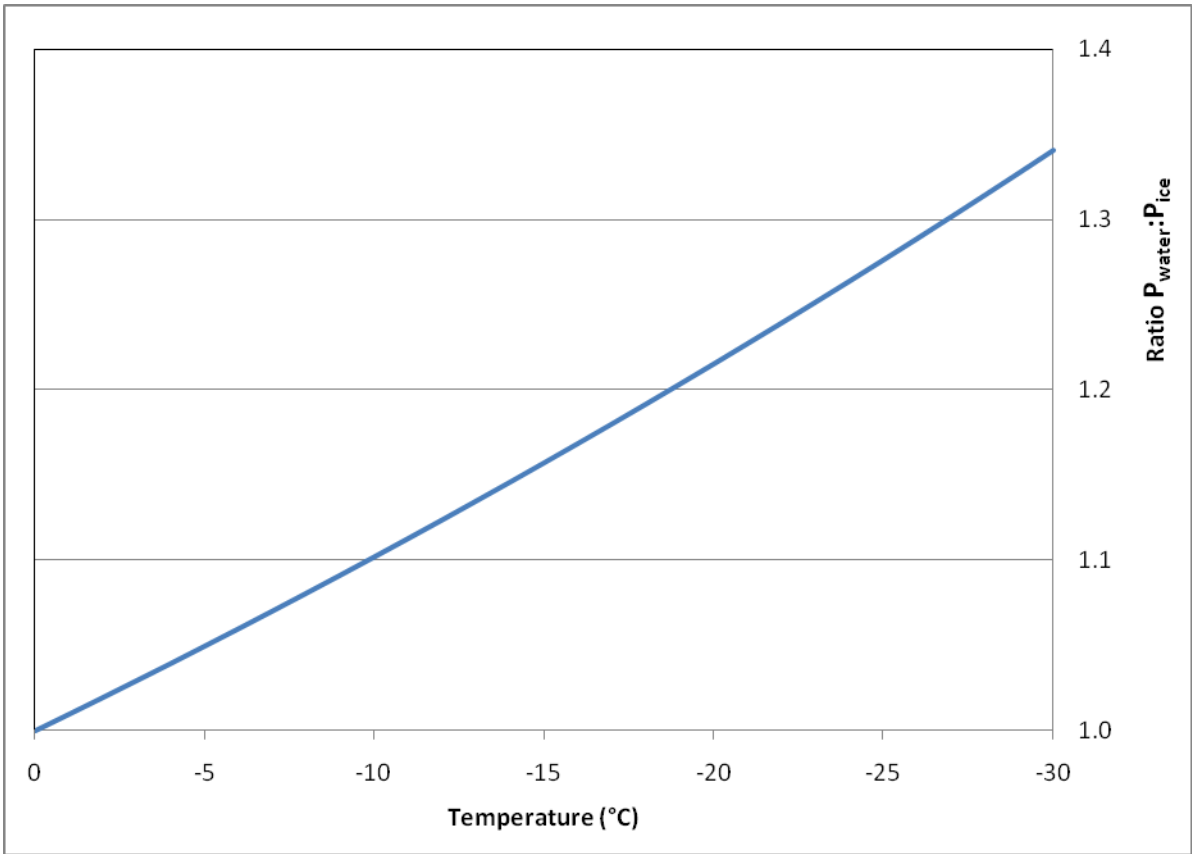

Figure 3-5 Ratio of vapour pressure over super-cooled water to vapour pressure over ice

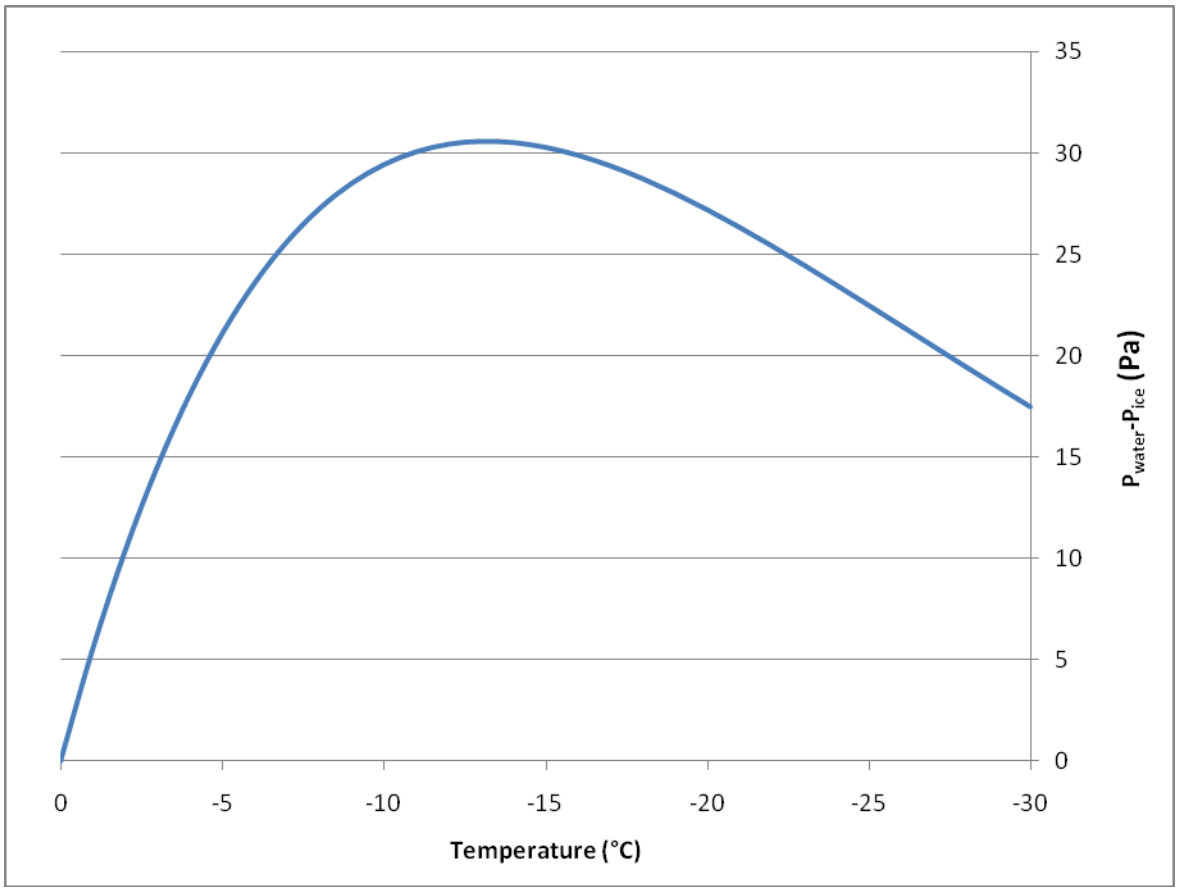

Figure 3-6 Difference in vapour pressure over super-cooled water and ice

Thus as the temperature decreases, increasing amounts of adsorbed water in capillaries will desorb, migrate to the ice and crystallize in a manner similar to ice lensing. This process will desiccate the pore causing the radius of curvature of the meniscus to decrease, which is related to vapour pressure above the capillary according to a modification of the Kelvin equation [Straube 2005]:

$$\ln\left(\frac{P_{v,cap}}{P_w}\right) = \frac{-2\sigma \cdot \cos\theta}{r \cdot \rho_w \cdot R_{wv} \cdot T} \tag{3-5}$$

where:

$P_{v,cap}$ = vapour pressure over the curved surface of water in a capillary pore [Pa]
P_w = water vapour pressure over a flat surface at the same temperature [Pa]
σ = surface tension water-air [N/m]
θ = contact angle [°]

r = pore radius of a cylindrical pore [m]
ρ_w = density of bulk water [~1000 kg/m^3]
R_{wv} = water vapour gas constant [461.5 J/kg·K]
T = temperature [K]

When the vapour pressure over super-cooled water equals the vapour pressure over ice no further water desorbs from capillaries to migrate to bulk ice in pores.

According to the disequilibrium theory, frost damage can be attributed to three separate mechanisms. First, ice crystal growth as desorbed water from capillaries crystallizes at the ice front can cause damage in a manner identical to ice lensing. This mechanism mostly affects large pores and cracks. Second, damage will occur if the rate of desorption of water in the capillaries is greater than the rate of volumetric flux to large open pores or the exterior surface of the material. Should this happen, a non-crystalline form of ice develops in the capillaries, exerting pressure on the solid matrix. Finally, super-cooled water that remains in the desiccated pores creates tensile forces on the solid matrix as the radius of curvature of the meniscus decreases, according to the Washburn equation:

$$P = \frac{-2\sigma \cos\theta}{r} \tag{3-6}$$

where:

P = capillary pressure [Pa]
σ = surface tension water-air [N/m]
θ = contact angle [°]
r = curvature radius of the meniscus [m]

3.2 Methods of Determining Freeze-Thaw Damage

Freeze-thaw damage in its most extreme form can be easily identified as a brick cracks, spalls and disintegrates (Figure 3-7) but damage occurs well before it is visually evident. Two common non-destructive methods used to determine if freeze-thaw damage has occurred in a material is to measure changes in elastic modulus and expansion.

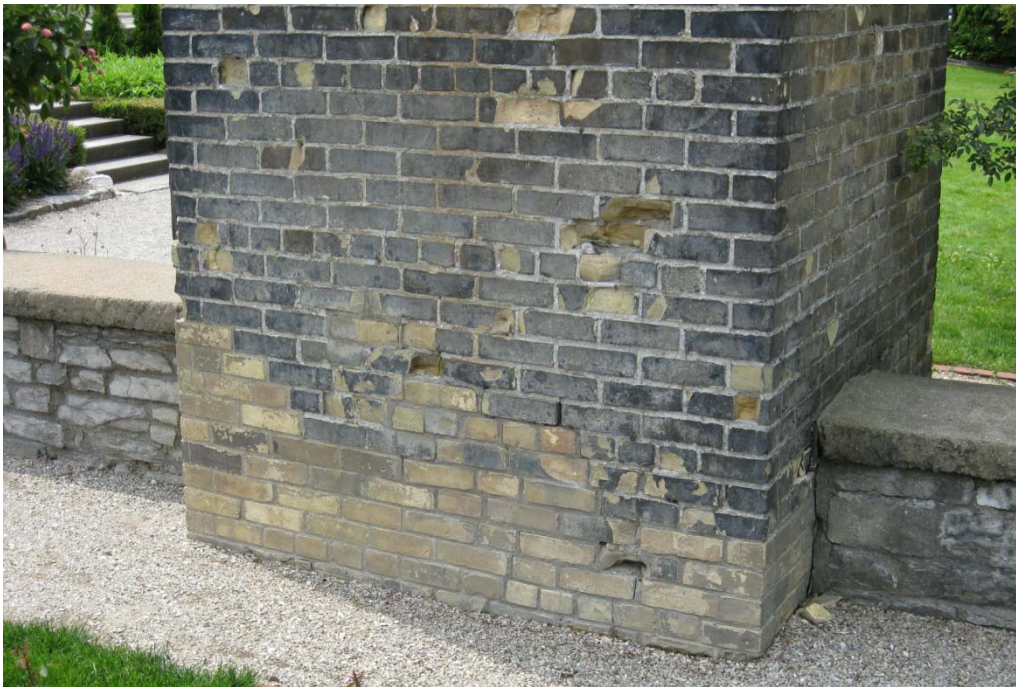

Figure 3-7 Spalling of brick due to frost action on an old chimney stack.

The dynamic elastic modulus of a material can be inferred from its natural frequency while under induced flexural vibration using a process such as that described in ASTM C 1548-02(2007). Dynamic E-modulus is related to the natural frequency of a rectangular object by the following equation:

$$E = 0.9465\left(\frac{mf_f^2}{b}\right)\left(\frac{L^3}{t^3}\right)T_1 \qquad (3\text{-}7)$$

where

E	=	Young's Modulus [Pa]
m	=	mass of the bar [g]
b	=	width of the bar [mm]
L	=	length of the bar [mm]
t	=	thickness of the bar [mm]
f_f	=	fundamental resonant frequency of the bar in flexure [Hz]
T_1	=	correction factor for fundamental flexural made to account for finite thickness of bar, Poisson's ratio, etc. [T1 to be calculated according to ASTM C 1548-02(2007)]

The dynamic elastic modulus of a specimen is measured prior to and subsequently after freeze-thaw cycling using an apparatus similar to that shown in Figure 3-8. If the E-modulus of the specimen after freeze-thaw cycling is less than 0.95 of the initial value damage is considered to have occurred [Fagerlund 1977, Prick 1997].

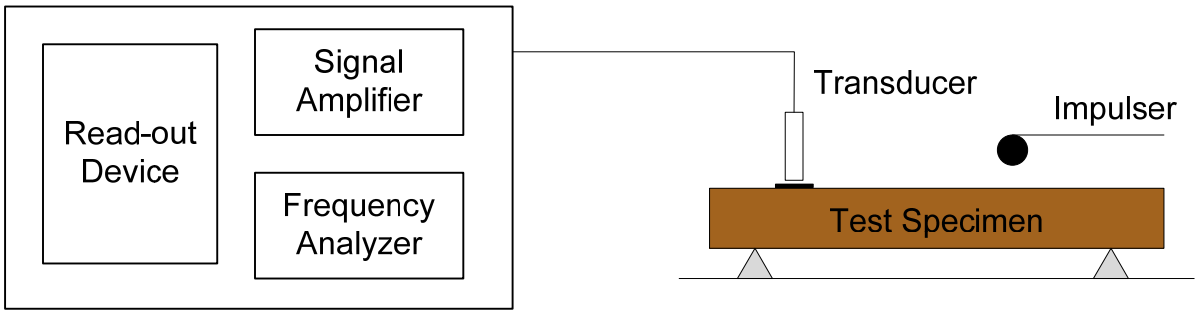

Figure 3-8 Diagram of test apparatus

The link between frost damage and permanent, irreversible expansion of material has been known for many decades [Ritchie 1968]. This should not be confused with thermal effect in which material will expand and contract elastically with temperature fluctuations but when brought to a reference temperature there is no permanent dimensional change. When frost damage occurs, each freeze-thaw cycle will cause a permanent dimensional expansion. Figure 3-9 illustrates the residual length change of water-saturated cement and porous glass immersed in benzene subjected to freeze thaw cycles. Multiple damaging freeze-thaw cycles leads to accumulated dimensional expansion, as shown in Figure 3-10.

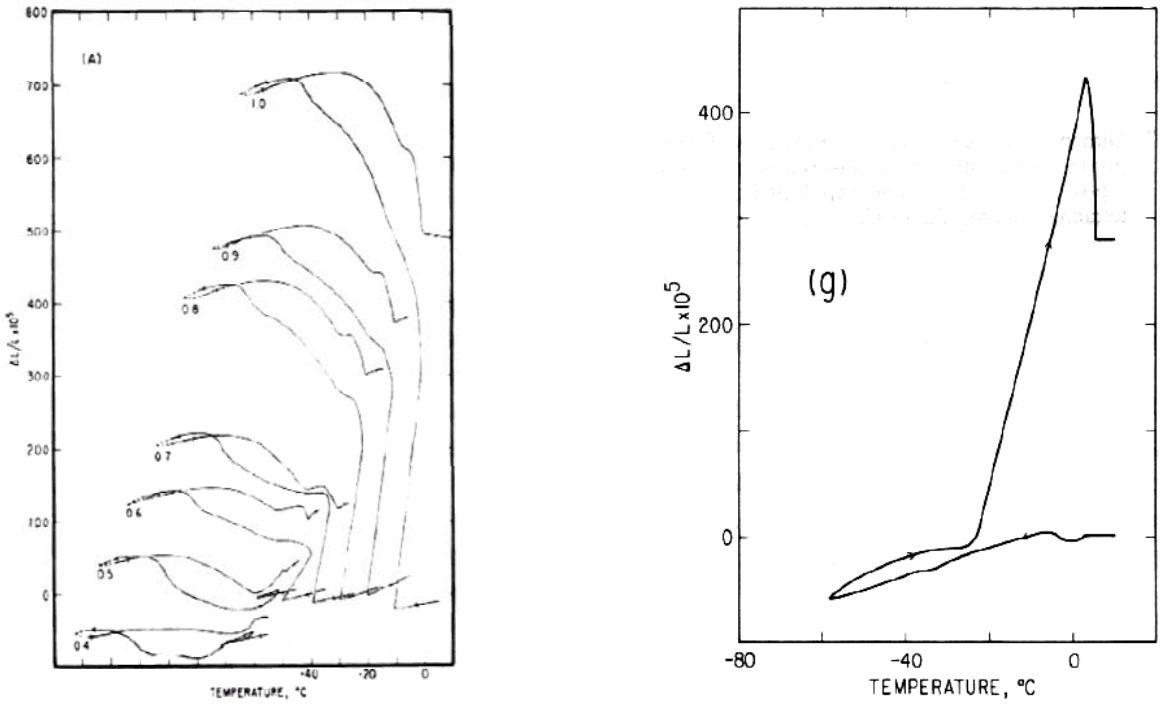

Figure 3-9 Length changes of water saturated concrete with various water/cement ratios; Dimensional changes of 5mm thick porous glass immersed in benzene. (Litvan 1988)

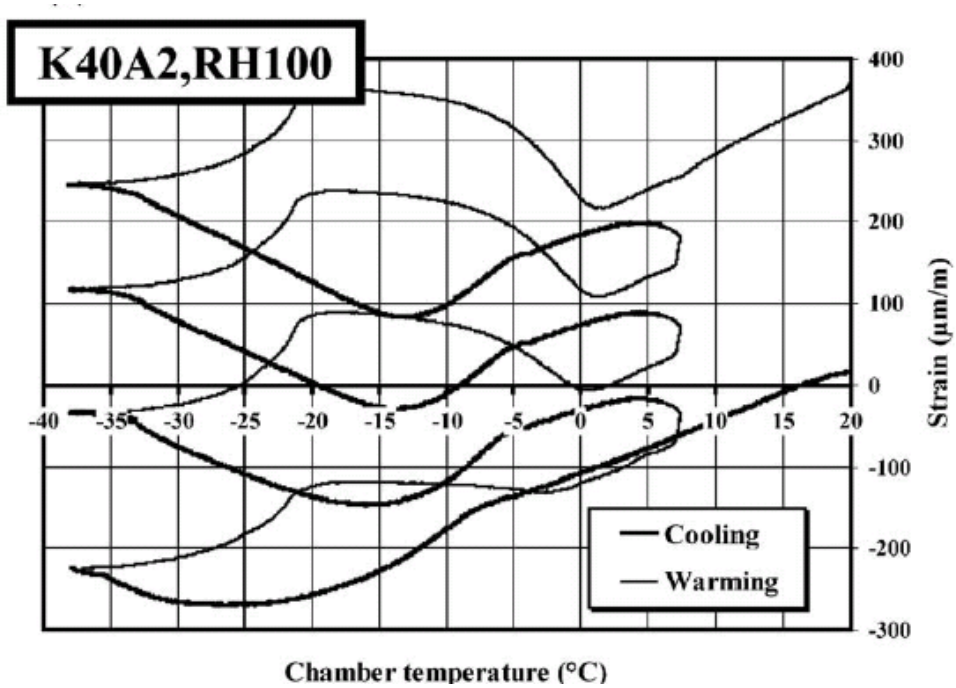

Figure 3-10 Accumulated axial strain in concrete over multiple freeze-thaw cycles (Pentalla 2002)

3.3 Factors Affecting the Severity of Freeze-Thaw Damage

3.3.1 Saturation

The occurrence of freeze-thaw damage is directly related to a material's degree of saturation. Damage will not occur if moisture is not present in sufficient quantity for any of the mechanisms discussed earlier to occur.

Experimentally it has been demonstrated that there exists a critical degree of saturation, S_{crit}, at which the necessary water required for frost damage would no longer be available [Ritchie 1964, Fagerlund 1979, Prick 1997]. In a study administered by Fagerlund, concrete samples cast in a single batch were distributed to five participating laboratories and subject to freeze-thaw cycles after having been wetted to various degrees of saturation. Frost damage was assessed both by the change in E-modulus and dilatometry. Figure 3-11 illustrates a typical plot of saturation versus strain used to determine S_{crit}. The general trend is for the material to experience increasing strains as the saturation is raised above S_{crit}.

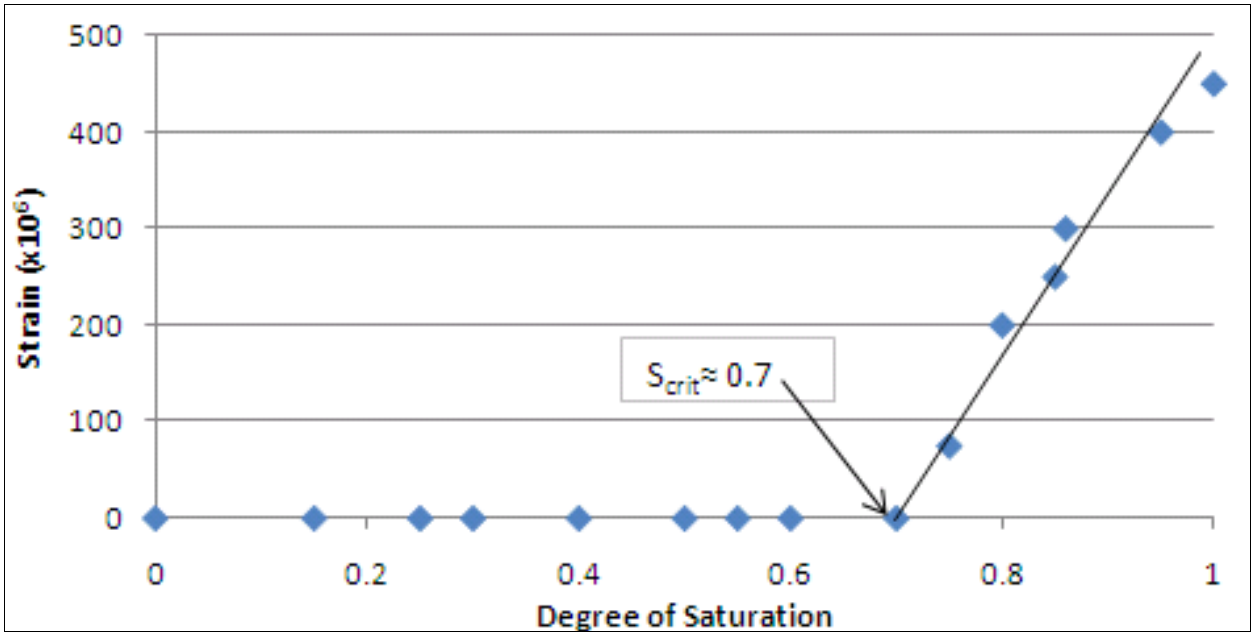

Figure 3-11 Idealized plot of expansion (microstrain) vs degree saturation used to determine S_{crit}

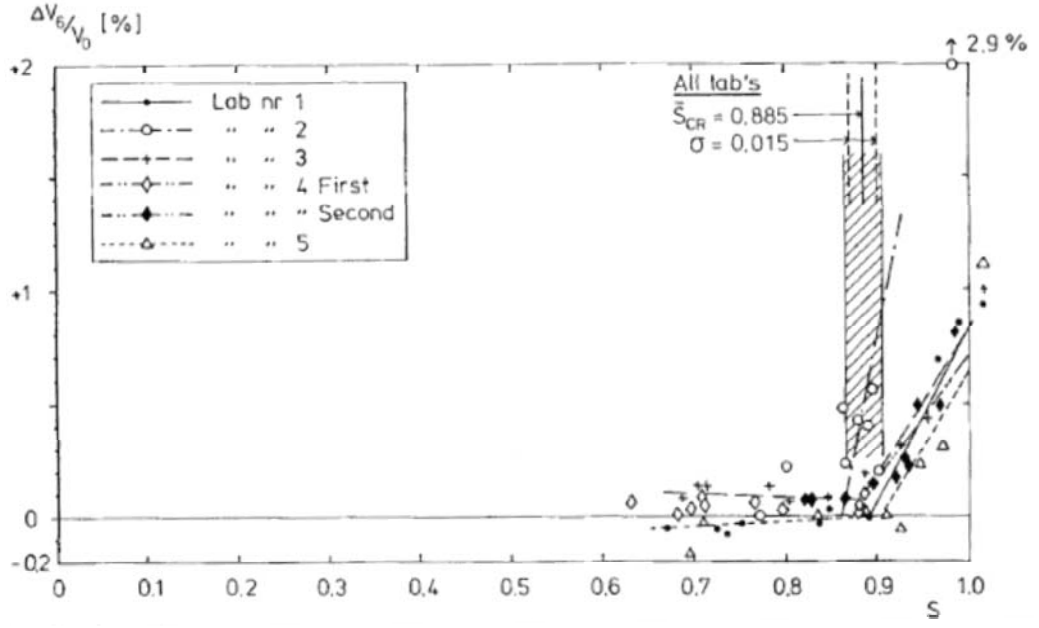

Figure 3-12 Change in volume plotted against degree of saturation [Fagerlund 1979]

Figure 3-12, taken from Fagerlund's paper, plots the degree of saturation of concrete samples versus change in volume. The degree of saturation at which damage occurs is remarkably consistent between all five laboratories, using both methods of determining frost damage. Prick [1997] conducted similar tests on limestone, the results of which are very much like Fagerlund's.

3.3.2 Freeze-Thaw Cycle

There are a number of parameters of a freeze-thaw cycle that impact the extent of frost damage in a material including the rate of cooling, the minimum temperature reached in the cycle, and the number of cycles.

Rate of cooling has a considerable affect on the severity of frost damage. This is possibly due to several reasons. According to the hydraulic pressure theory, ice formation will displace liquid water forcing it to flow through adjoining capillaries to partly filled pores. Rapid rates of cooling lead to a higher rate of ice formation increasing the flow rate, and subsequently the pressure, of water in capillaries.

In the disequilibrium theory, a high cooling rate will increase the rate at which water held in capillaries desorbs. If the desorption rate is higher than the redistribution rate, the accumulation of unstable water will cause damage. Conversely, low rates of cooling allow the solid matrix to creep in response to the tensile forces imposed on it by super-cooled water in desiccated pores. This has been confirmed experimentally: cement specimens with a high water/cement ratio of 0.7 were cooled from 0°C to -60°C using different freezing rates and it was discovered that no damage was sustained by specimens cooled at a rate of 2.5°C/hour while severe damage was inflicted on specimens cooled at a rate of 20°C/hour. It was concluded that "if the rate [of cooling] is very low even very vulnerable systems can go through freezing and thawing cycles without suffering damage" [Litvan 1988]. The importance of cooling rate has been corroborated by other researchers [Ritchie 1968].

In the study overseen by Fagerlund [1979] it appears that freezing rate only affects the severity of frost dilation but does not change the value of the critical degree of saturation. Five European laboratories determined the critical degree of saturation of concrete specimens. The rates of freezing used by the labs varied from -17°C/hour to -2.5°C/hour. Despite this wide range of freezing rates, there was a high level of consistency among the participants in determining the S_{crit} of the concrete. As a point of comparison, brick veneers, in Southern Ontario, have been shown to experience freezing rates of less than -5°C/hour [Straube 1998].

The minimum temperature of the cycle must be low enough to freeze the majority of water held in the pore space. Figure 3-2 illustrates that the freezing point of water in small pores can be significantly lower than that of bulk ice. If the minimum temperature of the cycle is just slightly less than 0°C, water held in a material with a fine pore structure will largely remain unfrozen leaving the material undamaged.

The number of damaging cycles experienced by a material affects the extent of frost damage as expansion of the material accumulates with each freeze-thaw cycle (see Figure 3-10). Even

though damage may not be visible with the initial cycles, the material has been irreparably weakened.

3.3.3 Material Properties

Based on the theories of frost damage discussed above, it is possible to identify properties of a material that may increase its susceptibility to freeze-thaw damage. Frost damage, as explained by the ice lensing theory, requires both small unfrozen capillaries as a water source and larger pores for ice crystal growth. Thus a material with a non-uniform pore size distribution may be more susceptible to frost damage. Conversely, a material with a tight pore size distribution will have very little super-cooled water available to form damaging ice lenses.

According to the disequilibrium theory, any condition that hinders the flow of desorbed water to an open material surface will increase the likelihood of damage. It follows that high porosity and high internal surface area may be problematic as a large amount of water is available to be desorbed, and low permeability will decrease the redistribution rate of unstable water.

Materials with a large distribution of pores of an "intermediate" size are increasingly prone to frost damage. Large pores readily fill with water but also have a higher drying rate than intermediate and small pores, therefore they tend to have water contents well below saturation. Water in small pores has a depressed freezing point, so there are fewer instances of temperatures being low enough to cause freezing than in intermediate size pores. There is less agreement on what actual size constitutes a dangerous, "intermediate" size pore diameter with varying estimates including <740nm [Maage 1988], 100nm-1000nm [Crawford 1984], and 8nm-60nm [Litvan 1973].

Material strength appears to have an indirect relation to freeze-thaw durability. As discussed in Section 3.1 the expansive forces imposed on a material due to frost action are far greater than its capacity to resist them. Strength is inversely related to the porosity of a material, so that low strength brick has a higher degree of porosity which renders it more susceptible to frost damage.

3.4 Summary

Frost damage has been attributed to several mechanisms including the volumetric expansion of water on freezing, hydraulic pressure effects and the formation of ice lenses driven by difference in chemical potential or vapour pressure between super-cooled water and ice. Despite only possessing a partial understanding of the physics of frost damage, procedures to identify frost damage are well established, including visual inspection, dilatometry and measurements of E-modulus. Furthermore several factors affecting the occurrence and severity of frost damage are well known such as moisture content during freezing, freezing rate, and material properties such as porosity and permeability.

Further research into the effect of the cooling rate on the degree of saturation and the extent of expansion would be useful, as would more investigations into the actual mechanisms and pore space characteristics that affect freeze thaw.

Chapter 4

Assessing the Risk of Freeze-Thaw Damage

4.1 Grading Clay Brick

In North America, manufactured clay brick must meet criteria established by ASTM International (ASTM) in the United States and the Canadian Standards Association (CSA) in Canada. ASTM C62-05 and ASTM C216-07a grade brick based on its resistance to frost damage as severe weathering (SW), moderate weathering (MW), or negligible weathering (NW). Facing brick must be of either grade SW or MW based on its exposure level as determined by the weathering index. The weathering index for a location is calculated by multiplying the number of days each year on which the air temperature cycles around 32°F (0°C) with the inches of annual winter rainfall. If a location has a weather index of 50 or greater, ASTM recommends using SW grade bricks. Almost the entire continental United States, and presumably all of Canada, has a weathering index of 50 or greater as shown in Figure 4-1.

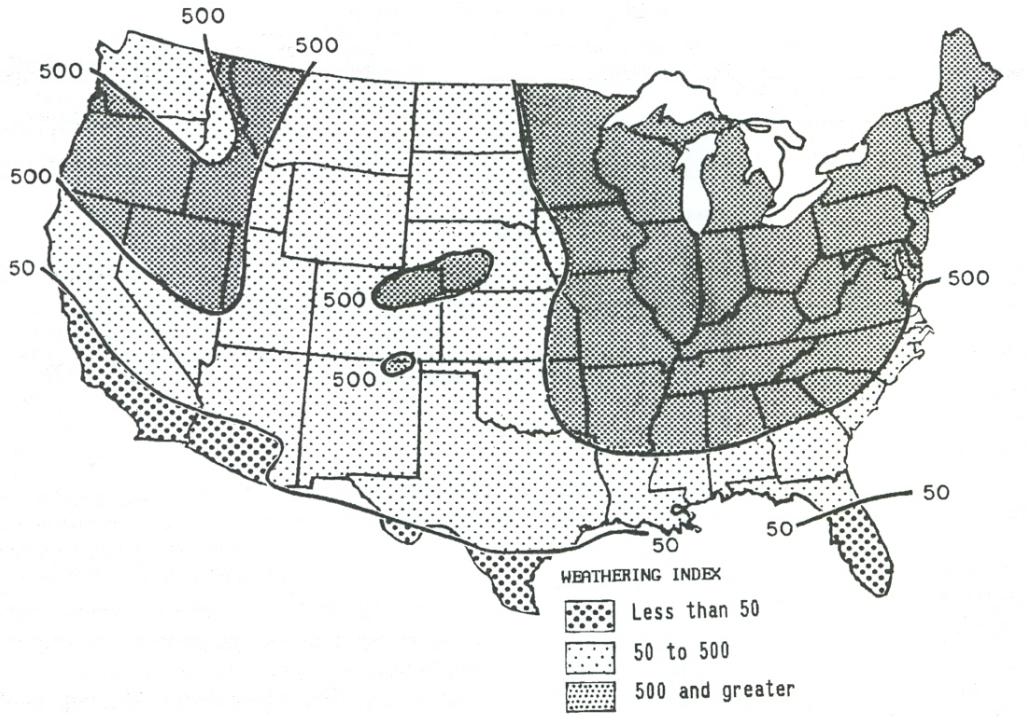

Figure 4-1 United States weathering index

CSA A82-06 grades brick as either Exterior Grade (EG) or Interior Grade (IG). Due to Canada's cooler climate, Exterior Grade brick is not differentiated between severe and moderate weathering.

ASTM and CSA have adopted very similar criteria for SW and EG bricks. In order for brick to be accepted as exterior grade or severe weathering, it must meet the criteria listed in Table 4-1. The compressive strength criteria are identical in both standards. The absorption and saturation criteria of the CSA are equal to the more stringent criteria for a 5-brick average of the ASTM standard, while the ASTM standard slightly relaxes the maximum allowable boiling absorption and saturation coefficient required of an individual brick. ASTM and CSA also specify that a brick needs only to pass either the maximum saturation coefficient or maximum cold water absorption criteria; it does not need to meet both. It should be noted that the procedures used in calculating the values of acceptance criteria are contained in a separate standard, ASTM C67-07a.

Table 4-1 Exterior Grade/Severe Weathering acceptance criteria by CSA and ASTM standards

	Compressive Strength		Max Boiling Absorption, 5-Hour	Max Saturation Coefficient	Max Cold Absorption, 24-Hour
	(MPa)	(psi)	(%)		(%)
CSA Individual Brick	17.2	-	17.0	0.78	8.0
CSA 5-Brick Average	20.7	-	-	-	-
ASTM Individual Brick	17.2	2500	20.0	0.80	8.0
ASTM 5-Brick Average	20.7	3000	17.0	0.78	-

In brief, and using CSA notation, cold water absorption is determined by weighing the dry mass full or half size brick specimens, M_1, submersing them in room temperature water for 24 hours, weighing their saturated mass, M_2. Absorption is calculated by:

$$Absorption,\% = 100 \times \frac{M_2 - M_1}{M_2} \tag{4-1}$$

Boiling absorption is determined by submersing full or half size brick specimens in water, heating the water to its boiling point for 5-hours, allowing the water to cool to room temperature and then weighing the saturated mass of the brick, M_3. Boiling absorption is calculated by:

$$BoilingAbsorption,\% = 100 \times \frac{M_3 - M_1}{M_3} \tag{4-2}$$

The saturation coefficient of a brick is calculated as:

$$SaturationCoefficient = \frac{M_2 - M_1}{M_3 - M_1} \tag{4-3}$$

The acceptance criteria used by ASTM and the CSA was selected to ensure adequate open pore space to accommodate expansion of water as it freezes [Crawford 1984]. The boiling absorption value is expected to be a fairly close representation of the maximum moisture a brick will absorb in field conditions. The 24-hour cold water absorption is an approximation of the likely moisture content after a severe wetting event. The saturation coefficient is a measure of the quantity of open pore space available under average wetting conditions. The intention is that the lower the coefficient of saturation, the more space is available to accommodate expansion of liquid water as it freezes. The 8% limit for water absorption after 24 hours is intended to ensure the brick does not too readily absorb water.

A brick that does not meet the acceptance criteria can still be approved provided it passes an omni-directional pass/fail freeze-thaw test specified by CSA A82-06 Clause 14 and ASTM C67-07a Clause 9. The freeze-thaw test specified by the CSA is essentially identical to the ASTM test, with only negligible differences. The test procedure can be summarized as follows. Half-brick samples, after being oven dried and cooled to room temperature, are soaked for approximately four hours in a thawing tank. They are then removed from the tank and the head face is laid in 12mm (½") of standing water and placed in a cold chamber for approximately twenty hours. This constitutes one freeze-thaw cycle and should be approximately 24 hours in duration. The samples are subjected to 50 cycles (taking ten weeks to complete if cycles are only carried out on standard business days) or until disintegration, which the CSA defines as 5% mass

loss (ASTM defines it as 3% mass loss) or the development of cracks in excess of the specimen's least dimension as determined by visual inspection. If after 50 cycles the specimens do not have a mass loss greater "than that permitted by the referenced unit specification for the appropriate classification" and has not developed cracks with a length greater "than that permitted by the reference unit specification for the appropriate classification" (wording taken from clause 9.4.3 of the ASTM standard), it is considered to have passed the test. This test is meant to replicate extreme field conditions of multiple freezing cycles while the brick is in a saturated condition.

4.2 Critique of Existing Methodology for Grading Brick

Criticism of the existing method of grading the durability of brick is longstanding. It is based on the fact that some bricks which pass the standard subsequently fail in service, while other brick fails the standard yet have been proven durable in practice [Butterworth 1964, Litvan 1975, Brampton Brick 1994].

The shortcoming of predicting durability of a material based on the acceptance criteria in the ASTM and CSA standards is that it is based on an incomplete understanding of the physics of freeze-thaw damage and an over-simplification of field exposure conditions. The saturation coefficient is based on the expectation that frost damage is principally due to the volumetric expansion of water as it freezes. As shown earlier, this is not the sole mechanism of freeze thaw damage although it may be the most important. Therefore, the inference between the saturation coefficient and durability that forms the basis of the ASTM/CSA acceptance criteria is at best a rough guide to in-service material durability; it is not a reliable measure of frost resistance.

The 50-cycle freeze-thaw test is even more problematic. For most uses of brick, especially walls, the mode of freezing is uni-directional; that is a freezing front advances inwardly from the outer face of the brick. The 50-cycle test is omni-directional, that is multiple freezing fronts advance from all exterior faces of the brick towards the centre. As already explained, this may build up hydraulic pressures in the centre of the brick that would not occur under the uni-directional mode of freezing experienced in service by most brick.

The 50-cycle test also is deficient in that no attempt is made to determine the saturation of the brick specimens as they are subjected to freeze-thaw cycles. This is worrisome as the degree of saturation of the brick during the test, S_{test}, may not closely approximate the degree of saturation of the brick when in service, $S_{service}$. Not controlling the degree of saturation of the brick while being tested, leads to two types of incorrect test results. Bricks that will reach a degree of saturation greater than S_{crit} in service, but absorbed less moisture than S_{crit} during the test, will eventually fail in service despite passing the test. Alternatively, if the moisture content of a brick never surpasses S_{crit} in service, but surpassed S_{crit} during the test, then the brick will be incorrectly rejected despite proving durable in service. The possible outcomes of the test are contained in Table 4-2.

Table 4-2. ASTM test vs service critical moisture contents

	$S_{service} > S_{crit}$	$S_{service} < S_{crit}$
$S_{test} > S_{crit}$	Correct Rejection	Incorrect Rejection
$S_{test} < S_{crit}$	Incorrect Approval	Correct Approval

Relying solely on acceptance criteria or the 50-cycle test does not provide an adequate basis for determining market eligibility of a product and can expose building owners to hefty maintenance or replacement costs in the case of incorrect approvals. Furthermore, in existing buildings, pass-fail criteria are not always very useful, as the masonry already exists and cannot be modified in situ. A designer may be able to reduce the moisture load on a masonry façade, and thereby reduce the risk of freeze-thaw damage, by changes in the building façade.

The fundamental problem with grading frost resistance of brick, as enshrined in the CSA/ASTM standards, is that no such thing exists. ASTM recognizes this in Appendix X4 of C216-07a which includes the disclaimer that "in severe exposures, even Grade SW brick may spall under certain conditions of moisture infiltration, chemical actions, or salt crystallization." This is just another way of saying that all materials will fail when subjected to harsh enough conditions. Thus, "freeze-thaw resistance" is a misleading concept because it implies that a material can be

capable of withstanding all possible damage mechanisms imposed by frost action under all conceivable circumstances.

A better approach to assessing the risk of frost damage in brick would be to have a test that could determine the critical degree of saturation of the brick and compare that to the maximum degree of saturation it will experience during freezing events. This is analogous to designing a structural member by ensuring that it possesses the strength to resist anticipated loads. There is no such thing as an inherently "load resistant" beam or column. So, when specifying a brick in new construction or planning a retrofit strategy, an engineer or architect should select a brick or pursue a strategy in which the predicted in-service moisture load will be less than the critical degree of saturation of the material. Developing a simple, inexpensive test to determine the critical moisture content of a brick is the focus of the remainder of this thesis.

4.3 Synopsis of Proposed Test Method to Determine Critical Degree of Saturation

The goals in developing this test method were to provide a fairly precise estimate of the critical moisture content of brick (assumed to exist because of the work of Fagerlund and others) at which it begins to experience freeze-thaw damage. After a review of possible methodologies for identifying freeze-thaw damage, including destructive compressive strength tests, visual observation and dynamic modulus, frost dilatometry was chosen. Frost dilatometry has the advantages of being a quantitative measure, non-destructive, requires only commonly available, relatively inexpensive equipment and can be of short duration. What follows is an overview of the test methodology developed and used in the experimental program. Chapters 5 to 7 examine in further detail the development of this method.

4.3.1 Preparation of Brick Specimens

The bricks selected for testing should be sliced into as many 10 mm thick specimens as possible by sawing parallel to the header face, i.e., the brick should be sliced like a loaf of bread. For a standard brick 8" (200 mm) in length, this will result in approximately 12 specimens, depending on the saw blade thickness. Many modern bricks have cores which will reduce the number of specimens that can be cut from a single brick. The 10 mm thickness was decided upon as it

allowed a high number of samples to be taken from a brick and it results in a high surface area to volume ratio which allows rapid heat transfer during freeze-thaw cycling.

Targets, which can be round-head slotted screws or rivets, should be installed at the ends of the long dimension of the sliced brick specimens. The targets should be secured with adhesive in pre-drilled holes wide enough to accommodate the stem but narrow enough that the head will sit flush to the brick surface, as per Figure 4-2 below.

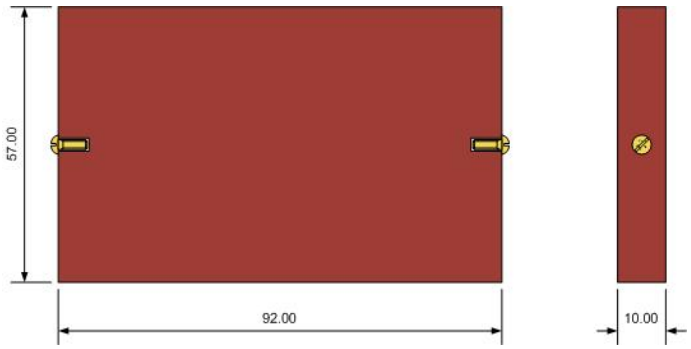

Figure 4-2 Typical brick sample with measuring pin targets.

The adhesive used to secure the pins to the brick must be able to survive prolonged boiling in water and drying at temperatures of 105°C. It was found that Lepage or JB-Kwik two-part steel epoxies provided satisfactory bonding under these conditions.

4.3.2 Material Properties

Following the preparation of the brick samples, the dry mass, saturated mass, capillary water uptake coefficient (A-value), and length of each specimen should be measured.

Specimens are typically dried in an oven at 105°C and measurements of the mass taken every hour after being placed in the oven. When the change in mass over two hours is less than 0.05%, the specimen is considered to have reached a dry state.

The saturated mass of a specimen can be determined using one of two methods: the boil method or the vacuum saturation method. The procedure for carrying out saturation by either method is

covered in Chapter 5 with a discussion of their relative merits. It may be helpful to take one specimen and determine its saturation moisture content using both the boil and the vacuum method. If the difference in saturation moisture content between the two methods is not great, perhaps less than 5%, boiling may be preferable as it is the more expedient method to saturate the specimens.

The A-value (capillary water uptake coefficient) of each brick sample should be determined by a water uptake test. Supports for the brick specimens are placed in a tray and water is poured into the tray until the supports are covered to a depth of 1 to 2 mm. The mass of each dry brick specimen is recorded and then each specimen can be placed on the supports with the largest face in contact with the water. At regular intervals, such as the schedule in Table 4-3, the specimens are removed from the water and the mass is recorded.

Table 4-3 Measurement schedule for the water uptake test

Measurement	Time Elapsed	Tolerance
1	1 min	5 sec
2	2 min	10 sec
3	5 min	30 sec
4	10 min	1 min
5	15 min	1 min
6	20 min	1 min
7	30 min	2 min
8	45 min	3 min
9	60 min	5 min
10	180 min	15 min

Each specimen's change in mass should be plotted against the square root of time for each measurement taken. An example of this plot is in Figure 4-3. Initially, the brick sample will rapidly absorb water until its capillaries are saturated. At this point the brick will continue to slowly absorb water as trapped gases dissolve and escape to the exterior. Highly, absorbent bricks may require additional measurements early in the test to determine the initial slope of the

curve, and low porous bricks may need to be in contact with water longer than three hours for the pore system to become mostly saturated.

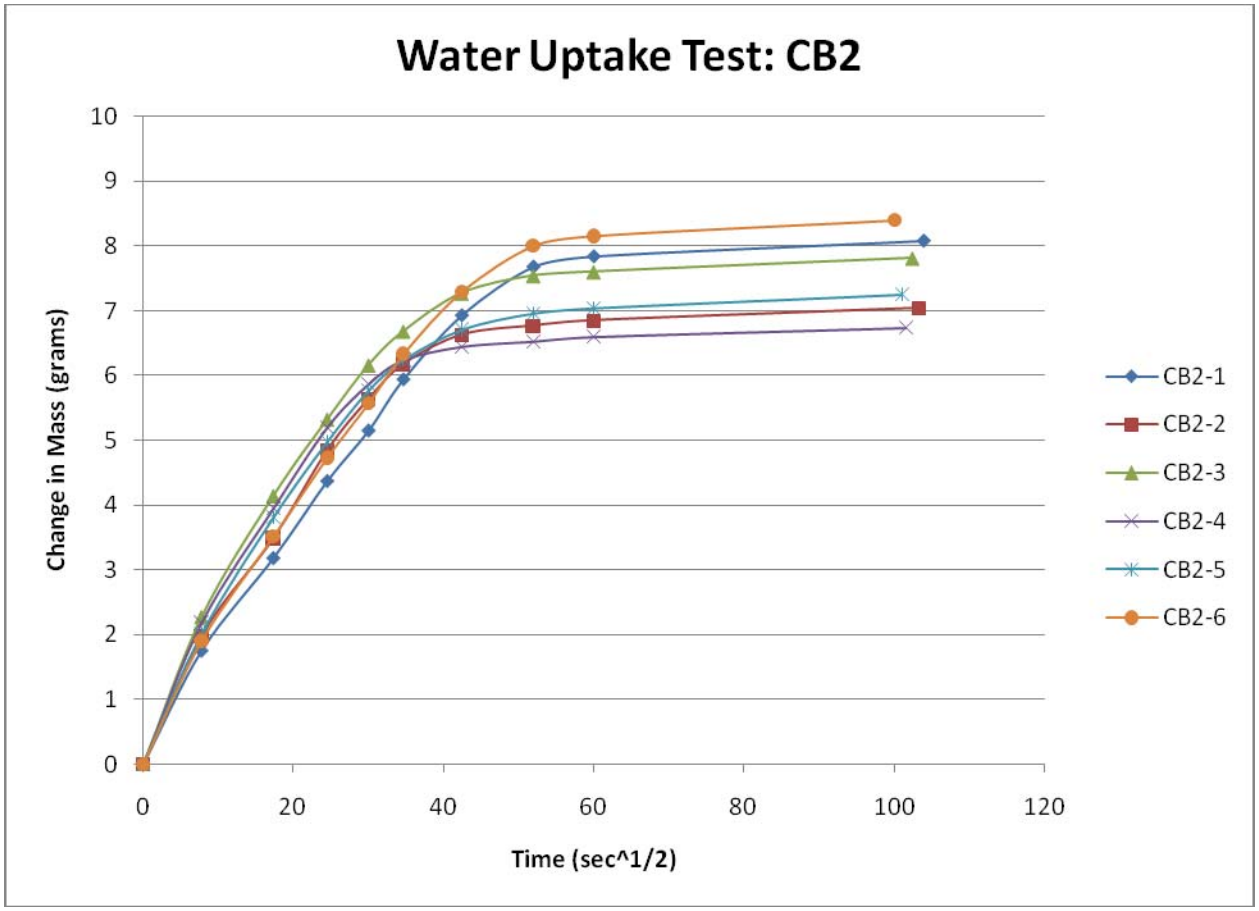

Figure 4-3 Typical results of the water uptake test

The A-value is calculated by dividing the initial slope of the curve by the surface area of the face in contact with water as per the following equation:

$$A-value = \frac{\sigma}{SA} \times 1000 \qquad (4\text{-}4)$$

Where:

A-value	water uptake coefficient ($kg/m^2s^{½}$)
σ	initial slope ($g/s^{½}$)
SA	surface area (m^2)

4.3.3 Freeze-Thaw Cycling

The length of each sample should be measured, in this study a ratchet-tightened outside micrometer accurate to ±0.001mm, was used to measure length by placing it in contact with the pins. A ratchet is necessary to ensure that a consistent tightening pressure is applied with each measurement. The micrometer should be calibrated on a gauge block prior to use. The flat face of the anvil and spindle are placed in contact with the rounded pins that have been secured to the ends of a specimen and then tightened with the ratchet stop until the measured length on the digital gauge no longer decreases. A record of the sample length is taken, the specimen rotated 180° and a second length measurement is made. The length is recorded to a one thousandth of a millimetre. The average of these two measurements will be considered the sample length. The orientation of the brick sample when the first measurement is taken must be marked so that the sample is subsequently measured in the same orientation. These precautions are important to ensure consistency among measurements. The samples occasionally seat differently when in contact with the micrometer depending on orientation; typically this ranges within ±0.005 mm. The instrument used in this study was a 3-4" Digimatic Outside Micrometer manufactured by Asimeto. This micrometer allowed expansion measurements to be made with a precision of about 10 microstrain.

The determination of S_{crit} is an iterative process. The first round of freeze thaw testing should determine the S_{crit} to the nearest 20% degree of saturation; and a second round will determine more precisely the degree of saturation at which frost damage occurs.

In the first round, five specimens from a brick have water added equal to 0.20, 0.40, 0.60, 0.80, and 1.00 of the saturation moisture content based on boil or vacuum saturation, as determined earlier. When wetting to low degrees of saturation, water can be simply placed in contact with the face of the specimen and be absorbed into the brick. To reach higher degrees of saturation a specimen may have to be saturated by using the boil or vacuum method and then dried to the desired moisture content. Seal the specimens by tightly wrapping them in plastic or aluminum tape, taking care to minimize the air space between the surface of the specimen and the sealant

material. The specimens must be set aside for at least 24 hours, prior to freezing, to allow moisture to distribute evenly throughout the pore space. For specimens with low A-values, approximately 0.005kg/m^{2}s^{½} or less, it may necessary to wait for up to 72 hours after wetting for redistribution to be mostly complete.

The wetted, wrapped samples should be subject to multiple freeze-thaw cycles; in this study the number of cycles was six. This can be done by placing the samples in a conventional freezer (cooled to approximately -18°C) for three hours and then allow them to thaw at room temperature for another three hours, or by placing the specimens in an un-insulated, watertight pouch and submersing in a chilled liquid bath that can be programmed to automatically cycles between temperatures of -15°C to 20°C.

After undergoing six freeze-thaw cycles, the wrapping around the specimens should be removed and the mass weighed to verify that the moisture content has not appreciable decreased during the freeze-thaw test. Next, the length of the specimen should be measured in order to calculate expansion experienced by the specimen during freezing using the same procedure as before. The expansion of the sample in terms of strain is calculated by the following equation:

$$\varepsilon = \frac{l_6 - l_0}{l_0} \times 10^6 \tag{4-5}$$

where

ε	expansion (microstrain)
l_0	initial specimen length (mm)
l_6	specimen length after six freeze-thaw cycles (mm)

Expansion greater than about 100 microstrain appears to be indicative of frost damage, as based on the experimental results of this study (see Chapter 7). Accordingly, this expansion magnitude will be used to define the saturation level at and above which frost damage is expected to occur (i.e., to determine S_{crit}); S_{crit} will be taken as the lowest saturation level for which expansion exceeds 100 microstrain after six cycles of freezing and thawing.

If the expansion of all samples tested in the first round is greater than 100 microstrain, S_{crit} must be less than 0.20 of the saturation moisture content. Select three more specimens from the brick and wet to 0.05, 0.10, and 0.15 of the saturation moisture content. Subject the specimens six cycles of freeze thaw testing following the same process as above, calculate the expansion at each increment of moisture content to determine S_{crit}.

If some of the samples experience an expansion greater than 100 microstrain, test three more samples at 0.05 increments of saturation between the highest degree of saturation at which the expansion was less than 100 microstrain and the lowest degree of saturation at which the expansion was greater than 100 microstrain. For example, if after the first round of freeze thaw testing the expansion in the sample at 0.80 degree of saturation was 238 microstrain and the expansion in the sample at 0.60 degree of saturation was 56 microstrain, the specimens used in the second round of freeze-thaw testing would be wet to 0.65, 0.70, and 0.75 degrees of saturation. Subject the samples to six freeze-thaw cycles and calculate the expansion to determine the S_{crit}.

If none of the samples that were wet based on maximum saturation as determined by the boil method, underwent expansion greater than 100 microstrain, all samples from that brick must be dried and the saturation moisture content determined using the vacuum saturation method (which, as described later, is greater than or equal to the boil saturation). Five samples should then be wet to 0.80, 0.85, 0.90, 0.95, and 1.00 of the vacuum saturation and put through six freeze-thaw cycles. Expansion is then calculated and S_{crit} is determined.

It is estimated that this test protocol will require 6 to 12 days to complete depending on the sample size and number of freeze-thaw cycles required to determine S_{crit}. Preparation of the specimens should be completed in one day. Determining material properties could take between 2 to 4 days depending on the number of bricks being tested and staffing. 1 day should be set aside to allow moisture redistribution, as explained earlier. Freeze-thaw cycling will take

between 2 to 6 days depending on the number of cycles required to determine S_{crit} to within 0.05 degrees of saturation.

4.4 Summary

The current method in North America for determining the durability of brick to frost action is to carry out a pass/fail test based on material properties or its ability to withstand a severe freeze-thaw test. The pass/fail approach is flawed because, in the case of acceptance criteria, it is based on an incomplete understanding of the physics of frost damage, in the case of the freeze-thaw test, one set of arbitrarily imposed conditions does not cover the range of exposures a brick could experience while in service nor does it accommodate different brick absorptivities and storage. More generally, frost resistance is not an inherent material property. An alternative approach, more consistent with engineering principles, is to determine the anticipated in-service moisture load and compare that to a material's critical degree of saturation, S_{crit}. A possible procedure for determining the S_{crit} of brick using frost dilatometry has been proposed.

Chapter 5

Measuring Degree of Saturation and Saturated Moisture Content

Measurements of saturated moisture content and degree of saturation require one to be able to determine the saturated mass of a material, which in turn is an indirect method of measuring the open void space of a material. It is important to distinguish between total void space and open void space. Porous materials may contain pores that are isolated from any other pore in the material, termed closed pores. Water entering the material from an external source will have no means of entering closed pores. Therefore, when determining open void space, disconnected pores can be considered part of the solid matrix. Gravimetric, liquid saturation methods of determining the open pore space of a material are based on weighing the material in a dry and saturated state. The void space is calculated by the following equation:

$$V_v = \left(M_{sat} - M_{dry}\right) / \rho_{liquid} \tag{5-1}$$

where

V_v = open void volume [m^3]
M_{sat} = mass of the saturated material [kg]
M_{dry} = mass of the dry material [kg]
ρ_{liquid} = liquid density [kg/m^3]

There are some difficulties in obtaining an accurate measure of saturated mass. As liquid enters a dry material, most of the air initially held in the pore space is expelled. However, air can become trapped by the wetting front in dead-end pores (see Figure 5-1). Dead-end pores are gradually filled over time as trapped gasses dissolve, are replaced by liquid water, and subsequently degas to the surrounding atmosphere.

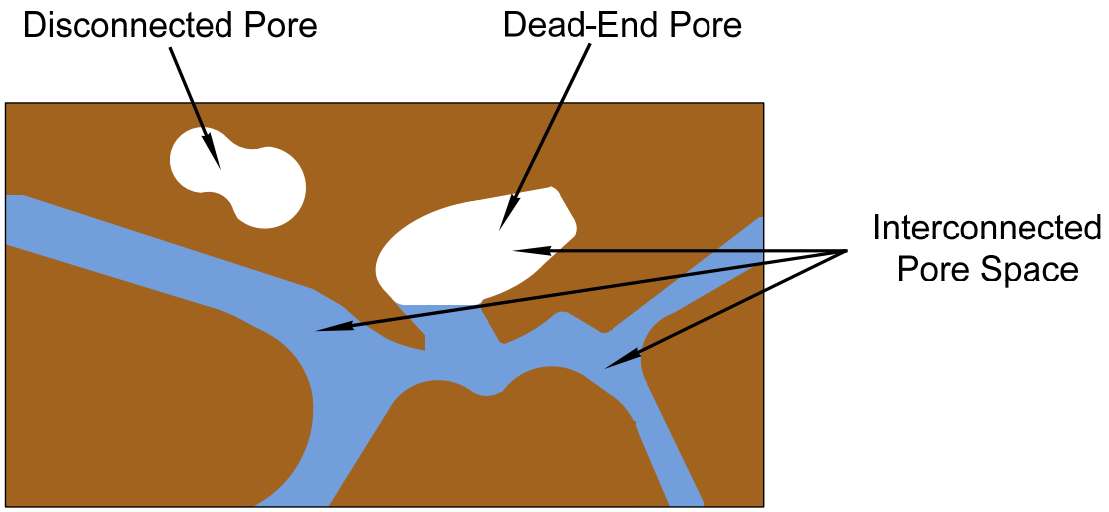

Figure 5-1 Idealization of a liquid-saturated pore space

The replacement of trapped air with water in dead end pores can be a very slow process. In an experiment by Gummerson [1980], the header face of a clay brick was placed in contact with water, while all other surfaces were free to evaporate, similar to a water uptake test. The brick was then weighed at intervals over the next two years, plotted in Figure 5-2. The water reached the top surface of the brick within one day, filling about 82% of the open pore space. Then, the brick gradually continued to gain mass over the following two years as water slowly displaced air trapped in dead end pores. At the end of the two years, gas still remained in approximately 2% of the interconnected pore space.

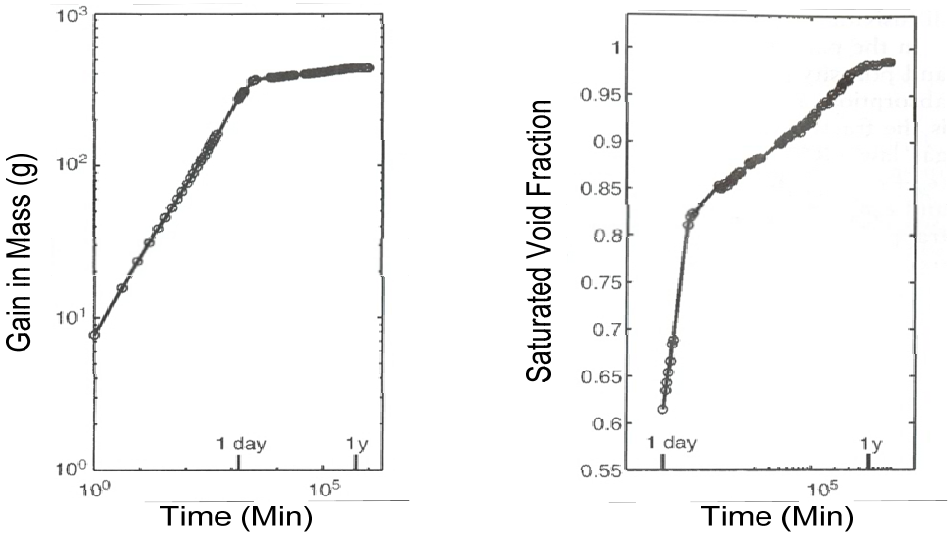

Figure 5-2 Long-term water uptake of a clay brick [Gummerson 1980]

In order to gain an accurate measure of a material's saturated mass, trapped gas must be minimized. It is not feasible, however, to wait two years for gasses to slowly dissolve out of the pore space. Consequently, two techniques are commonly used to minimize the amount of air trapped in the pore space when saturating a material, namely boiling and the vacuum saturation.

5.1 Boil Method

The boiling method is a simple way to approximate the open porosity of a material. A dry sample is weighed and then fully submersed in boiling water. Viscosity of water decreases as a function of increasing temperature (see Figure 5-3) allowing it to more easily travel through capillaries and pores when heated. Upon reaching the boiling point, steam is generated inside the material which drives out air initially retained in the pore space. After a pre-determined length of time passes, the water is allowed to cool down to room temperature while the brick specimens are kept fully submersed. As the specimens cool, pockets of steam within the pore space collapse creating a suction force that draws in additional water.

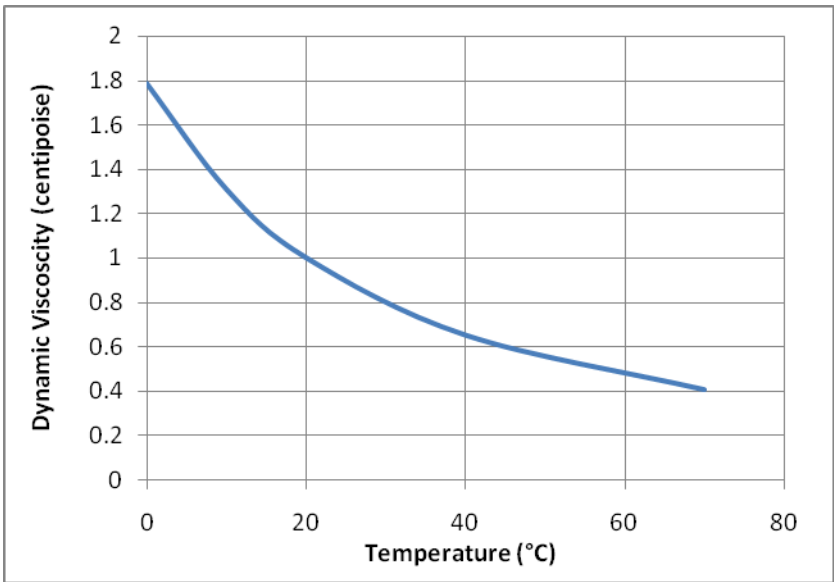

Figure 5-3 Dynamic viscosity of water as a function of temperature [Bear 1972]

5.1.1 ASTM/CSA Procedure

An identical procedure for the boil method is given in both ASTM C 67-07a and CSA A82-06 for full- or half-brick specimens. According to these two standards, the boiling test is to be conducted following a 24-hour soak in water at room temperature. It is then placed in a bath and the water is heated to boiling within 1 hour. According to the CSA standard, the water is boiled continuously for 5 hours (1, 2, or 5 hours in the ASTM standard), then allowed to cool to between 15°C and 30°C for a minimum of 12 hours or a maximum of 72 hours (no time constraints given in the ASTM standard). Upon cooling the specimens are removed and surface water is removed with a damp cloth. The specimens are weighed within 2 minutes of removal (5 minutes in the ASTM standard). The void volume is then calculated according to equation 4-2, page 34.

5.1.2 Optimizing the Boil Method for Reduced Sample Sizes

The boiling method is a two step procedure. The specimens must be boiled and then allowed to soak for prescribed amounts of time. The specimens intended for use in the test procedure proposed here are smaller than full- or half-sized bricks. As water has far less distance to

penetrate in these specimens it was found that the boil and soak timeframes prescribed in the ASTM and CSA standards are lengthier than required.

Four modern brick of the same lot manufactured by Canada Brick (now Hanson Brick) in the mid-1990s were sliced into specimens of varying thickness between 16 and 23mm. The specimens were boiled for various lengths of time, ranging from 1 to 24 hours, at which point the samples were removed from the boiling water and weighed. As the temperature of the wet specimens was close to the boiling point, the time between removal and weighing was kept to a minimum as water near the surface of the specimen quickly evaporated. Therefore the measured mass of boil saturated specimens will be slightly lower than the actual mass. Assuming that the amount of water loss was similar each time the specimens were boiled and weighed, a comparison of the amount of water absorbed by the specimen is possible (see Figure 5-4). Most of the water absorbed by the specimens occurred within the first hour. The moisture content slightly increased after 5-hours, and only marginal gains in moisture content were realized with an addition 19 hours of boiling. The difference in water absorbed between 1-hour and 5-hour boiling was more pronounced in specimens taken from Canada Brick 3, which has a lower porosity than the other bricks, indicating that additional boiling may be beneficial for specimens from low porosity bricks.

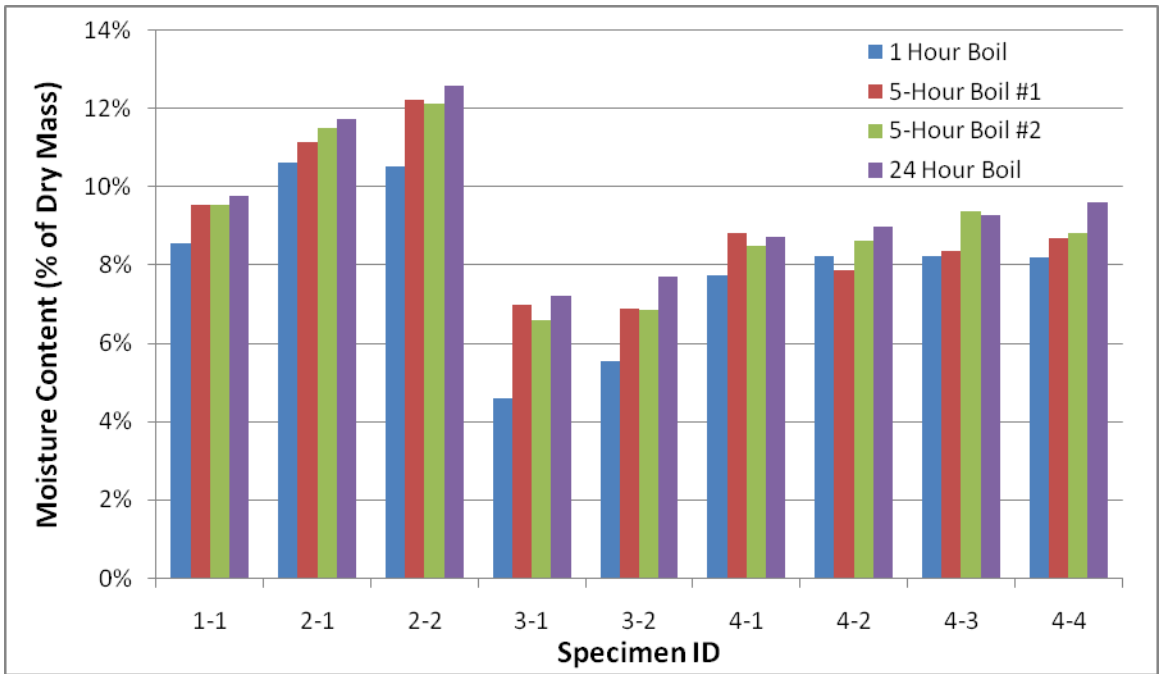

Figure 5-4 Water absorption of brick specimens by boiling

Due to the small size of the specimens used in the proposed test, the optimal length of time to allow the sliced brick specimens to soak, following the boil phase, appears to be far lower than the 12 hours required in the CSA standard for full or half bricks. Specimens, from the four bricks, were boiled for 5 hours and allowed to soak for 14 hours on two separate occasions. On both occasions the dry mass of the brick was recorded prior to entering the water and the samples were weighed at the end of the 5-hour boil and 14-hour soak procedure. During the first cycle, the mass of the specimens was recorded every hour of the 5 hour boil phase, while on the second occasion the specimens were weighed at intervals during the soaking phase (test data can be found in Appendix A). By combining the two sets of data in Figure 5-5 & Table 5-1, it is clear that the majority of the water is absorbed in the first hour of the boil and soak phases.

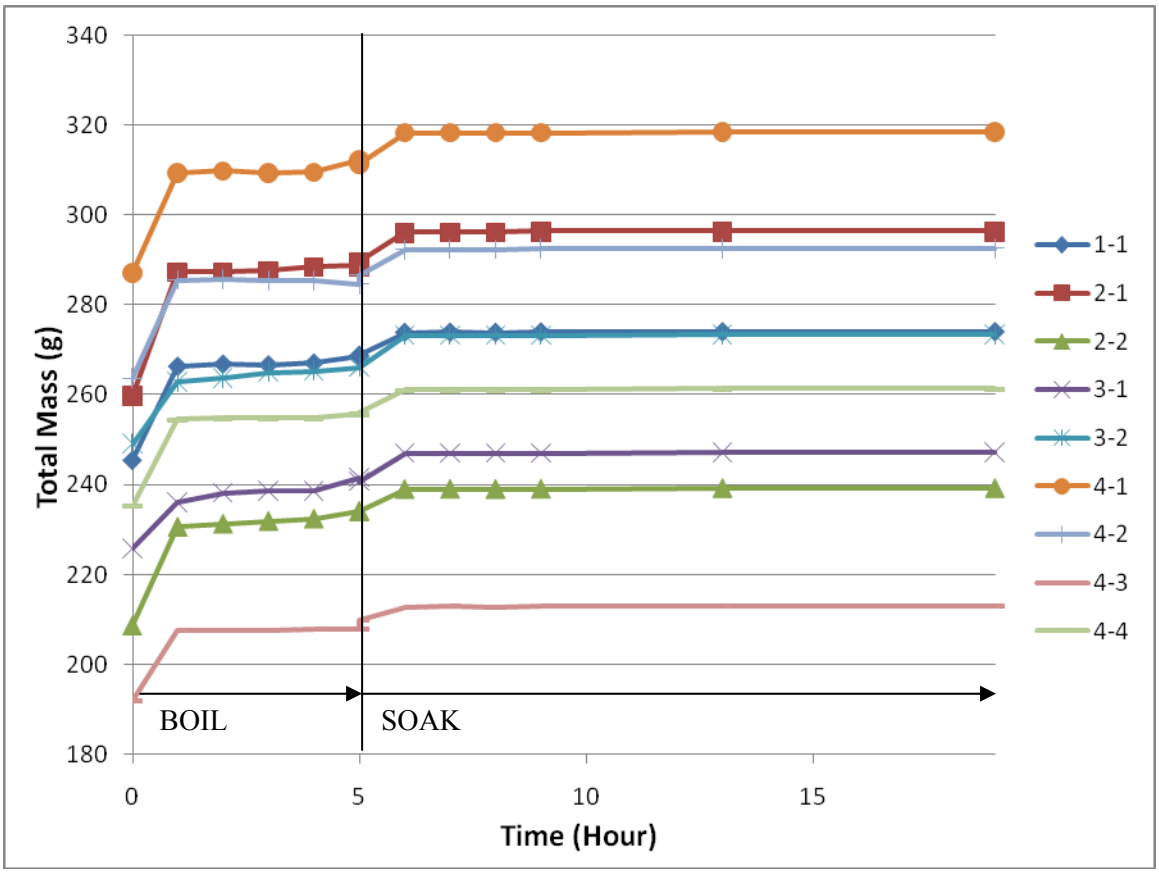

Figure 5-5 Water absorption over time by boiling and soaking

Table 5-1 Water absorption of Canada Brick

Specimen ID		Time (hours)												
		BOIL						SOAK						
		0	1	2	3	4	5	5	6	7	8	9	13	19
1-1	Mass (g)	245.39	266.40	266.89	266.72	267.12	268.80	268.83	273.98	274.03	273.98	274.08	274.10	274.15
	% Change	-	8.56%	0.18%	-0.06%	0.15%	0.63%	-	1.92%	0.02%	-0.02%	0.04%	0.01%	0.02%
2-1	Mass (g)	259.79	287.37	287.41	287.68	288.48	288.73	289.67	296.13	296.23	296.22	296.31	296.33	296.44
	% Change	-	10.62%	0.01%	0.09%	0.28%	0.09%	-	2.23%	0.03%	0.00%	0.03%	0.01%	0.04%
2-2	Mass (g)	208.78	230.75	231.42	232.03	232.56	234.31	234.12	239.13	239.16	239.14	239.17	239.33	239.33
	% Change	-	10.52%	0.29%	0.26%	0.23%	0.75%	-	2.14%	0.01%	-0.01%	0.01%	0.07%	0.00%
3-1	Mass (g)	225.88	236.22	238.25	238.67	238.62	241.67	240.80	247.10	247.05	247.04	247.12	247.20	247.27
	% Change	-	4.58%	0.86%	0.18%	-0.02%	1.28%	-	2.62%	-0.02%	0.00%	0.03%	0.03%	0.03%
3-2	Mass (g)	249.06	262.85	263.7	265.05	265.34	266.20	266.13	273.23	273.27	273.28	273.32	273.40	273.48
	% Change	-	5.54%	0.32%	0.51%	0.11%	0.32%	-	2.67%	0.01%	0.00%	0.01%	0.03%	0.03%
4-1	Mass (g)	287.11	309.35	309.88	309.34	309.62	312.45	311.46	318.35	318.37	318.35	318.42	318.52	318.61
	% Change	-	7.75%	0.17%	-0.17%	0.09%	0.91%	-	2.21%	0.01%	-0.01%	0.02%	0.03%	0.03%
4-2	Mass (g)	263.81	285.50	285.64	285.32	285.42	284.53	286.58	292.25	292.33	292.31	292.37	292.39	292.49
	% Change	-	8.22%	0.05%	-0.11%	0.04%	-0.31%	-	1.98%	0.03%	-0.01%	0.02%	0.01%	0.03%
4-3	Mass (g)	191.96	207.73	207.82	207.81	207.91	208.02	209.97	212.89	212.97	212.95	212.99	213.03	213.11
	% Change	-	8.22%	0.04%	0.00%	0.05%	0.05%	-	1.39%	0.04%	-0.01%	0.02%	0.02%	0.04%
4-4	Mass (g)	235.18	254.48	254.72	254.76	254.72	255.63	255.96	261.06	261.13	261.15	261.14	261.22	261.34
	% Change	-	8.21%	0.09%	0.02%	-0.02%	0.36%	-	1.99%	0.03%	0.01%	0.00%	0.03%	0.05%

Comparisons of water absorbed by the 1-hour boil & 1-hour soak (1B+1S) to the amount of water absorbed by the 5-hour boil and 14 or 18-hour soak (5B+14/18S) verify that little additional moisture is gained by lengthening the duration of each phase, as can be seen in Figure 5-6.

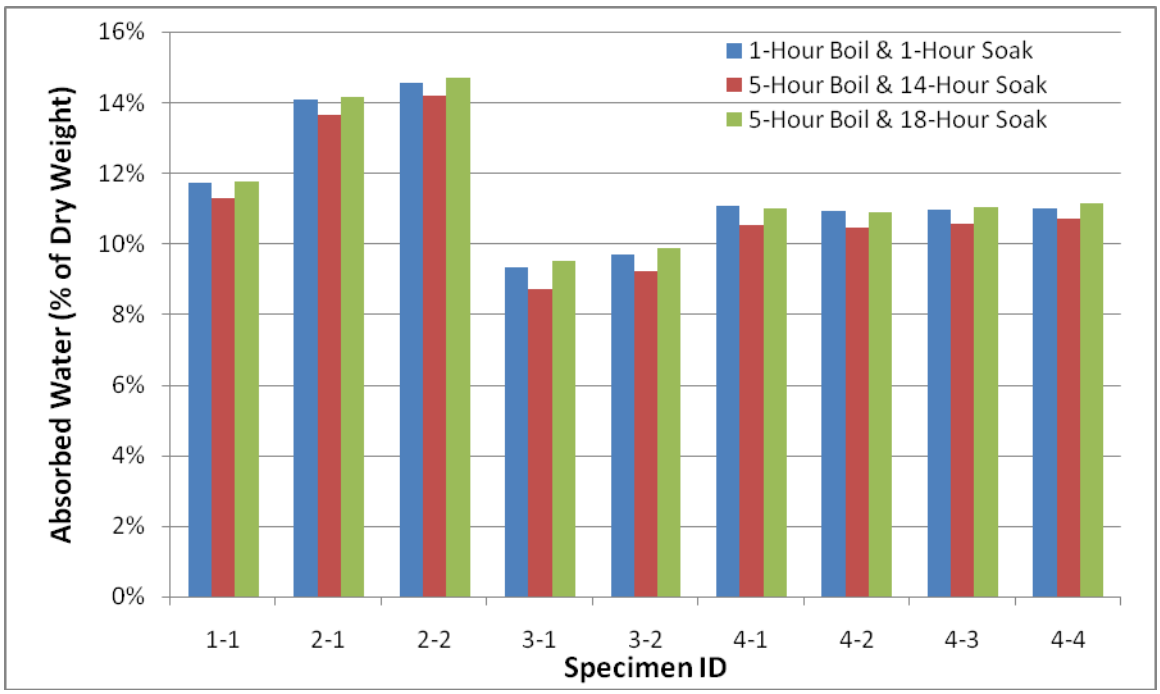

Figure 5-6 Water absorption of 1B+1S versus 5B+14/18S

Subsequently, three additional Canada Brick bricks were sliced into six 1 cm thick specimens and subjected to three rounds of 1B+1S saturation and one round of 5B+14S saturation, the results are summarized in Table 5-2 and presented in Figure 5-7 on the following page. There is some variability in the amount of water absorbed over the three occasions in which the specimens were saturated using 1B+1S. The ratio of minimum to maximum mass of water absorbed using 1B+1S ranges between 0.90 and 0.96. The average amount of moisture absorbed by the specimens using 1B+1S is approximately 5% less than using 5B+14S. This source of error underestimates the open porosity of the brick, which will increase the value of S_{crit}.

Table 5-2 Repeated boiling saturation of Canada Brick #3

		Sample ID					
		CB3-1	CB3-2	CB3-3	CB3-4	CB3-5	CB3-6
1-Hr Boil & 1-Hr Soak #1	Saturated Mass (g)	133.78	148.81	126.61	142.23	141.47	161.10
	H_2O Mass (g)	7.88	9.03	7.50	8.61	8.60	10.70
	H_2O (% of Dry Mass)	6.26%	6.46%	6.30%	6.44%	6.47%	7.11%
1-Hr Boil & 1-Hr Soak #2	Saturated Mass (g)	134.53	149.45	127.29	142.88	142.33	161.53
	H_2O Mass (g)	8.68	9.72	8.22	9.33	9.53	11.19
	H_2O (% of Dry Mass)	6.90%	6.96%	6.90%	6.99%	7.18%	7.44%
1-Hr Boil & 1-Hr Soak #3	Saturated Mass (g)	134.28	148.92	126.83	142.41	141.79	161.03
	H_2O Mass (g)	8.42	9.16	7.75	8.80	8.97	10.67
	H_2O (% of Dry Mass)	6.69%	6.55%	6.51%	6.59%	6.75%	7.10%
5-Hr Boil & 14-Hr Soak	Saturated Mass (g)	134.54	149.34	127.3	142.93	142.39	161.67
	H_2O Mass (g)	8.73	9.64	8.25	9.39	9.62	11.36
	H_2O (% of Dry Mass)	6.94%	6.90%	6.93%	7.03%	7.25%	7.56%
	Average of 1B+1S	6.62%	6.66%	6.57%	6.67%	6.80%	7.22%
	Ratio of Min:Max 1B+1S	0.91	0.93	0.91	0.92	0.90	0.96
	Difference between Avg 1B+1S and 5B+14S (% of Dry Mass)	-0.32%	-0.24%	-0.36%	-0.36%	-0.44%	-0.34%

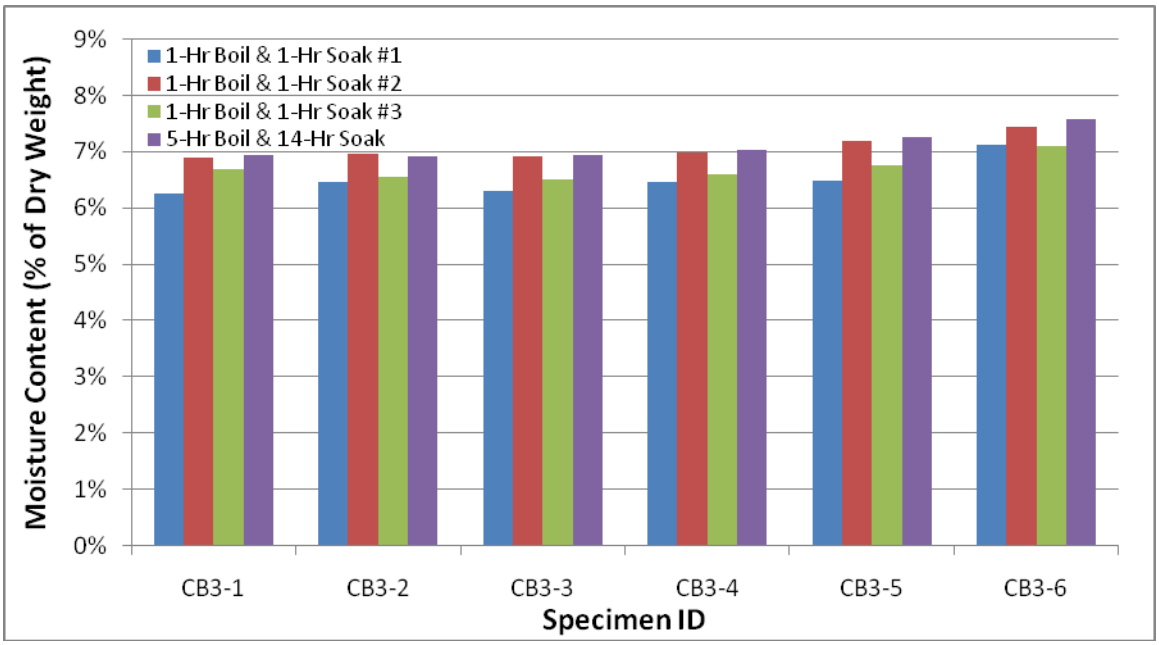

Figure 5-7 Water absorption of Canada Brick #3

The discrepancy in repeated measurements of the saturated mass of a specimen using the boiling method is a cause for concern as this lowers the precision of saturated moisture content and degree of saturation.

5.2 Vacuum Saturation

The intent when vacuum saturating is to evacuate as much of the air as possible from the pore space prior to submerging the material in a liquid. This will remove most of the trapped gas in dead end pores allowing them to be filled with water. As a perfect vacuum cannot be achieved in practice, some gas will still remain trapped in the pore space. Therefore, open porosity calculated by vacuum saturation is slightly less than the actual open porosity.

5.2.1 Vacuum Saturation Procedure

No ASTM or CSA standards were located that regulate how vacuum saturation of a material is to be performed. The apparatus used in this study is shown in Figure 5-8.

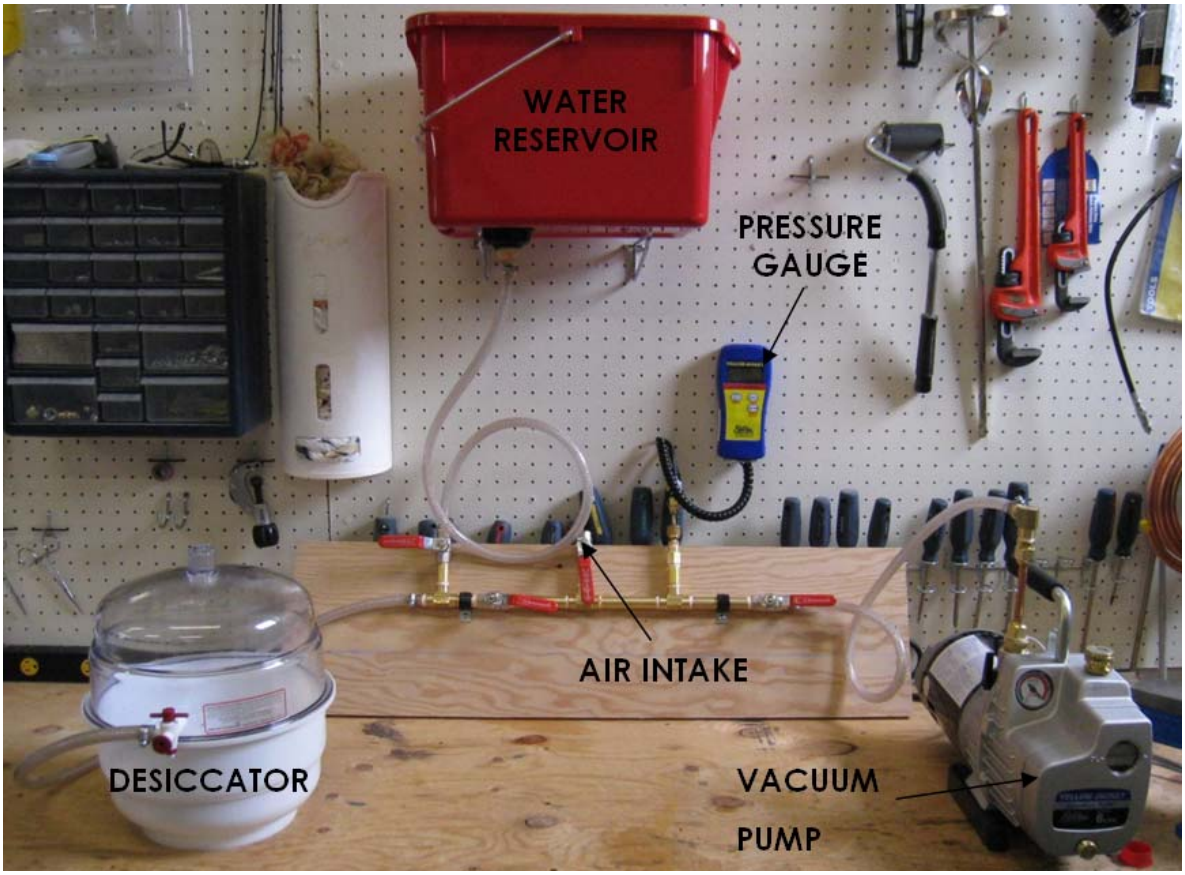

Figure 5-8 Vacuum saturation apparatus

The procedure used to vacuum saturate brick specimens in this study is:

1) Brick specimens are placed in a vacuum desiccator on level supports to ensure that water can freely flow around all sides.

2) A vacuum pump is used to draw down the pressure in the desiccator to at least 0.01 Atm (equivalent to -100.3kPa, -29.6inHg, 7600micronHg, or 10millibar), as illustrated in Figure 5-9. Vacuum pressures achieved in this study ranged from 700 to 1000 micronHg (0.0009 to 0.0013 Atm).

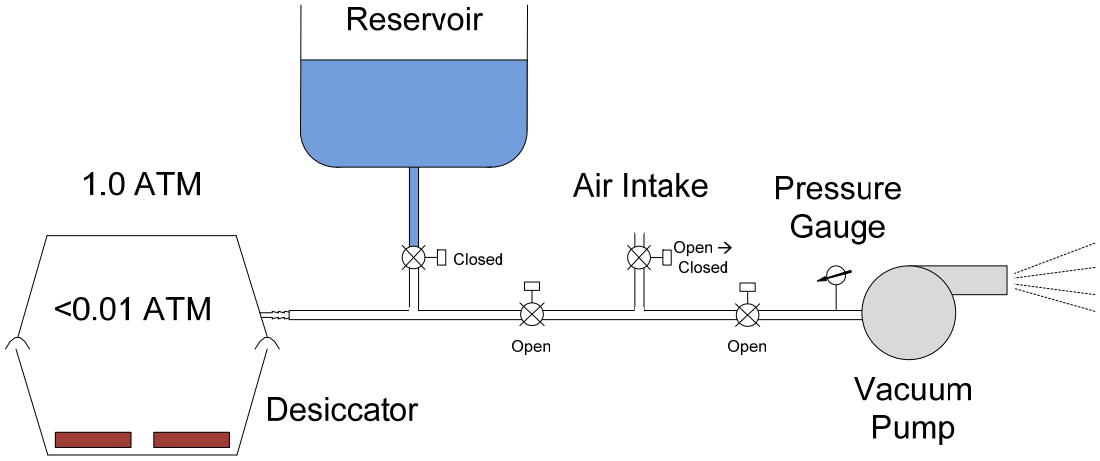

Figure 5-9 Vacuum saturation apparatus; pressure in desiccator less than 0.01Atm

3) Upon reaching the required vacuum pressure, the vacuum pump is isolated from the desiccator and allowed to return to atmospheric pressure as illustrated in Figure 5-10.

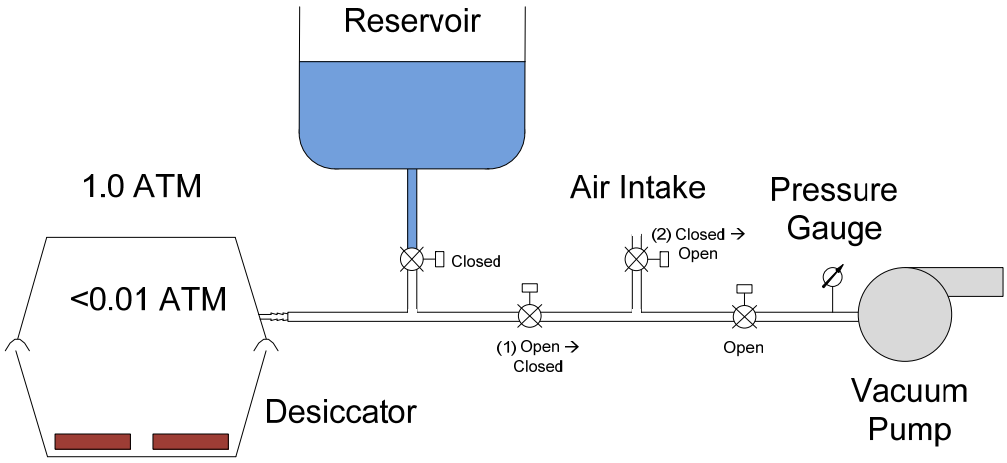

Figure 5-10 Vacuum pump isolated from desiccator

4) The valve to the reservoir is opened allowing distilled water to flood the desiccator until the bricks are fully immersed as demonstrated in Figure 5-11.

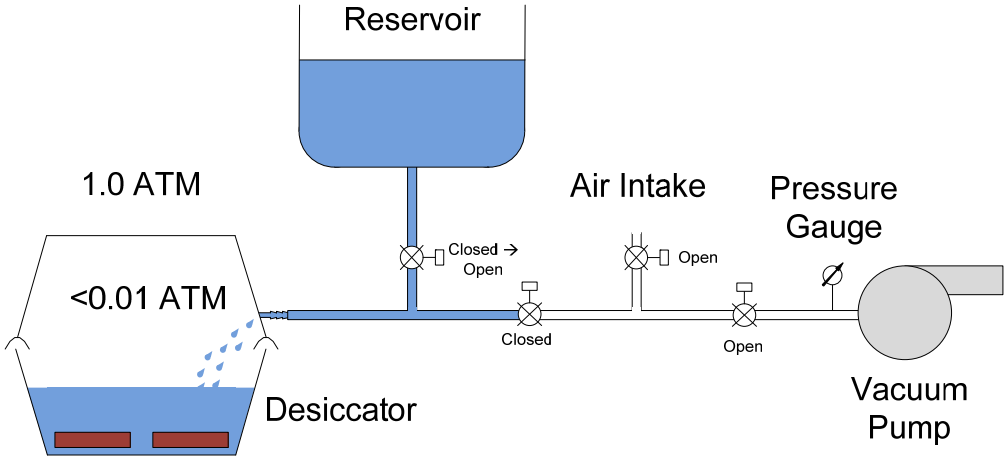

Figure 5-11 Specimens in the desiccator are submersed in distilled water

5) After the bricks are fully immersed, the water source is shut off. The air intake valve is opened purging any remaining water in the hoses and restores the air pressure in the desiccator to atmospheric as shown in Figure 5-12. The specimens are left to soak for at least one hour and then the saturated mass is recorded.

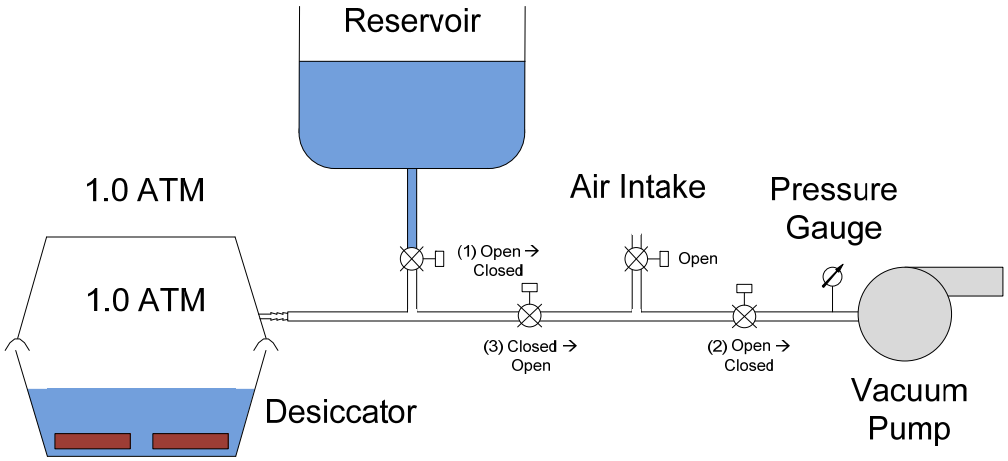

Figure 5-12 Water purged from lines and desiccator pressure returns to atmospheric

5.2.2 Factors Affecting Vacuum Saturation

There are a number of variables in the vacuum saturation procedure that influence the effectiveness of vacuum saturation. One of the most important is the minimum vacuum pressure reached in the desiccator prior to submerging the specimens. The Canada Brick specimens were saturated under vacuum pressures ranging from 0.001 to 0.265 atmospheres. Moisture content appears to vary linearly with vacuum pressure as can be seen in Figure 5-13. It was found that the value of moisture content expressed as a percentage of these specimen's dry mass appears to be linear at pressures less than 0.3 ATM; decreasing by 0.5% for each 0.1 ATM rise above perfect vacuum.

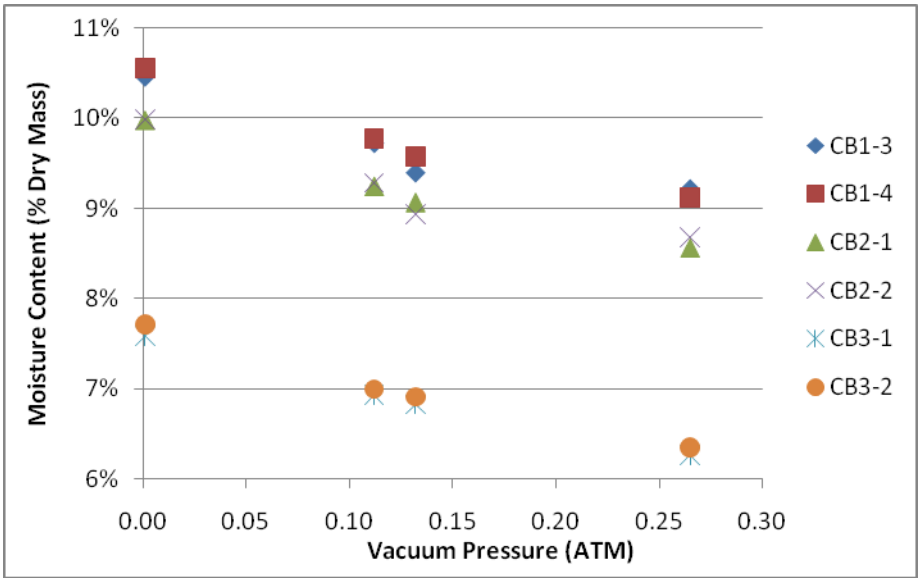

Figure 5-13 Moisture content of brick specimens vary with vacuum pressure

The duration of the soak required once atmospheric pressure has been reintroduced to the desiccator appears to be quite short. It was expected that the soak time required to reach saturation would be quite short. Unlike cold water saturation there should be almost no trapped gases to slowly dissolve out of the material. The ability of water to fully saturate the material would be solely limited by its liquid viscosity. To be conservative the specimens were allowed to soak for an hour. A comparison of the results of vacuum saturated mass of Upper Canada College Brick #8 after soaking for either 1 hour or 15 minutes as is shown in Table 5-3. The average difference in saturated mass of all the specimens comprising the sample was 0.01g,

suggesting that the soak time of 1 hour is far longer than necessary. This should be corroborated by further comparisons of soak durations on brick of varying water uptake coefficients.

Table 5-3 Difference in vacuum saturated mass based on duration of soak

Specimen ID	Dry Mass (g)	1-Hour Soak Saturated Mass (g)	1-Hour Soak H_2O Mass (g)	15-Minute Soak Saturated Mass (g)	15-Minute Soak H_2O Mass (g)	Difference (g)
UC8-1	101.07	120.29	19.22	120.28	19.21	-0.01
UC8-2	96.17	114.31	18.14	114.33	18.16	0.02
UC8-3	96.74	114.93	18.19	114.94	18.2	0.01
UC8-4	90.01	106.83	16.82	106.87	16.86	0.04
UC8-5	88.13	104.63	16.50	104.56	16.43	-0.07
UC8-6	87.08	103.39	16.31	103.41	16.33	0.02
UC8-7	102.27	121.55	19.28	121.52	19.25	-0.03
UC8-8	87.09	103.59	16.50	103.55	16.46	-0.04
UC8-9	90.42	107.48	17.06	107.49	17.07	0.01
UC8-10	86.01	102.16	16.15	102.16	16.15	0.00
UC8-11	89.88	106.67	16.79	106.62	16.74	-0.05
UC8-12	88.67	105.16	16.49	105.15	16.48	-0.01
					Average	**-0.01**

The brick specimens must be completely dry when placed in the desiccator. If specimens come into contact with even small amounts of water prior to lowering the pressure in the vacuum desiccator the water will be absorbed in the pore space and trap some gas in dead end pores. Capillary pressures are frequently higher than the pressure difference between trapped gasses and vacuum, which is at most 0.1MPa.

In Fagerlund's [1979] study, water used to saturate concrete specimens was de-aired so that it contains no dissolved gases. A de-aired water source was not available for this study and distilled water was substituted. The benefit of de-aired water as opposed to other sources was not quantified in any published study reviewed by the author and it could not be quantified in the current study. Nevertheless, given the prevalent use of de-aired water in other studies it may be of importance.

5.3 Comparison of Boiling and Vacuum Saturation

There are differences in the efficacy of boiling and vacuum saturation to determine the saturated moisture content of a material, in the repeatability of their results, and in the variance of specimen moisture contents over a sample. Furthermore, there is a difference in each procedure's equipment requirements and difficulty of performance.

Saturated moisture content of brick as determined by vacuum saturation was found to be always equal to or greater than that of boiling saturation. The moisture content of seven sample bricks used in this study as determined by boiling and vacuum saturation are contained in Table 5-4. The Canada Brick samples absorbed approximately 20% more moisture and the Upper Canada College bricks absorbed approximately 5% more moisture when vacuum saturated compared to boiling. The old Montreal bricks have identical moisture contents irrespective of the method used to saturate. Vacuum saturation appears to be more effective than boiling for materials with low saturation moisture contents. However, the Upper Canada College and Old Montreal bricks have similar saturation moisture contents yet the effect of vacuum saturation over boiling differs markedly between the two sets of brick.

Table 5-4 Sample brick moisture contents using boiling and vacuum saturation

	Moisture Content (% Dry Mass)		
Sample ID	Boil	Vacuum	Difference
CB1	8.68%	10.29%	18.5%
CB2	8.20%	9.87%	20.4%
CB3	6.51%	7.72%	18.6%
UC6	14.92%	15.56%	4.3%
UC8	17.80%	18.89%	6.1%
OM1	14.01%	14.01%	0.0%
OM2	15.25%	15.25%	0.0%

The results of vacuum saturation have greater repeatability than those of boiling saturation. The moisture contents of the six specimens from Canada Brick #3 over three rounds of boiling are

presented in Figure 5-14. The ratio of minimum to maximum value of moisture content of the specimens tested ranged from 0.90 to 0.96.

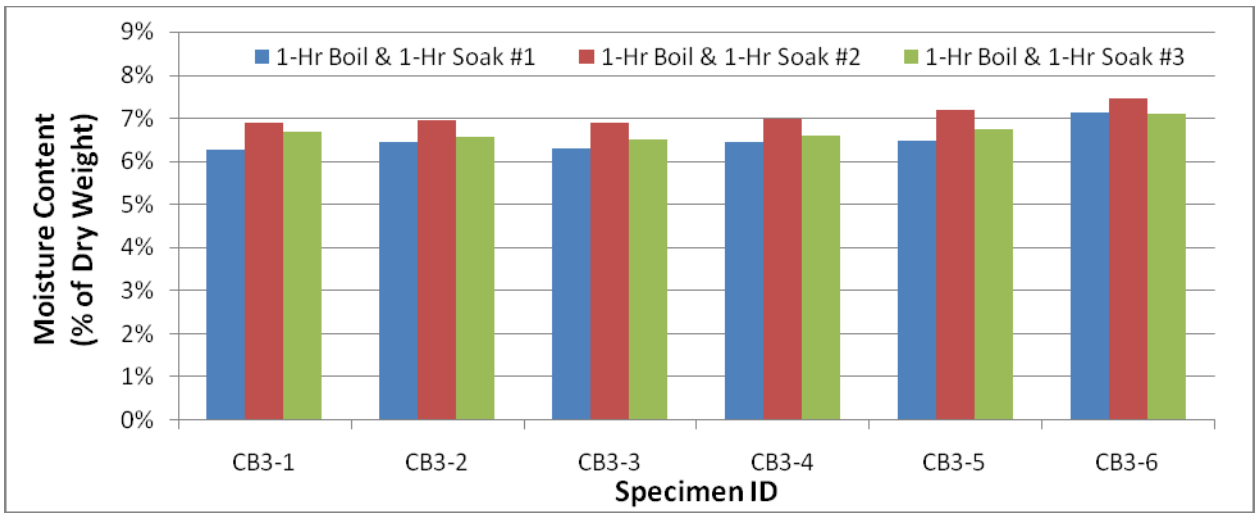

Figure 5-14 Repeatability of boiling saturation test results

The moisture contents of the twelve specimens taken from Upper Canada College brick 8 over three rounds of vacuum saturation are presented in Figure 5-15. The ratio of minimum to maximum value of moisture content of the specimens tested ranged from 0.99 to 1.00.

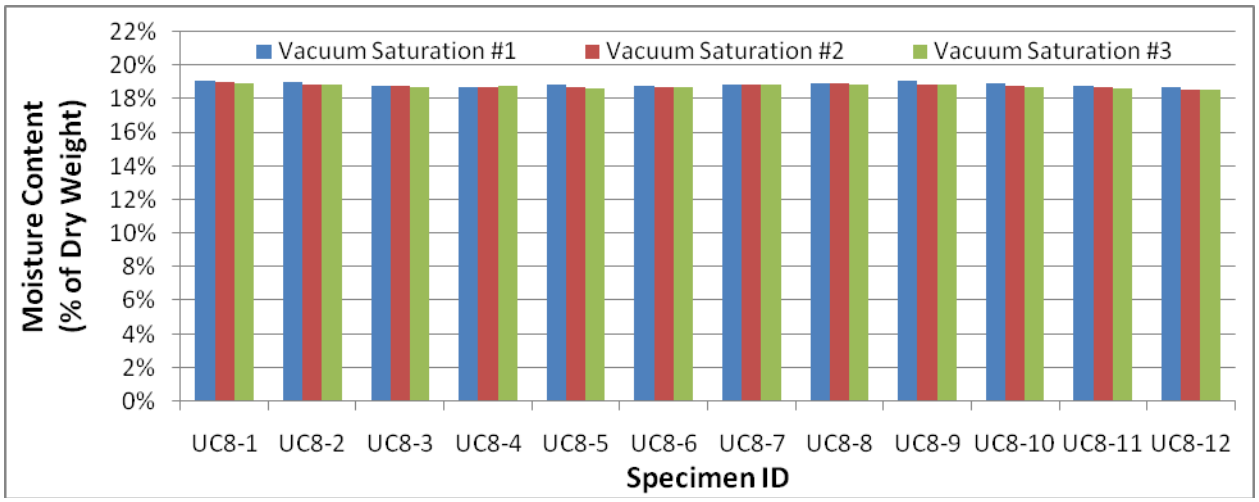

Figure 5-15 Repeatability of vacuum saturation test results

The porosity and saturated moisture content of brick is never completely uniform throughout, hence there will be some variability of these properties in the specimens taken from a brick. It is desirable to minimize the measured variability of the specimen moisture contents so that outliers

will not disproportionately affect a sample's mean moisture content. The variability of specimen moisture contents within a sample tends to be less when using vacuum saturation as compared to boiling saturation. This was quantified by comparing the standard deviation and ratio of maximum to minimum moisture content of each sample's set of specimens using vacuum and boiling saturation (Table 5-5).

Table 5-5 Variability of sample bricks' moisture content

Sample ID	Standard Deviation of Specimen Moisture Content (% Dry Mass)		Ratio Min:Max of Specimen Moisture Content	
	Boil	Vacuum	Boil	Vacuum
CB1	0.29%	0.21%	0.92	0.95
CB2	0.31%	0.10%	0.91	0.98
CB3	0.31%	0.26%	0.88	0.91
UC6	0.12%	0.14%	0.98	0.98
UC8	0.12%	0.13%	0.98	0.98
OM1	0.14%	0.14%	0.97	0.96
OM2	0.29%	0.29%	0.95	0.94

There is less variability in the specimen moisture contents of the Canada Brick samples when using vacuum saturation than boiling saturation while the Upper Canada College and Old Montreal brick samples have essentially the same degree of variability in their specimen moisture contents irrespective of saturation technique. Similar to average sample moisture content, the effect of vacuum saturation on reducing the variability when measuring specimen moisture contents is more pronounced for brick with low porosity.

5.4 Summary

Calculating the degree of saturation of a material requires the knowledge of the total open porosity of the material. The simplest method of determining total open porosity is a liquid, gravimetric approach which necessitates that one be capable of fully saturating the pore space with water. Boiling and vacuum saturation are commonly used to fill most of the pore space of a material with water by minimizing the volume of gas trapped in dead-end pore spaces by advancing wetting fronts.

The boil method is a two-part process in which trapped gasses are flushed out of pores by steam generated during the boil phase and then when specimens are subsequently cooled, water is sucked into the pore space as pockets of steam collapse. In order to saturate specimens of similar dimension to that used in the proposed test method, it is only necessary to boil the specimen for one hour followed by soaking for one hour.

Vacuum saturation works by evacuating almost all gasses from the material prior to submersion in water. Vacuum saturation is heavily dependent on achieving a low vacuum. It appears that for every 0.1 ATM increase above perfect vacuum the moisture content drops by approximately 0.5% of the dry mass of the specimen. This indicates a vacuum pressure of less than 0.01 ATM is adequate for consistent estimates of saturated moisture content using vacuum saturation.

Vacuum saturation is equal or superior to boiling saturation in estimating the saturated moisture content of brick and reduces the variability within a sample. Furthermore, it always offers superior repeatability in multiple measurements of saturated moisture content. It appears the sole advantage of boiling saturation is that both the equipment requirements and complexity of the procedure are simple enough that it can be carried out in any modestly equipped laboratory requiring only a minimal amount of employee training. Additionally, it does provide data that is of almost equal accuracy to that of vacuum saturation for some brick with high porosity.

ASTM or CSA standards for vacuum saturation could not be located and a method for vacuum saturation was developed based on the experience of others. Further research should be undertaken into the effect of vacuum pressure, soak duration and use of de-aired water on saturated moisture content of brick using vacuum saturation.

Chapter 6

Moisture Storage and Distribution in Brick

Assessing the degree of saturation at which freeze-thaw damage occurs (S_{crit}) by using the proposed test procedure requires the ability to wet brick specimens to precise target moisture contents. In addition to achieving the target moisture content, the brick specimens must stay at or close to this target moisture content for the duration of freeze-thaw cycling. Finally, the moisture added to a specimen must be uniformly distributed throughout the specimen so that the moisture content at any one part of the specimen is consistent throughout the entire specimen. Ensuring that these three requirements can be met and were met during the testing reported here is the subject of this chapter.

6.1 Wetting Brick Specimens

There are two methods that allow one to wet brick specimens to precise moisture contents. The simplest method is to simply deposit water on the surface of the specimen and allow it to be absorbed by capillary suction. This method is most useful for wetting specimens that have a high water uptake coefficient to low moisture contents.

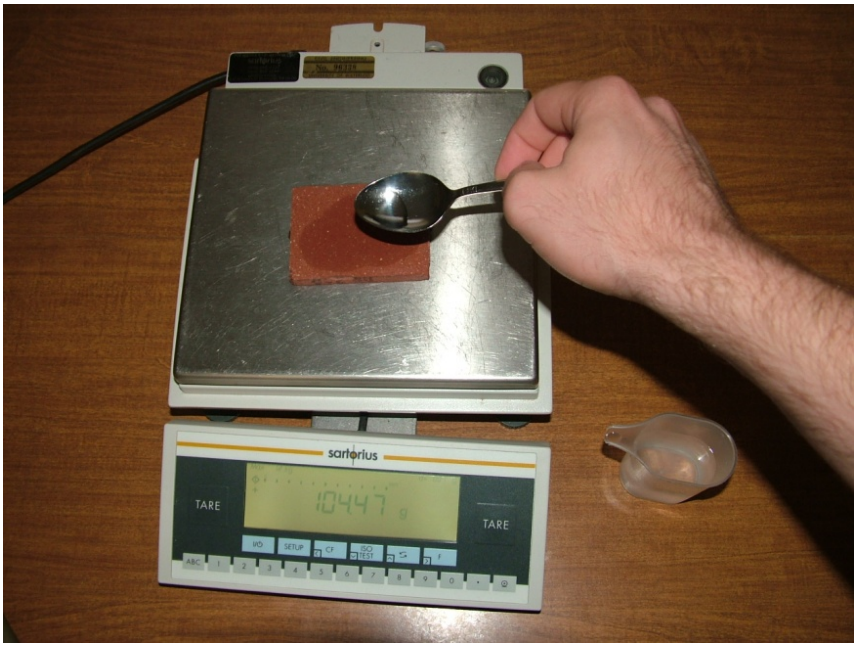

Figure 6-1 Surface wetting of a brick specimen

Water uptake curves are useful to estimate the greatest moisture content a specimen can absorb by surface deposition. For example, if one examines the water uptake curve of Canada Brick 2-4 in Figure 4-6, one would see it can absorb approximately 7g of water, and from initial testing its 1-hour boil moisture uptake was determined to be approximately 10g. It follows that surface wetting can be used to reach moisture contents less than 70% of boil porosity.

The other approach is to saturate the specimen by either boiling or under a vacuum and then dry it down to the desired moisture content. This method should be used when wetting the specimen to high moisture contents, typically greater than 60%.

Figure 6-2 Drying a saturated specimen to a target moisture content

The actual moisture contents reached by using these two methods are very close to the initial target moisture contents. Table 6-1 presents the average difference between actual moisture contents and target moisture contents for the Upper Canada College and Old Montreal bricks that were tested in this study, the data this table is based on is found in Appendix C.

Table 6-1 Difference between target and actual moisture contents

Sample ID	Average $\lvert M_{target}-M_{actual}\rvert$ |g|	$\lvert M_{target}-M_{actual}\rvert / (M_{target}-M_{dry})$ (%)
OM1	0.03	0.3%
OM2	0.02	0.3%
UC6	0.02	0.6%
UC8	0.02	0.4%
Overall	0.02	0.4%

The average difference between the actual moisture contents and the target moisture contents is typically 0.02 grams and in relative terms the actual moisture content of most specimens differed from the target moisture content by 0.4%. One can conclude that a close correlation between actual and target moisture contents is achievable.

6.2 Moisture Retention

Once the specimens have been wet to the desired moisture content, they must be sealed with a vapour impermeable material to retain the moisture over the course of freeze-thaw cycling. The specimens should be sealed, air tight with a vapour impermeable material. For this study the specimens were initially wrapped with cellophane and then double sealed tight with a plastic tape as demonstrated in Figure 6-3.

The specimens were weighed in their wet and wrapped condition prior to and after freeze-thaw cycling. There was at least a three day time lapse between initial and final weighing of each specimen. Table 6-2 presents the average difference between initial and final wet and wrapped mass of specimens taken from the Upper Canada College and the Old Montreal set. The raw data this table is based on is found in Appendix C.

Figure 6-3 Sealing a brick specimen

The mass of the wrapped samples was essentially unchanged between measurements, indicating that no moisture escaped the wrapped samples during freeze-thaw testing. Once the wrapping was removed, there is a slight decrease in mass of the wetted samples of 0.05g or more. This negligible difference in mass is due to water vapour diffusing out of the specimen and condensing on the wrapping. The moisture content of the specimens at the completion of the freeze-thaw testing is typically less than half a percent lower than the target moisture content in terms of boiling porosity. Moisture retention of sealed specimens was deemed adequate for the purposes of the proposed freeze-thaw test.

Table 6-2 Moisture retention in Old Montreal & Upper Canada brick samples

Sample ID	Avg ΔM_{wrap} (g)	Avg ΔM_{wet} (g)	ΔMC (%)
OM1	0.02	-0.05	-0.3%
OM2	-0.02	-0.09	-0.5%
UC6	-0.01	-0.05	-0.2%
UC8	-0.02	-0.07	-0.4%
Overall	-0.01	-0.06	-0.4%

6.3 Moisture Redistribution

After the specimens have been wetted and sealed, they must be allowed to sit for a period of time to allow the moisture to distribute itself evenly throughout the pore space. The purpose is to ensure that the moisture content at any one part of a specimen is equal to the moisture content of all other parts of the specimen. If a specimen is subjected to freeze-thaw cycling with localized pockets of elevated moisture content, it may display evidence of freeze-thaw damage that shouldn't have occurred had the additional moisture been allowed to distribute itself evenly.

No simple test exists to determine how long it takes for moisture to evenly redistribute throughout a material. Hygrothermal computer models, such as WUFI [Künzel 1995], offer a reliable means to estimate moisture redistribution times. To assess the time for uniform moisture redistribution in the small brick samples used in this research project, a WUFI study was undertaken.

The material properties of a brick required for modelling moisture transport with WUFI are porosity (m^3/m^3) and A-value ($kg/m^2s^{½}$) [Water Absorption Coefficient]. The material properties of the bricks modelled for this study are listed in Table 6-3.

Table 6-3 Material properties of brick modelled in WUFI

Specimen ID	A-Value ($kg/m^2s^{½}$)	Dry Density (kg/m^3)	$Porosity_{vacuum}$ (m^3/m^3)
OM1	0.293	2021	0.285
OM2	0.323	1986	0.307
CB1	0.032	2212	0.228
CB2	0.028	2223	0.219
CB3	0.005	2249	0.172
UC6	0.220	1957	0.394
UC8	0.257	1950	0.364

Based on this small data set, by plotting A-value on a logarithmic scale against porosity in Figure 6-4, an empirical expression can be developed relating A-value to porosity:

$$A = 0.0006e^{17.47P} \quad (6\text{-}1)$$

where:

A = water uptake coefficient [kg/m^{2}s^{½}]
P = porosity [m^3/m^3]

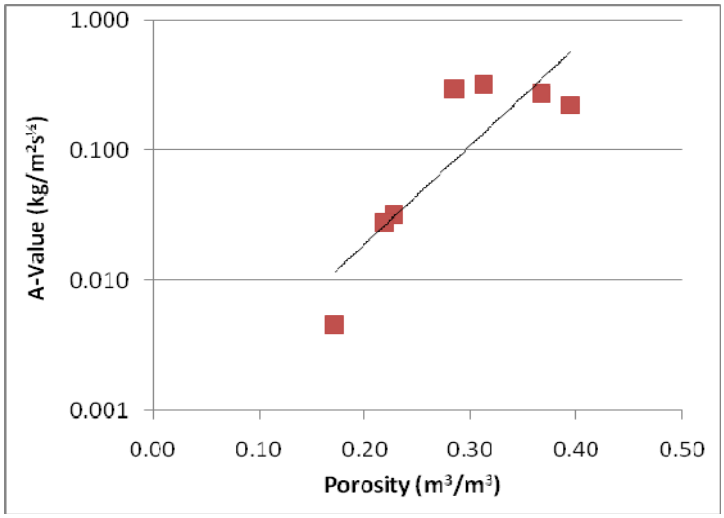

Figure 6-4 A-Value and porosity of brick

6.3.1 Creating a WUFI Model

Parameters which affect redistribution times are specimen length, degree of saturation, A-value, and porosity. Each is accounted for in the WUFI model. The thickness and degree of saturation were modelled by splitting the brick into two parts: saturated and dry. The length of the saturated part is equal to the total length multiplied by the degree of saturation. For example, to model a 10 mm thick specimen with a degree of saturation of 0.2, the length of the saturated material would be 2 mm, and the length of the dry portion is equal to the remainder, in this case 8 mm. A vapour impermeable layer must be added at each end, such as thick polyethylene, to ensure there is no vapour diffusion out of the brick (this models the wrapping actually used) as shown in Figure 6-5.

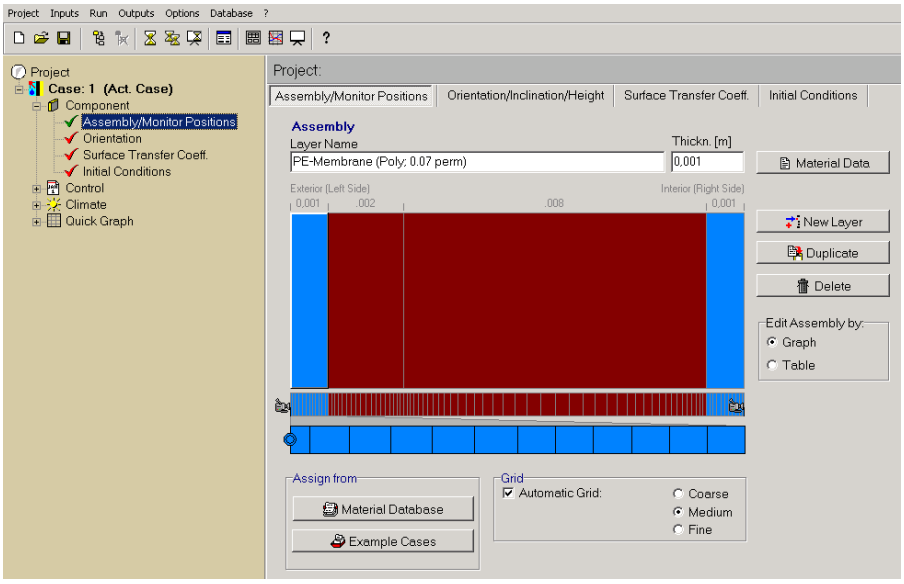

Figure 6-5 WUFI material configuration

Material properties of the brick to be modelled are entered in the material data table. For this study, the generic brick material data table was modified to include the dry density, A-value and porosity of each brick as in Figure 6-6. Free water saturation is equal to porosity multiplied by bulk density of water, approximated as 1000 kg/m^3.

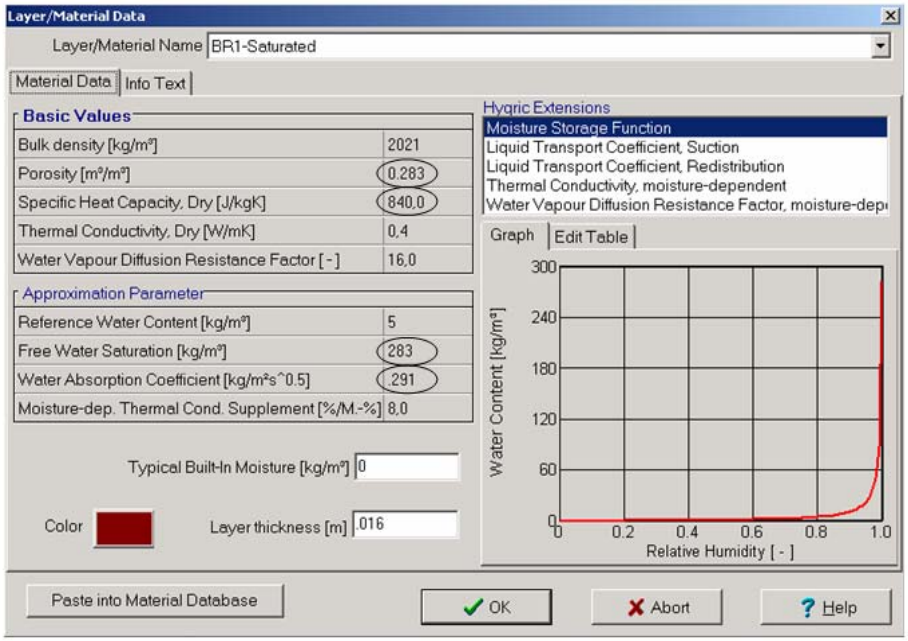

Figure 6-6 Modified material data table

The initial water content in the saturated portion of the brick must be set equal to free water saturation, that is, the entire porosity is filled with water. The initial water content in the dry portion of the brick is always 0 (Figure 6-7).

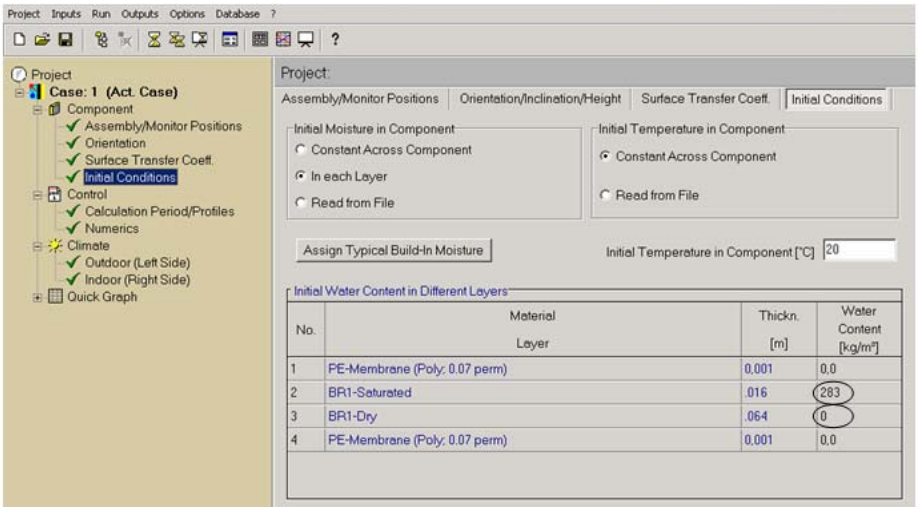

Figure 6-7 Initial water content

Lastly, the indoor and outdoor climate should be set equal to a constant temperature and humidity typifying indoor conditions. In this study, the temperature was set to 20°C and the humidity set to 50%RH for all models (Figure 6-8).

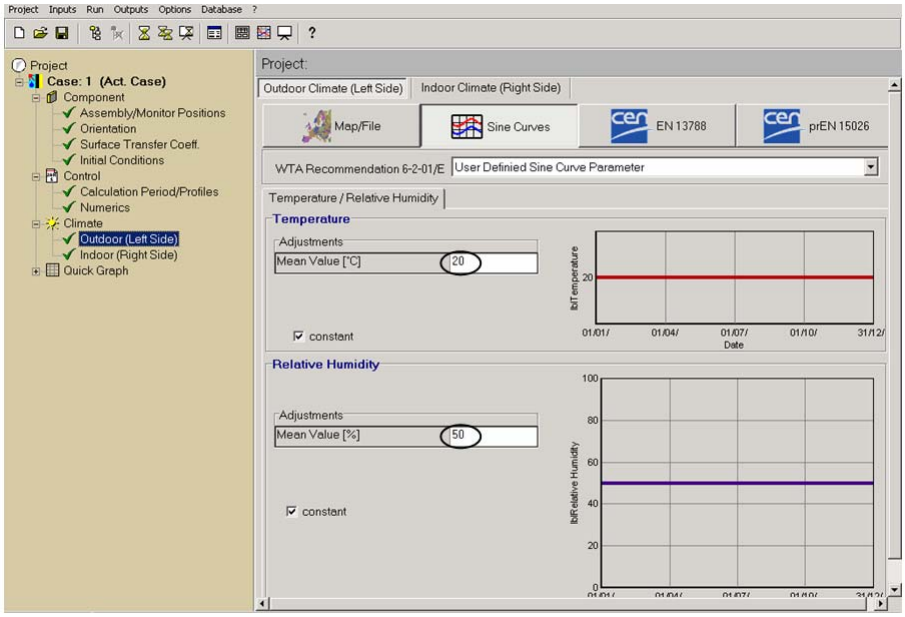

Figure 6-8 Constant indoor temperature and humidity

6.3.2 Modelled Redistribution Times

With all modelling, the boundary conditions dictate whether the model will accurately predict actual behaviour. The WUFI model should reflect how the brick is actually wet. With surface applied wetting, moisture must distribute through both the thickness and across the face of the specimen as shown in Figure 6-9.

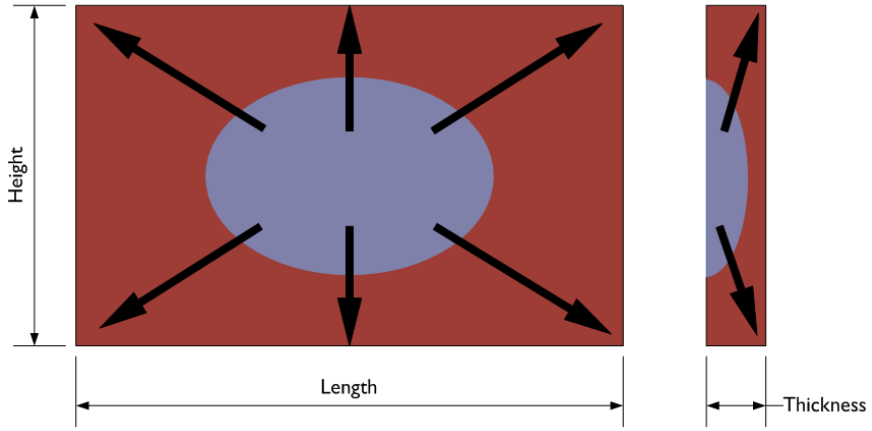

Figure 6-9 Moisture distribution: surface wetting

When wetting by saturating a specimen and then drying it down to the desired degree of saturation, moisture only needs to be redistributed through the thickness of the specimen, illustrated in Figure 6-10.

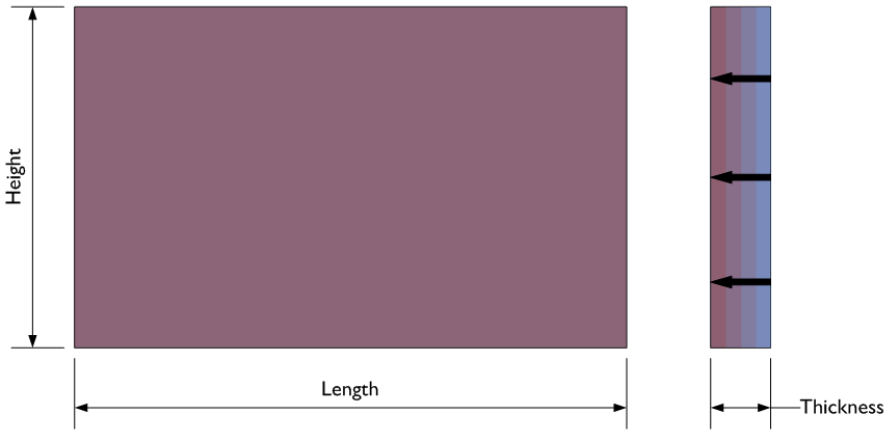

Figure 6-10 Moisture distribution: drying saturated brick

The redistribution times of all bricks used in this study were modelled across both their thickness, 10mm, and across an idealized length, 80mm, at incremental degrees of saturation. Redistribution rate slows asymptotically as the moisture content of each portion of the material reaches equilibrium. The redistribution time was decided to be set equal to the length of time required to reach 97.5% of the equilibrium moisture content in the dry portion of the brick, demonstrated in Figure 6-11. The results of all these simulations are presented in Table 6-4 on the following page.

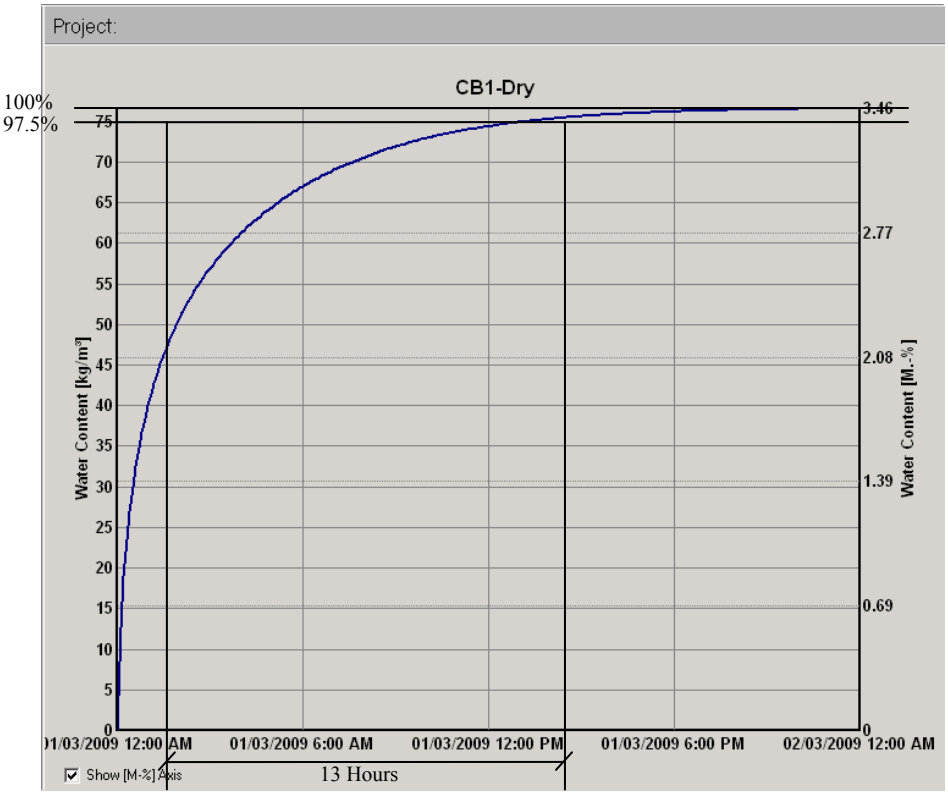

Figure 6-11 Estimating redistribution times

The redistribution times based on the material thickness closely reflects the process of wetting by saturation drying and should be a fair approximation of surface wetting times if care is taken to deposit the moisture evenly across the face of the material. The length distribution was included to model the greatest possible redistribution time. The time required to redistribute across the

length of a specimen is of significantly greater duration than that required to distribute across a specimen's thickness for the specimens recommended in this study.

Table 6-4 Estimated moisture redistribution times

		Moisture Redistribution Time (Hours) Degree of Saturation								
	Specimen ID	10%	20%	30%	40%	50%	60%	70%	80%	90%
Specimen Thickness (10 mm)	OM1	-	1.0	-	0.6	-	0.25	-	0.15	-
	OM2	-	1.0	-	0.55	-	0.25	-	0.15	-
	CB1	-	19	-	12	-	5	-	2	-
	CB2	-	21	-	13	-	6	-	2	-
	CB3	15	52	85	104	118	111	74	56	26
	UC6	-	1.7	-	0.9	-	0.4	-	0.2	-
	UC8	-	1.5	-	0.85	-	0.4	-	0.2	-
Specimen Length (80 mm)	OM1	-	40	-	21	-	8	-	3.5	-
	OM2	-	39	-	21	-	8	-	3.5	-
	CB1	-	984	-	720	-	384	-	132	-
	CB2	-	1008	-	744	-	384	-	132	-
	CB3	672	2304	3683	4761	5678	5329	3816	2592	1135
	UC6	-	72	-	36	-	18	-	7	-
	UC8	-	70	-	37	-	18.5	-	7.5	-

The A-value has a large effect on distribution times, but it also limits how much moisture can be absorbed by surface wetting. Based on water uptake data (see Appendices B and C), after 10 minutes of surface contact the degree of saturation of Canada Brick #3 was 0.1, of Canada Bricks #1 & #2 was 0.4, and of the Old Montreal and Upper Canada Bricks was 0.7. Therefore, drying from saturation, represented by the thickness distribution, is the only way to wet Canada Brick 3 which has the longest redistribution time of 118 hours, or 5 days, at a degree of saturation equal to 0.5. For the other bricks, a 24-hour period to allow redistribution appears to be adequate.

6.3.3 Implications of the WUFI Model

The length of the specimen has a large impact on redistribution time. For the specimens modelled, the length (80mm) was 8 times greater than the thickness (10mm) but it took on average 45 times longer for the moisture to be redistributed over the length than the thickness. As displayed in Figures 6-12 and 6-13, the shape of the curves relating redistribution time and

degree of saturation are similar. Assuming that material length and redistribution time are related geometrically, an empirical formula relating the two parameters was developed:

$$\frac{T_2}{T_1} = \left(\frac{L_2}{L_1}\right)^{1.85} \tag{6-2}$$

where:

T_1 = Modelled Redistribution Time [Hour]
T_2 = Adjusted Redistribution Time [Hour]
L_1 = Modelled Length of Specimen [mm]
L_2 = Adjusted Length of Specimen [mm]

This relationship should be validated by further modelling as it is based on only two data sets, but if true, it would allow redistribution times to be estimated for any material length after an initial curve has been created.

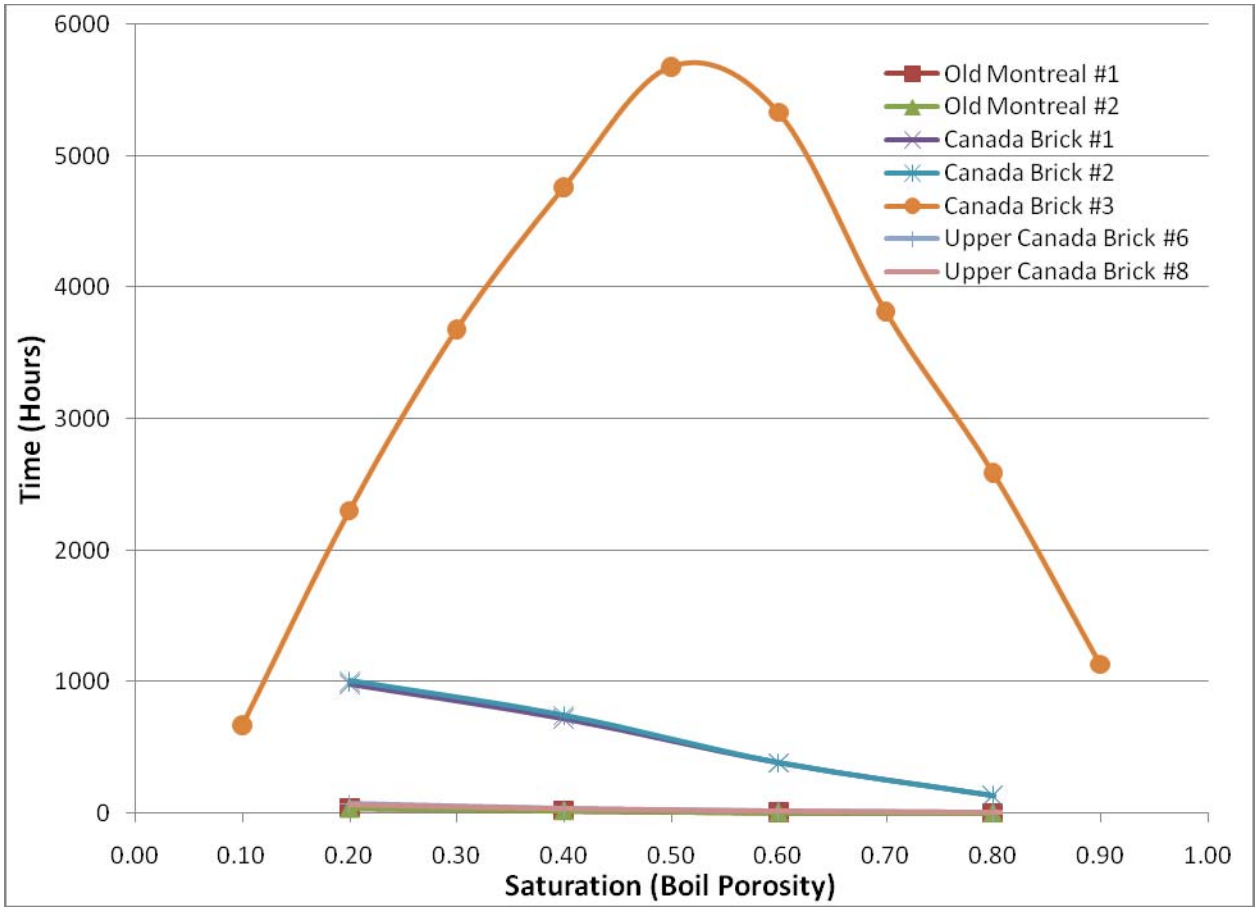

Figure 6-12 Moisture redistribution curve: specimen length of 80mm

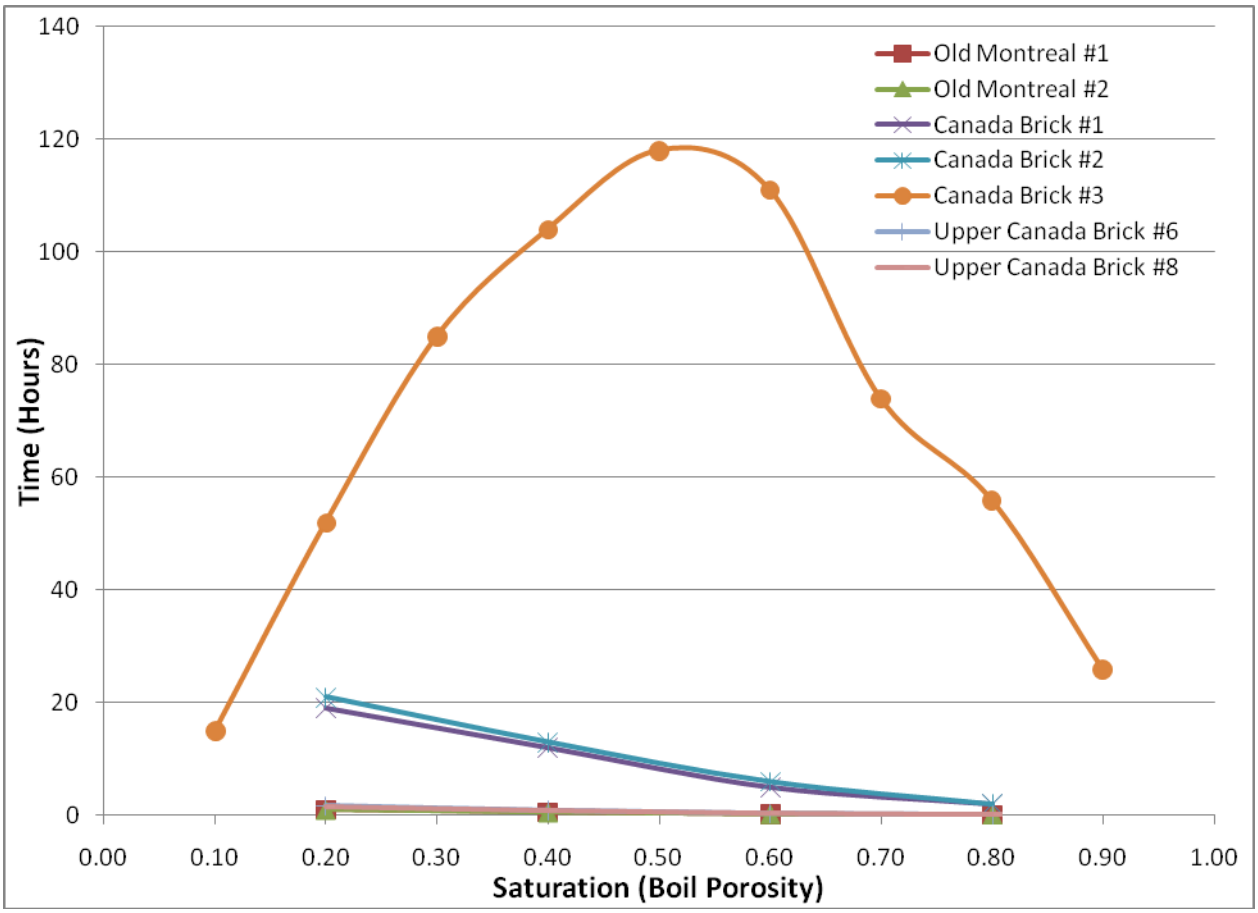

Figure 6-13 Moisture redistribution curve: specimen length of 10mm

The bell shaped curve is common to all materials, as the A-value increases the maximum point of the curve is located at a lower degree of saturation (Figure 6-14). The upward slope of the curve is due to the fact that at low degrees of saturation, vapour diffusion is the primary mode of moisture transport. Diffusion slows as the degree of saturation increases and the pores become increasingly blocked to diffusion as they fill with liquid water. The subsequent decreasing slope is caused by increased capillary transport, which becomes the primary mode of moisture redistribution.

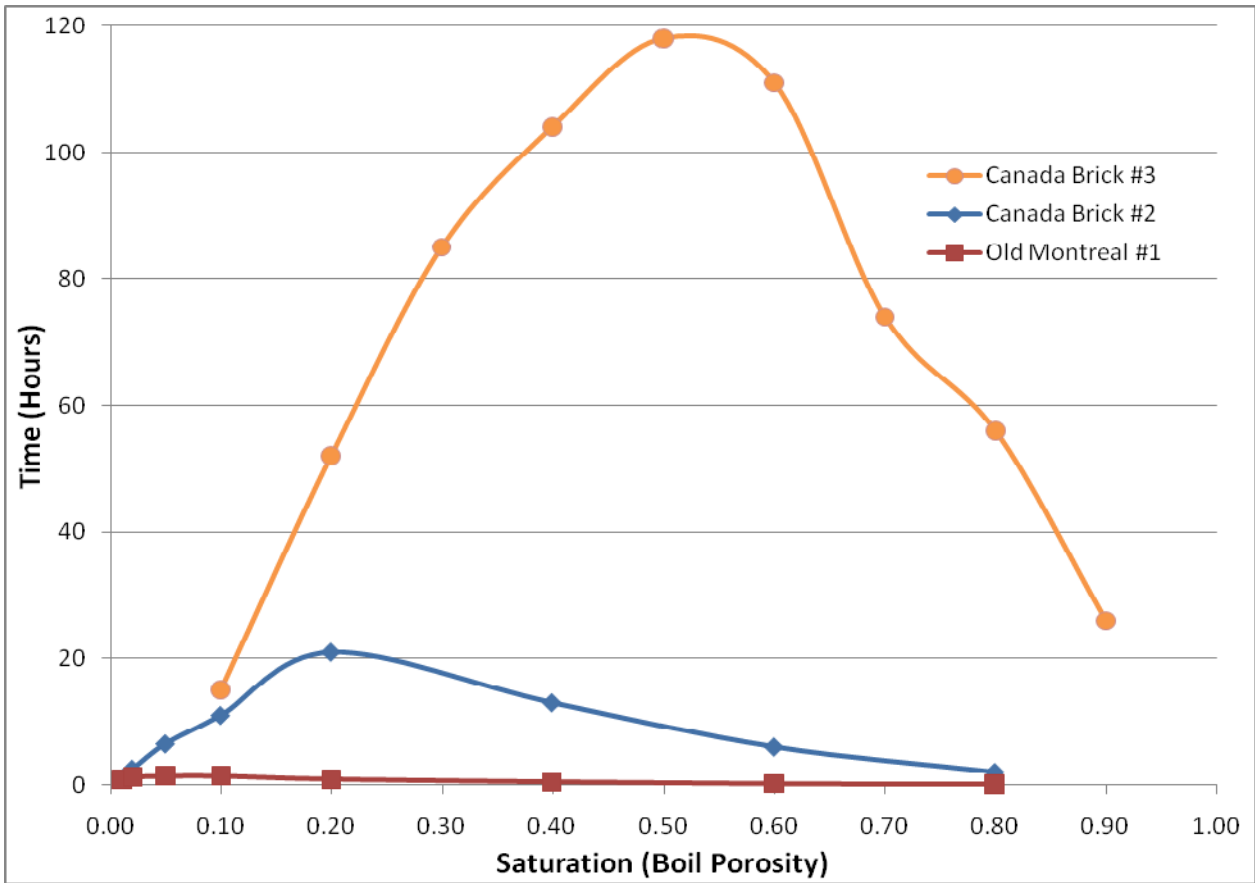

Figure 6-14 Moisture redistribution curve is bell-shaped for all specimens

Porosity and A-value were isolated to determine their effect on the WUFI model. If density, moisture content and A-value are held constant, redistribution appears to be a polynomial function of porosity (Figure 6-15). However, when porosity is held constant, A-value and redistribution time are related by a power-law relationship (Figure 6-16).

This serves to underscore that A-value has a greater and opposite effect on redistribution times than porosity. When combined with the data that suggests A-value increases exponentially with porosity, then as porosity and A-value increase, the effect of the A-value on lowering redistribution times will outweigh the effect of porosity in increasing it.

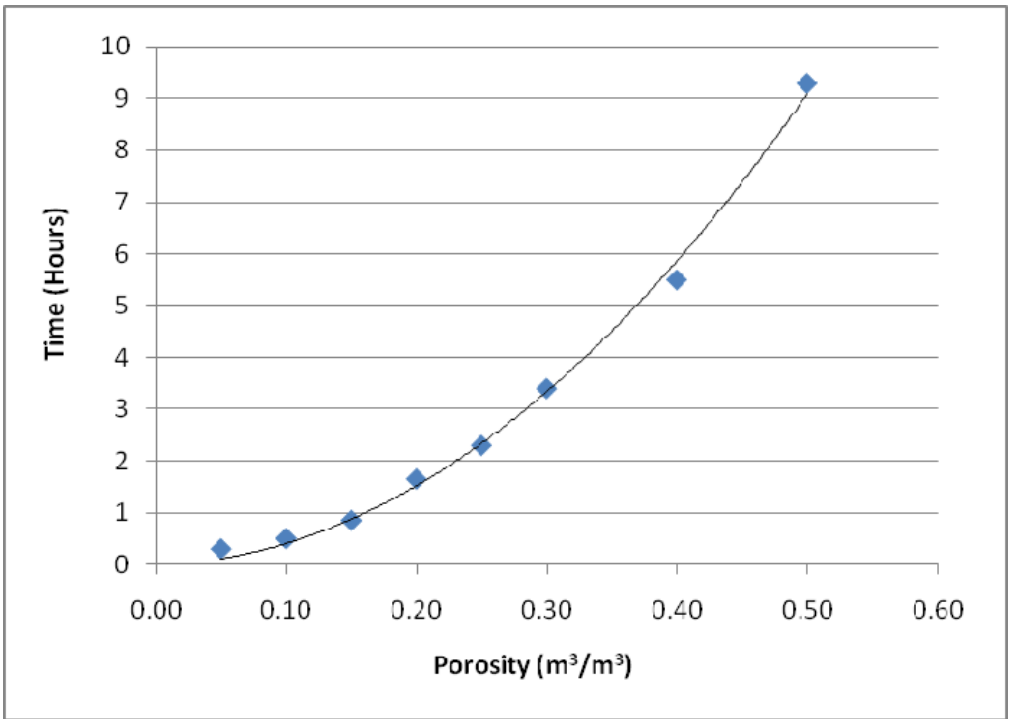

Figure 6-15 Effect of porosity on moisture redistribution

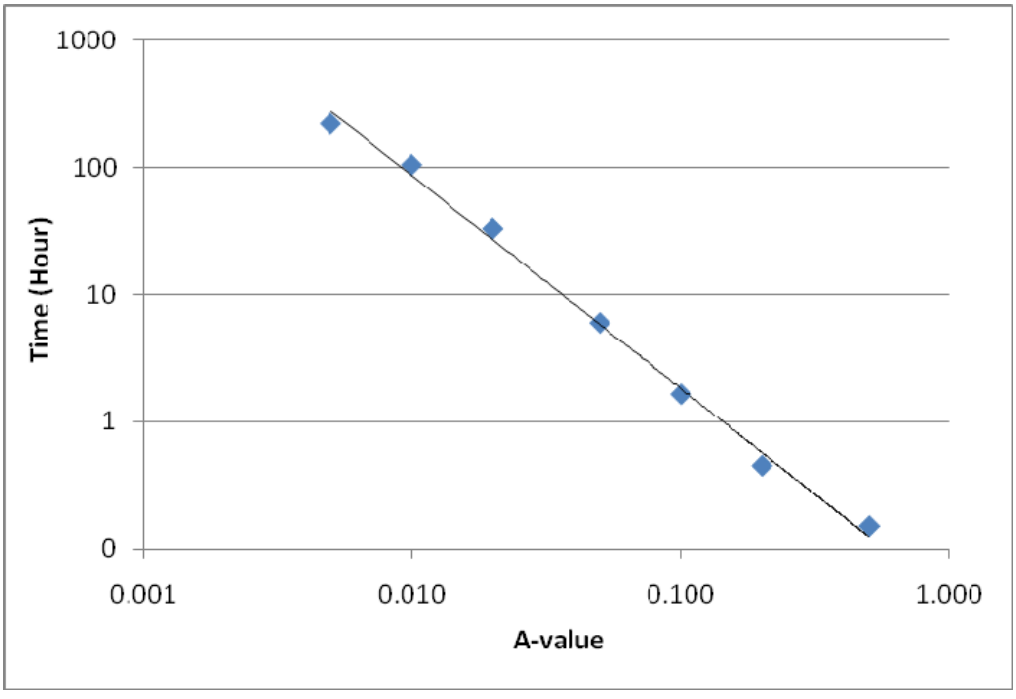

Figure 6-16 Effect of A-value on moisture redistribution

6.4 Summary

Given the small specimen sizes used in this study, wetting to target moisture contents was achieved with a high degree of accuracy, typically within 0.02 g, by either depositing water on the surface of the specimen and allowing it to be absorbed through capillary suction or by fully saturating the specimen and then drying it down to the desired moisture content. When sealed with cellophane and wrapped in plastic tape it was found that a specimen's moisture content was stable, typically only decreasing by 0.06 g.

Upon sealing the specimens, a length of time should be allowed to pass before freezing to allow the moisture added to the specimen to evenly distribute itself throughout the pore space of the material. Specimens with a large length to thickness ratio allow rapid and uniform redistribution of moisture. Based on WUFI simulations for each brick used in this study, it appears that redistribution occurs within 24 hours for most brick. Redistribution in bricks with a low A-value, such as Canada Brick #3 at 0.005 $kg/m^2s^{½}$, may take up to 72 hours.

There were several interesting relationships between material properties and redistribution times. It was found that the time required for water to evenly distribute throughout a specimen increases as porosity rises or A-value decreases. However, A-value appears to be related to porosity exponentially so that the effect of porosity on moisture redistribution is dwarfed by that of A-value.

Chapter 7
Frost Dilation of Brick

The parameters chosen for the freeze-thaw cycle used in this study are discussed in this chapter and include the temperature extremes of the cycle, the freezing rate, and the number of cycles. Strain measurements, used to determine if frost damage occurred in a specimen, were completed using a digital outside micrometer. The results of the freeze-thaw testing, presented for each set of brick samples, confirms that there is a S_{crit} value for the clay bricks tested and that it can occur over a wide range of values for different brick.

7.1 Freeze-Thaw Cycling Parameters

Freeze-thaw cycling is defined by its minimum and maximum temperature, rate of temperature change, the duration of time that specimens are held at minimum & maximum temperatures, and the number of cycles.

The minimum temperature of the cycle must be low enough to freeze the majority of capillary bound water (refer back to Figure 3-2). Capillary radius and freezing point depression are related by the Kelvin Equation (Equation 3-2). Pore size distributions of brick taken from previous studies [Maage 1984, Pentalla 2002] indicate that most capillaries and pores in brick have diameters greater than 0.016μm (Figure 7-1) which using the Kelvin Equation corresponds to a minimum freezing temperature of 258K or -15°C.

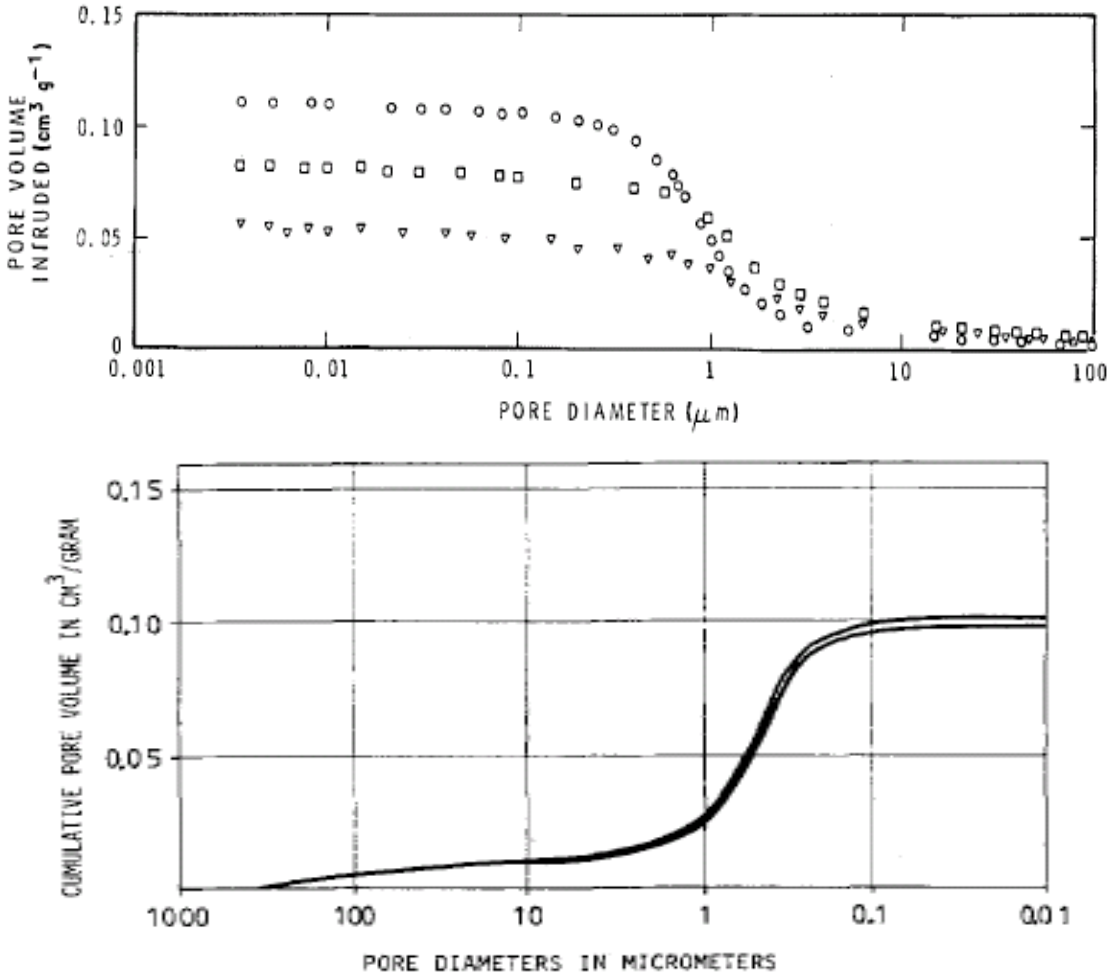

Figure 7-1 Pore size distributions of clay brick [Maage 1984, Pentalla 2002]

The maximum temperature of the freeze thaw cycle simply needs to be above 0°C. However, the length of time it takes for the specimen to thaw will decrease as the maximum temperature is increased. Hence, warming to a temperature of 15 or 20°C is a reasonable and convenient maximum target.

Additionally, it is desirable and often practical to expose the specimen to the minimum and maximum temperature for a period of time to ensure that the entire specimen reaches a uniform temperature. Although further research is needed, an hour seems appropriate for the specimen shapes and sizes used here based on computer simulations (Figure 7-4). Larger samples will require more time.

Freezing rate only appears to effect whether frost damage occurs but does not appear to affect the value of S_{crit} (see discussion of Fagerlund's experiments with concrete in section 3.3.2 page 29). A freezing rate must be selected that is large enough to damage the material. Freezing rates much higher than natural exposure, which in south-western Ontario is at most -5°C/hour [Straube 1998], may create failure mechanisms not possible in the field. A freezing rate of -17.5°C/hour was chosen as an expedient compromise between testing speed and real life cooling rates.

Expansion due to frost damage will occur after exposure to an initial freeze-thaw cycle but is cumulative over multiple cycles. Therefore, it may be easier to measure the change in strain after a number of freeze-thaw cycles have occurred. The specimens were subject to six freeze-thaw cycles between length measurements, following Fagerlund's precedent. It may prove useful to increase the number of cycles a specimen is exposed to, prior to measuring length, so that it experiences strain, when damage occurs, far beyond that which could be attributed to instrument error.

In this study, specimens were subjected to freeze-thaw cycles by sealing and submersing them in a programmable temperature controlled refrigerating circulator manufactured by VWR filled with a half ethylene-glycol, half water mixture, (Figure 7-3). The minimum and maximum temperatures of the cycles were -15°C and 20°C. The rate of freezing was -17.5°C/hour. The specimens were held at the maximum and minimum temperatures for one hour. The temperature gradient of one freeze thaw cycle is displayed in Figure 7-2.

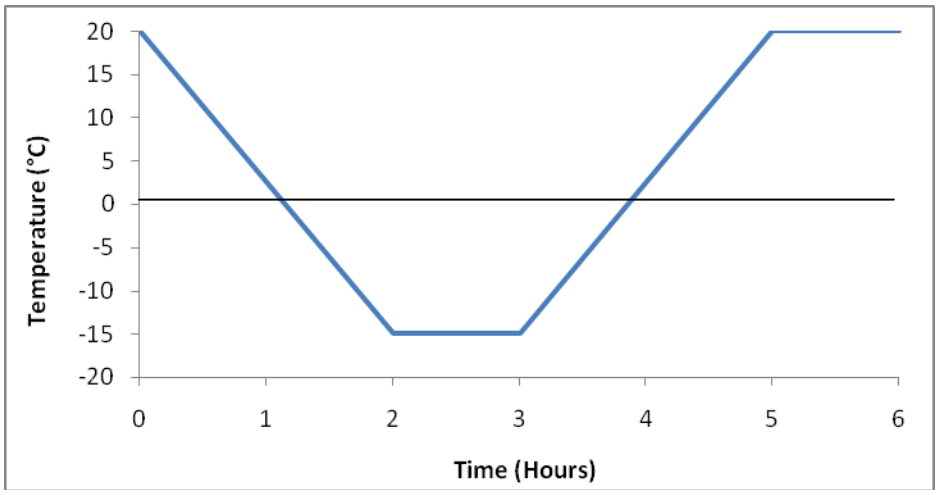

Figure 7-2 Temperature profile of a single freeze-thaw cycle

Figure 7-3 VWR refrigerating circulator with programmable temperature controller

Commercial or residential freezers can be used for freeze-thaw cycling. Specimens can be frozen by being placing in a freezer and then thawed at room temperature by removing them. Most standard freezers have a minimum temperature of about -18°C ensuring that most capillary held water will freeze. The rate of freezing will be beyond the control of the user as it is in current ASTM and CSA standards. A WUFI simulation of a 10mm thick slice of completely saturated

brick at an initial temperature of 20°C, exposed to an air temperature of -18°C was created to model this approach to freezing a specimen. It was found that the specimen reached a temperature of -18°C after approximately 2 hours of exposure, Figure 7-4. The chilled water bath used in the results reported here will cause the brick samples to cool down more quickly, and as it is automated, the need to physically move specimens back and forth between a freezer and a thawing space is eliminated.

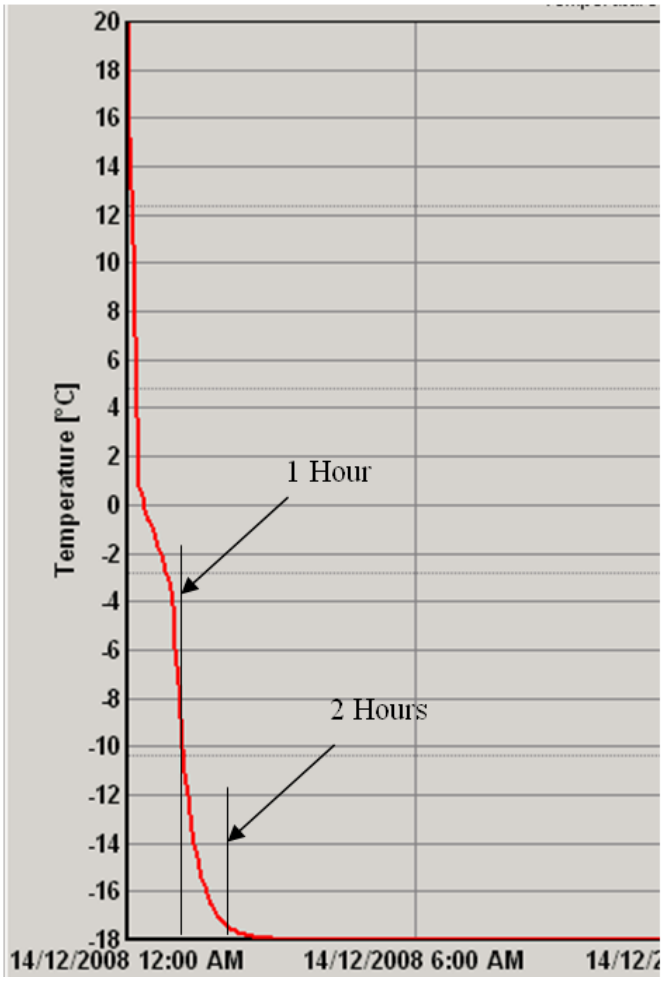

Figure 7-4 WUFI generated temperature profile of a specimen placed in typical freezer

7.2 Freeze-Thaw Dilation of Brick

Several rounds of freeze-thaw cycling were carried out on each set of brick to determine its S_{crit}. In the initial round of freezing, specimens from a brick were wet over a wide range of saturation

values to provide a rough estimate of S_{crit}. A second and possibly third round of freeze-thaw cycling on remaining undamaged specimens was subsequently undertaken to more precisely identify the value of S_{crit}. Brick specimens that were not damaged in the initial round of freeze-thaw testing were reused in later rounds however, once a specimen experienced dilation it was disqualified for use in any future testing.

The temperature of specimens undergoing freeze-thaw cycling was never directly measured. Based on WUFI simulations, such as the one above, and given the small volume of the specimens used, a three hour freezing phase was considered adequate to ensure that the temperature of the specimens reached the minimum of -15°C necessary to freeze of the majority of capillary held water.

The occurrence of frost damage in a specimen following exposure to freeze-thaw cycles is ascertained by measuring permanent expansion in microstrain (see Equation 4-5). Given that the measurements by the micrometer were accurate to within ±0.005mm, only expansion greater than 100 microstrain (equivalent to approximately 0.01 mm) was considered indicative of frost damage.

The proposed method was used to determine the critical degree of saturation for three sets of brick. The dilation experienced by specimens at various degrees of saturation, based on the vacuum method, is plotted for each set of brick in Figures 7-5 to 7-7 (based on the measured data contained in Appendices B and C).

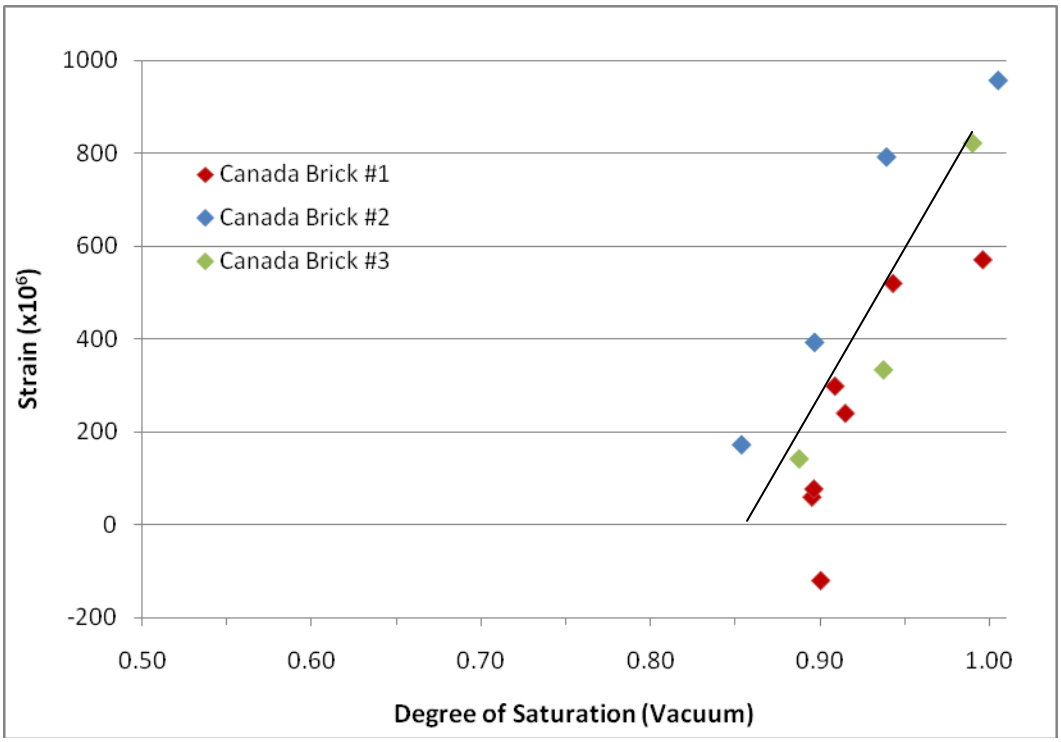

Figure 7-5 Frost dilatometry: Canada Brick

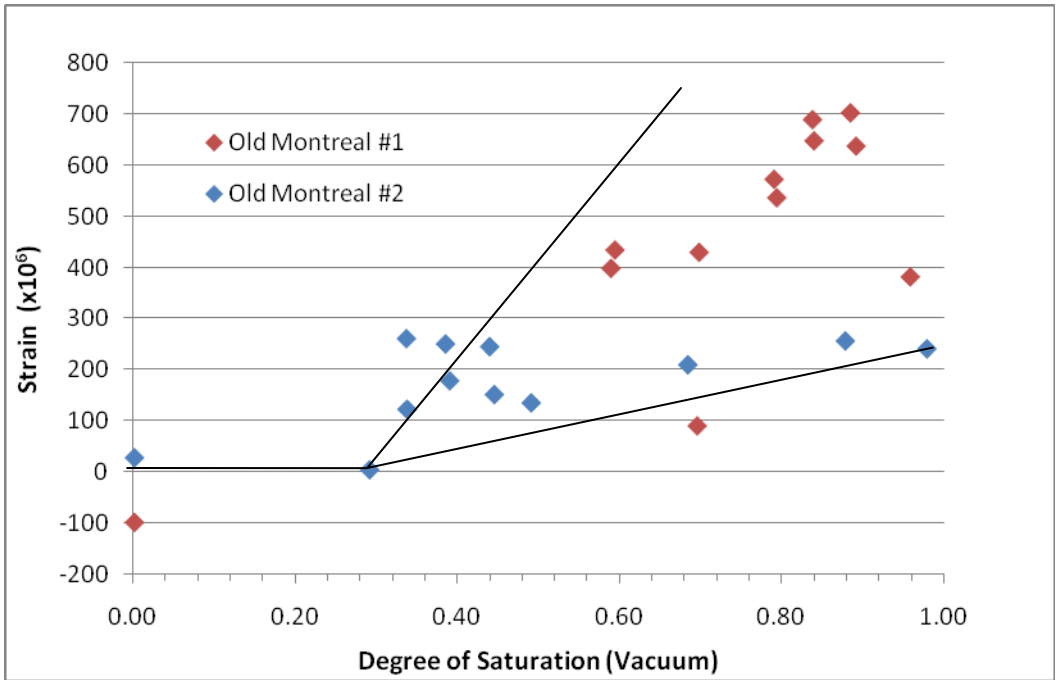

Figure 7-6 Frost dilatometry: Old Montreal Brick

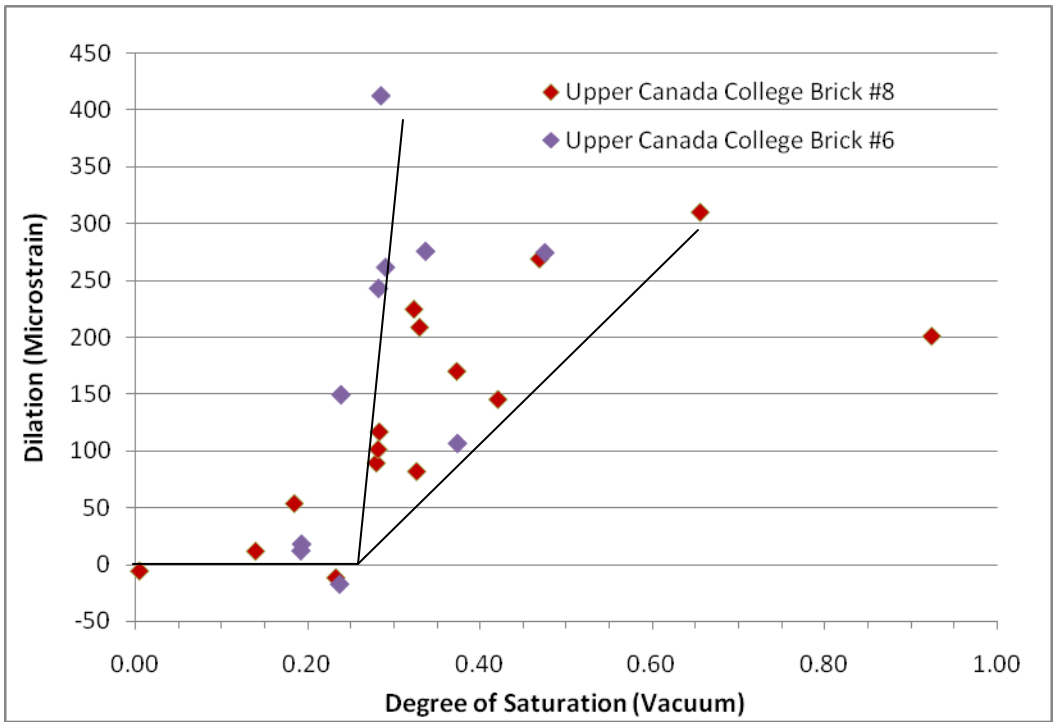

Figure 7-7 Frost dilatometry: Upper Canada College

All three sets of brick appear to have a clearly defined critical degree of saturation below which frost dilation does not take place. When subjected to freeze thaw cycles above S_{crit}, frost dilation tends to increase as the saturation level rises. The tendency for frost dilation to increase as a function of saturation is far from linear, especially with the Upper Canada College and Old Montreal set of brick.

The value of S_{crit} varies widely between the three sets of brick. The S_{crit} of Canada Brick is approximately 0.87, of Old Montreal brick is 0.30, and of Upper Canada College is 0.25. This wide difference between S_{crit} values ran counter to expectations. The S_{crit} value for the set of Canada Brick can be readily explained by the hydraulic pressure and disequilibrium theories.

It is less clear why the value of S_{crit} for Old Montreal (OM) and Upper Canada College (UCC) is so low. The disequilibrium theory states that damage is caused by capillary water desorbing faster than it can be distributed to the material surface or large interior pore spaces, which

requires either high water content or low permeability material. Neither condition is true of the UCC and OM samples at their critical degrees of saturation. Hydraulic pressure similarly requires the specimens to have a high degree of saturation in order for damaging flow pressures to exist in capillaries. Ice lensing is a possible explanation, but without knowledge of the pore size distribution of either set of brick it is difficult to know if they contain the requisite mix of large pores and small capillaries. However, although the physics of frost damage are still unclear, the dilatometric results for the UCC and OM set of bricks should not be discounted.

7.3 Summary

Freeze-thaw cycling of brick specimens requires consideration of several basic parameters. In this study a minimum temperature of -15°C was selected to ensure that the majority of pore-held water freezes. The maximum temperature of the cycle was 20°C to allow rapid thawing. Based on WUFI modeling and taking into consideration the specimen's high ratio of surface area to volume it was thought that exposure to the minimum and maximum temperatures for one hour would allow complete freezing and thawing to occur. A freezing rate of -17.5C/hour was selected as a compromise between test expediency and reported in-field freezing rates. Six freeze-thaw cycles were carried out between length measurements based on Fagerlund's precedent.

The use of dilatometry on specimens exposed to freeze-thaw cycles over a range of degrees of saturation demonstrates that a critical degree of saturation exists in clay brick. In all three sets of brick tested in this study, there exists a clear saturation threshold below which frost damage does not occur and above which permanent, irreversible expansion of the material occurs in increasing magnitude. This threshold varies widely among brick and appears to be somewhat related to porosity or A-value. Those bricks with high porosity and high A-value had a low critical degree of saturation whereas those bricks with low porosity and low A-value had a high critical degree of saturation. The reasons for this are not immediately clear and require further investigation.

Chapter 8
Conclusions and Recommendations

Current methods for assessing the resistance of brick to freeze-thaw damage are deficient, and are even less useful for making decisions with respect to existing or historic solid masonry buildings. The approach enshrined in North American test standards of determining "frost resistance" of a material based on acceptance criteria has for a long time been acknowledged as an unreliable guide to brick durability. The other alternative, subjecting brick to a severe freeze-thaw test, does not replicate the broad range of in-service conditions across North America. The underlying problem with a pass/fail approach to assessing durability is that "frost resistance" as a material property does not really exist anymore than strength does; given a high enough moisture loading with an aggressive rate of freezing it appears that all brick will suffer frost damage.

An alternative approach, promoted in this thesis, is to select a brick that can safely accommodate a predicted in-service moisture load. This requires knowledge of a brick's critical degree of saturation (S_{crit}), which is the moisture content above which freeze-thaw damage likely occurs, and accurate models to predict in-service moisture loading. A test method to determine S_{crit} based on expansion due to freeze-thaw damage is proposed in this thesis. The test method was demonstrated to be capable of determining S_{crit} to within ±0.05 degrees of saturation. The equipment and time requirements are not onerous. Major equipment includes a vacuum pump, desiccator, and outside micrometer. A freezer, saw, drill press, and balance accurate to one hundredth of a gram are also necessary but likely to be already part of a modestly equipped laboratory. The duration of the test will typically be between 6 to 12 days.

Knowledge of the critical degree of saturation of a material would be useful for design of new buildings and the retrofit of existing buildings. When selecting brick to be used in new construction predicted moisture loads in terms of degree of saturation would be compared to the material's S_{crit}. If the predicted moisture load is less than S_{crit} the material could safely be used, but if it is greater than S_{crit} a substitute material would have to be specified. In existing buildings the effect of a proposed retrofit strategy on the moisture content of walls would have to be

compared to the S_{crit} of the existing brick. If the proposed retrofit strategy does not increase the moisture content above S_{crit} the strategy could be safely pursued, but if it is expected to raise the moisture content above S_{crit} then the retrofit plan should be modified. In both cases knowledge of a material's S_{crit} provides the designer with a threshold value to determine whether the material can withstand predicted in-service moisture loads during freezing events.

The vacuum method is preferred to boiling saturation for determining the maximum degree of saturation. The boiling method tends to underestimate the saturated mass of brick versus vacuum saturation. Furthermore the vacuum saturation method offers greater repeatability and less variability among specimens in a sample brick. While the equipment requirements of vacuum saturation are greater and the procedure is more complex than the boiling method this should not pose a barrier for modern commercial testing laboratories.

It is possible to very accurately wet brick specimens to target moisture contents, on average within 0.4% of the target. The moisture content of sealed specimens over several days was found to remain almost constant with a typical moisture content loss of 0.04%. The length of time to allow uniform moisture redistribution was predicted to be 24 hours for most specimens and up to 72 hours for specimens with very low water absorption values at low target moisture contents based on hygrothermal modeling.

The results of frost dilatometry on the three sets of brick considered reveal that a distinct S_{crit} does exist in clay brick and its value varies significantly among different types and eras of brick. The S_{crit} of Canada Brick (a modern extruded brick) was approximately 0.87, and was 0.25 and 0.30 for brick from the Upper Canada College (1950s vintage) and the Old Montreal (1880s molded brick) sets respectively. S_{crit} may be inversely related to porosity or A-value, the reasons for this are not immediately clear and require further investigation.

It is recommended that further research be pursued in several areas. The ability of existing hygrothermal models, such as WUFI, to predict in-service moisture loads was beyond the scope of this study. This must to be demonstrated in order for the value of S_{crit} to have maximum utility.

The purpose of this study was to demonstrate that a critical degree of saturation exists in brick and that has been accomplished, however further parametric studies should follow.

A better understanding of vacuum saturation and the relative importance of its various parameters is required. This would form the basis of creating a standard method for performing vacuum saturation of building materials.

The effect of freezing rate on frost dilation requires further clarification. This study proceeded on the assumption that freezing rate only affected the severity of dilation but did not change the degree of saturation at which it occurred. Although corroborating evidence for this assumption was sparse, no contrary evidence was unearthed.

A better method for measuring strain should be pursued as length determined by the outside digital micrometer could be affected by operator error. Increasing the number of freezing cycles may cause significantly larger strains to develop in specimens experiencing frost damage and this should lower the precision and accuracy of the length determination required but this needs verification.

Lastly, a larger sample size is needed to corroborate the findings of this study. The results of the seven bricks used to demonstrate the methodology of the proposed S_{crit} test, while encouraging, would benefit from much larger sample sizes.

Bibliography

Anderson, Lindsay. "Spalling Brick – Material, Design or Construction Problem?" Journal of Performance of Constructed Facilities, Nov. 1999: 163-171.

ASTM C62-05. "Standard Specification for Building Brick (Solid Masonry Units Made From Clay or Shale)." West Conshohocken, PA: 2008 ed.

ASTM C67-07a. "Standard Test Methods for Sampling and Testing Brick and Structural Clay Tile." West Conshohocken, PA: 2008 ed.

ASTM C216-07a. "Standard Specification for Facing Brick (Solid Masonry Units Made From Clay or Shale)". West Conshohocken, PA: 2008 ed.

ASTM C1548-02(2007). "Standard Test Method for Dynamic Young's Modulus, Shear Modulus, and Poisson's Ratio of Refractory Materials by Impulse Excitation of Vibration." West Conshohocken, PA: 2008 ed.

Bear, Jacob. Dynamics of Fluids in Porous Media. Mineola, NY: Dover Publications, Inc., 1988.

Brampton Brick Limited. "A Position Paper on Current Canadian Standard Durability Tests". Brampton, June 1994.

Butterworth, B. and L.W. Baldwin. "Laboratory Test and the Durability of Brick: The Indirect Appraisal of Durability (continued)." Transactions of the British Ceramics Society 63.11 (1964): 647-661.

Crawford, C.B., "Frost Durability of Clay Bricks – Evaluation Criteria and Quality Control". Proceedings of the CBAC/DBR Manufacturers' Symposium. NRCC, Ottawa, April 1984.

CSA A82-06. "Fired masonry brick made from clay or shale." Mississauga, ON: 2006 ed.

Drysdale, R.G., A.A. Hamid, and L.R. Baker. Masonry Structures: Behaviour and Design. Englewood Cliffs, NJ: Prentice-Hall, 1994.

Fagerlund, G. "The critical degree of saturation method of assessing the freeze/thaw resistance of concrete." Materials and Structures 10.58 (1977): 217-230.

Fagerlund, G. "The international cooperative test of the critical degree of saturation method of assessing the freeze/thaw resistance of concrete." Materials and Structures 10.58 (1977): 231-253.

Gummerson, R.J., C. Hall, and W.D.Hoff. "Capillary water transport in masonry structures: building construction applications of Darcy's law." Construction Papers 1 (1980): 17-27.

Hall, Christopher, and William Hoff. Water Transport in Brick, Stone and Concrete. New York, NY: Spon Press, 2002.

Krischer, O., and W. Kast. "Die Wissenschaftlichen Grundlagen der Trocknungstechnik, 3" Auflage, Springer-Verlag, Berlin: 1978.

Krus, M., and A. Holm. "Simple Methods to Approximate the Liquid Transport Coefficients Describing the Absorption and Drying." Proceedings of the 5th Symposium 'Building Physics in the Nordic Countries. Göteborg, Sweden, August 24-26, 1999: 241-248.

Krus, M., and T.A.Vik. "Determination of Hygric Material Properties and Calculation of the Moisture Balance of Wooden Prisms." Proceedings of the 5th Symposium 'Building Physics in the Nordic Countries. Göteborg, Sweden, August 24-26, 1999: 313-320.

Künzel, H. Simultaneous Heat and Moisture Transport in Building Components: One- and two-dimensional calculation using simple parameters. Diss. Fraunhofer Institute of Building Physics, Germany, 1995.

Lindmark, Sture. Frost Resistance of Swedish Cement. Diss. Lund University, Sweden, 1998.

Litvan, G. "Phase Transition of Adsorbates III: Heat Effects and Dimensional Changes in Nonequilibrium Temperature Cycles" Journal of Colloid and Interface Science 38.1 (1972): 75-83.

Litvan, G. "Pore Structure and Frost Susceptibility of Building Materials". Research Paper No.584, NRCC, 1973.

Litvan, G. "Testing the Frost Susceptibility of Bricks". Masonry: Past and Present, ASTM STP 589. 1975: 123-132.

Litvan, G. "The Mechanism of Frost Action in Concrete – Theory and Practical Implications". Proceedings of Workshop on Low Temperature Effects on Concrete. IRC/NRCC, Ottawa, Sept. 1988: 116-127.

Maage, M. "Frost resistance and pore size distribution in bricks". Materials and Structures 17.101 (1984): 345-350.

Pazera, M. Development of Experimental Methods for Characterizing Water Vapour Transmission in Building Materials. Diss. Syracuse University, NY, 2007.

Pentalla, Vesa, and Fahim Al-Neshawy. "Stress and strain state of concrete during freezing and thawing cycles." Cement and Concrete Research 32 (2002): 1407-1420.

Petković, J. Moisture and ion transport in layered porous building materials: a Nuclear Magnetic Resonance study. Diss. Technical University of Eindhoven, Netherlands, 2005.

Prick, Angélique. "Critical Degree of Saturation as a Threshold Moisture Level in Frost Weathering of Limestones." Permafrost and Periglacial Processes 8 (1997): 91-99.

Ritchie, T. "Factors Affecting Frost Damage to Clay Bricks." Building Research Note No.62, NRCC, 1968.

Roppel, James. "Masonry walls treated with water-repellents." MASc Thesis. University of Waterloo, ON, 2003.

Sissons, Malcom. "Brick in the Twenty-First Century". Proceedings of the 8th Canadian Masonry Symposium. Jasper, AB, May 31- June 3, 1998: 1-5.

Straube, John, and Eric Burnett. Building Science for Building Enclosures. Westford, MA: Building Science Press, 2005.

Straube, John, and Eric Burnett. "Field Measurements of Masonry Veneer Exposure Conditions." Proceedings of the 8th Canadian Masonry Symposium. Jasper, AB, May 31-June 3, 1998: 208-221.

Taber, S. "Mechanics of Frost Heaving." Journal of Geology 38 (1930): 303-317.

Watt, David and B. Colson. "Investigating the effects of humidity and salt crystallisation on medieval masonry." Building and Environment 35 (2002): 737-749.

Wessman, L. "Studies of frost resistance of natural stone." Report TVBM-3077, Lund Institute of Technology, Lund, Sweden, 1997.

Wight, Jane. Brick Building in England: From the Middle Ages to 1550. London, UK: John Baker, 1972.

Appendix A

Material Data: Initial Canada Brick Sample

Table A.1 Initial Canada Brick material data

Specimen ID	Dimensions				Dry	Density	
	Length mm	Height mm	Thickness mm	Volume mm^3	Mass g	Specimen kg/m^3	Average kg/m^3
1-1	88	70	19	117040	245.36	2096	2096
2-1	87	71	20	123540	259.67	2102	2003
2-2	87	70	18	109620	208.66	1903	
3-1	88	70	18	110880	225.90	2037	2083
3-2	88	70	19	117040	249.05	2128	
4-1	89	69	23	141243	287.09	2033	1991
4-2	88	70	22	135520	263.76	1946	
4-3	88	70	16	98560	191.93	1947	
4-4	88	69	19	115368	235.14	2038	

Table A.2 Water uptake by boiling in initial Canada Brick specimens (basis of Figure 5-4)

			Duration of Boil			
		Dry	1-Hour	5-Hour	5-Hour	24-Hour
1-1	Mass (g)	245.39	266.40	268.80	268.83	269.35
	Water (g)		21.01	23.41	23.44	23.96
	MC (%)		8.6%	9.5%	9.6%	9.8%
2-1	Mass (g)	259.79	287.37	288.73	289.67	290.29
	Water (g)		27.58	28.94	29.88	30.50
	MC (%)		10.6%	11.1%	11.5%	11.7%
2-2	Mass (g)	208.78	230.75	234.31	234.12	235.05
	Water (g)		21.97	25.53	25.34	26.27
	MC (%)		10.5%	12.2%	12.1%	12.6%
3-1	Mass (g)	225.88	236.22	241.67	240.80	242.21
	Water (g)		10.34	15.79	14.92	16.33
	MC (%)		4.6%	7.0%	6.6%	7.2%
3-2	Mass (g)	249.06	262.85	266.2	266.13	268.24
	Water (g)		13.79	17.14	17.07	19.18
	MC (%)		5.5%	6.9%	6.9%	7.7%
4-1	Mass (g)	287.11	309.35	312.45	311.46	312.15
	Water (g)		22.24	25.34	24.35	25.04
	MC (%)		7.7%	8.8%	8.5%	8.7%
4-2	Mass (g)	263.81	285.50	284.53	286.58	287.53
	Water (g)		21.69	20.72	22.77	23.72
	MC (%)		8.2%	7.9%	8.6%	9.0%
4-3	Mass (g)	191.96	207.73	208.02	209.97	209.74
	Water (g)		15.77	16.06	18.01	17.78
	MC (%)		8.2%	8.4%	9.4%	9.3%
4-4	Mass (g)	235.18	254.48	255.63	255.96	257.74
	Water (g)		19.30	20.45	20.78	22.56
	MC (%)		8.2%	8.7%	8.8%	9.6%

Table A.3 Water uptake by boil & soak in initial Canada Brick specimens (basis of Figure 5-6)

			Duration of Boil+Soak		
		Dry	1+1	5+14	5+18
1-1	Mass (g)	245.39	274.13	273.09	274.23
	Water (g)		28.74	27.70	28.84
	MC (%)		11.7%	11.3%	11.8%
2-1	Mass (g)	259.79	296.38	295.22	296.54
	Water (g)		36.59	35.43	36.75
	MC (%)		14.1%	13.6%	14.1%
2-2	Mass (g)	208.78	239.16	238.39	239.45
	Water (g)		30.38	29.61	30.67
	MC (%)		14.6%	14.2%	14.7%
3-1	Mass (g)	225.88	246.92	245.53	247.35
	Water (g)		21.04	19.65	21.47
	MC (%)		9.3%	8.7%	9.5%
3-2	Mass (g)	249.06	273.18	272.04	273.61
	Water (g)		24.12	22.98	24.55
	MC (%)		9.7%	9.2%	9.9%
4-1	Mass (g)	287.11	318.88	317.27	318.68
	Water (g)		31.77	30.16	31.57
	MC (%)		11.1%	10.5%	11.0%
4-2	Mass (g)	263.81	292.58	291.38	292.56
	Water (g)		28.77	27.57	28.75
	MC (%)		10.9%	10.5%	10.9%
4-3	Mass (g)	191.96	213.01	212.23	213.16
	Water (g)		21.05	20.27	21.20
	MC (%)		11.0%	10.6%	11.0%
4-4	Mass (g)	235.18	261.02	260.37	261.35
	Water (g)		25.84	25.19	26.17
	MC (%)		11.0%	10.7%	11.1%

Appendix B

Material Data: Canada Brick #1, 2, 3

Table B.1 Vacuum & boiling saturation

Specimen ID		Mass (g) Dry	Mass (g) Sat_{Vac}	Mass (g) Dry	Mass (g) Sat_{Boil}	Mass (g) Dry	Mass (g) Sat_{Boil}	Mass (g) Dry	Mass (g) Sat_{Boil}
CB1-1	Mass (g)	161.10	177.55	161.14	174.90				
	% Change	-	10.21%	-	8.54%				
CB1-2	Mass (g)	140.28	154.55	140.29	152.43				
	% Change	-	10.17%	-	8.65%				
CB1-3	Mass (g)	125.79	138.95	125.86	137.14				
	% Change	-	10.46%	-	8.96%				
CB1-4	Mass (g)	146.36	161.81	146.46	159.61				
	% Change	-	10.56%	-	8.98%				
CB1-5	Mass (g)	152.23	167.55	152.26	164.87				
	% Change	-	10.06%	-	8.28%				
CB2-1	Mass (g)	147.02	161.69	147.09	158.73				
	% Change	-	9.98%	-	7.91%				
CB2-2	Mass (g)	128.21	141.01	128.75	139.01				
	% Change	-	9.98%	-	7.97%				
CB2-3	Mass (g)	142.88	157.02	142.89	154.35				
	% Change	-	9.90%	-	8.02%				
CB2-4	Mass (g)	121.16	133.13	121.17	131.03				
	% Change	-	9.88%	-	8.14%				
CB2-5	Mass (g)	130.70	143.46	130.70	142.01				
	% Change	-	9.76%	-	8.65%				
CB2-6	Mass (g)	151.23	165.97	151.24	164.11	Mass (g)		Mass (g)	
	% Change	-	9.75%	-	8.51%	Dry	Sat_{Boil}	Dry	Sat_{Boil}
CB3-1	Mass (g)	125.94	135.49	125.90	133.78	125.85	134.53	125.86	134.28
	% Change	-	7.58%	-	6.26%	-	6.90%	-	6.69%
CB3-2	Mass (g)	139.81	150.59	139.78	148.81	139.73	149.45	139.76	148.92
	% Change	-	7.71%	-	6.46%	-	6.96%	-	6.55%
CB3-3	Mass (g)	119.14	128.03	119.11	126.61	119.07	127.29	119.08	126.83
	% Change	-	7.46%	-	6.30%	-	6.90%	-	6.51%
CB3-4	Mass (g)	132.87	143.09	133.62	142.23	133.55	142.88	133.61	142.41
	% Change	-	7.69%	-	6.44%	-	6.99%	-	6.59%
CB3-5	Mass (g)	150.50	162.78	132.87	141.47	132.80	142.33	132.82	141.79
	% Change	-	8.16%	-	6.47%	-	7.18%	-	6.75%
CB3-6	Mass (g)	161.10	177.55	150.40	161.10	150.34	161.53	150.36	161.03
	% Change	-	10.21%	-	7.11%	-	7.44%	-	7.10%

Table B.2 Water uptake test & A-value

Specimen ID		Time (Mins) 0	1	5	10	15	20	30	45	60	180	Surface Area (mm2)	A-Value kg/m^2√s
	Mass (g)	161.16	163.34	165.03	166.61	167.63	168.54	169.69	170.29	170.36	170.64	6003	
CB1-1	TimeStamp	19:08	19:09	19:13	19:18	19:23	19:28	19:38	19:53	20:08	22:08		
	Time($s^{½}$)	0	8	17	24	30	35	42	52	60	104		0.033
	Mass (g)	140.31	142.68	144.58	146.13	147.04	147.60	148.09	148.26	148.27	148.44	6003	
CB1-2	TimeStamp	19:11	19:12	19:16	19:21	19:26	19:31	19:41	19:56	20:11	22:11		
	Time($s^{½}$)	0	8	17	24	30	35	42	52	60	104		0.031
	Mass (g)	125.87	128.44	130.59	131.94	132.6	132.91	133.02	133.08	133.12	133.31	5520	
CB1-3	TimeStamp	19:14	19:15	19:19	19:24	19:29	19:34	19:44	19:59	20:14	22:14		
	Time($s^{½}$)	0	8	17	24	30	35	42	52	60	104		0.031
CB1-4	Mass (g)	146.47	149.09	151.19	152.67	153.49	154.04	154.5	154.68	154.72	154.93	5740	
	TimeStamp	19:17	19:18	19:22	19:27	19:32	19:37	19:47	20:02	20:17	22:17		
	Time($s^{½}$)	0	8	17	24	30	35	42	52	60	104		0.033
	Mass (g)	152.28	154.41	156.25	157.63	158.71	159.50	160.39	160.69	160.71	160.91	6003	
CB1-5	TimeStamp	19:20	19:21	19:25	19:30	19:35	19:40	19:50	20:05	20:20	22:20		
	Time($s^{½}$)	0	8	17	24	30	35	42	52	60	104		0.032
	Mass (g)	147.10	148.85	150.28	151.47	152.25	153.04	154.03	154.78	154.94	155.18	6072	
CB2-1	TimeStamp	8:30	8:31	8:35	8:40	8:45	8:50	9:00	9:15	9:30	11:30		
	Time($s^{½}$)	0	8	17	24	30	35	42	52	60	104		0.027

	Mass (g)	128.74	130.72	132.23	133.59	134.38	134.92	135.37	135.51	135.59	135.78	6072	
CB2-2	TimeStamp	8:33	8:34	8:38	8:43	8:48	8:53	9:03	9:18	9:33	11:31		
	Time($s^{1/2}$)	0	8	17	24	30	35	42	52	60	103		0.026
	Mass (g)	142.90	145.17	147.04	148.22	149.06	149.58	150.17	150.44	150.50	150.71	5589	
CB2-3	TimeStamp	8:36	8:37	8:41	8:46	8:51	8:56	9:06	9:21	9:36	11:31		
	Time($s^{1/2}$)	0	8	17	24	30	35	42	52	60	102		0.031
	Mass (g)	121.16	123.34	125.11	126.36	127.03	127.40	127.61	127.69	127.76	127.90	5520	
CB2-4	TimeStamp	8:39	8:40	8:44	8:49	8:54	8:59	9:09	9:24	9:39	11:31		
	Time($s^{1/2}$)	0	8	17	24	30	35	42	52	60	102		0.028
	Mass (g)	130.71	132.72	134.52	135.69	136.48	136.95	137.42	137.67	137.75	137.96	6003	
CB2-5	TimeStamp	8:42	8:43	8:47	8:52	8:57	9:02	9:12	9:27	9:42	11:32		
	Time($s^{1/2}$)	0	8	17	24	30	35	42	52	60	101		0.026
CB2-6	Mass (g)	151.24	153.14	154.75	155.97	156.81	157.57	158.53	159.24	159.39	159.63	6003	
	TimeStamp	8:45	8:46	8:50	8:55	9:00	9:05	9:15	9:30	9:45	11:32		
	Time($s^{1/2}$)	0	8	17	24	30	35	42	52	60	100		0.029
	Mass (g)	125.95	126.33	126.53	126.74	126.81	126.92	127.09	127.27	127.38	128.12	5628	
CB3-1	TimeStamp	11:40	11:41	11:45	11:50	11:55	12:00	12:10	12:25	12:40	14:46		
	Time($s^{1/2}$)	0	8	17	24	30	35	42	52	60	106		0.0036
	Mass (g)	139.79	140.18	140.44	140.66	140.75	140.83	141.01	141.19	141.32	142.13	5628	
CB3-2	TimeStamp	11:43	11:44	11:48	11:53	11:58	12:03	12:13	12:28	12:43	14:47		
	Time($s^{1/2}$)	0	8	17	24	30	35	42	52	60	105		0.0040
	Mass (g)	119.13	119.61	119.91	120.11	120.20	120.34	120.49	120.68	120.84	121.58	5168	
CB3-3	TimeStamp	11:46	11:47	11:51	11:56	12:01	12:06	12:16	12:31	12:46	14:47		
	Time($s^{1/2}$)	0	8	17	24	30	35	42	52	60	104		0.0045

	Mass (g)	133.64	134.12	134.39	134.60	134.74	134.89	135.04	135.21	135.38	136.14	5092	
CB3-4	TimeStamp	11:49	11:50	11:54	11:59	12:04	12:09	12:19	12:34	12:49	14:48		
	Time($s^{1/2}$)	0	8	17	24	30	35	42	52	60	104		0.0047
	Mass (g)	132.89	133.36	133.70	133.90	134.04	134.14	134.34	134.52	134.76	135.61	5712	
CB3-5	TimeStamp	11:52	11:53	11:57	12:02	12:07	12:12	12:22	12:37	12:52	14:48		
	Time($s^{1/2}$)	0	8	17	24	30	35	42	52	60	103		0.0046
	Mass (g)	150.46	151.00	151.41	151.67	151.88	152.00	152.25	152.53	152.74	153.78	5712	
CB3-6	TimeStamp	11:55	11:56	12:00	12:05	12:10	12:15	12:25	12:49	12:55	14:48		
	Time($s^{1/2}$)	0	8	17	24	30	35	42	52	60	102		0.0057

Table B.3 Moisture wetting, moisture retention, and frost dilatometry for Canada Brick #1

	M_{sat} (g)	S_{target}	M_{dry} (g)	M_{wet} (g)	M_{wrap} (g)	$L_{0,1}$ (mm)	$L_{0,2}$ (mm)	$L_{0,avg}$ (mm)	M_{wrap} (g)	M_{wet} (g)	S_{actual}	$L_{6,1}$ (mm)	$L_{6,2}$ (mm)	$L_{6,avg}$ (mm)	L_6-L_0 (mm)	Strain (x 10^6)
DATE:	**February 9, 2009**								**February 13, 2009**							
CB1-3	138.95	-	125.79	137.92	141.69	9.98	9.96	9.97	141.69	137.83	0.915	9.98	10.00	9.99	0.020	240
CB1-4	161.81	-	146.36	160.38	164.14	10.41	10.41	10.41	164.12	160.27	0.900	10.40	10.40	10.40	-0.010	-119
DATE:	**March 3, 2009**								**March 11, 2009**							
CB1-3	138.95	-	125.79	137.64	140.72	9.97	10.01	9.99	140.75	137.57	0.895	9.98	10.01	10.00	0.005	60
CB1-4	161.81	-	146.36	160.42	163.32	10.40	10.39	10.40	163.36	160.40	0.909	10.42	10.42	10.42	0.025	298
DATE:	**June 10, 2009**								**June 12, 2009**							
CB1-3	138.95	1.00	125.79	138.96	141.90	83.432	83.428	83.430	141.87	138.90	0.996	83.480	83.475	83.478	0.047	569
DATE:	**June 12, 2009**								**June 15, 2009**							
CB1-4	161.81	0.95	146.36	161.01	164.12	83.867	83.869	83.868	164.13	160.93	0.943	83.914	83.909	83.912	0.044	519
CB1-5	167.55	0.90	152.23	166.03	169.05	90.607	90.613	90.610	169.09	165.96	0.896	90.613	90.621	90.617	0.007	77

Table B.4 Moisture wetting, moisture retention, and frost dilatometry for Canada Brick #2

	M_{sat} (g)	S_{target}	M_{dry} (g)	M_{wet} (g)	M_{wrap} (g)	$L_{0,1}$ (mm)	$L_{0,2}$ (mm)	$L_{0,avg}$ (mm)	M_{wrap} (g)	M_{wet} (g)	S_{actual}	$L_{6,1}$ (mm)	$L_{6,2}$ (mm)	$L_{6,avg}$ (mm)	L_6-L_0 (mm)	Strain (x 10^6)
DATE:				**June 10, 2009**							**June 12, 2009**					
CB2-3	157.02	1.00	142.88	157.02	160.43	84.203	84.191	84.197	160.41	157.09	1.005	84.278	84.277	84.278	0.081	956
DATE:				**June 12, 2009**							**June 15, 2009**					
CB2-4	133.13	0.95	121.16	132.53	135.36	83.431	83.435	83.433	135.36	132.4	0.939	83.489	83.509	83.499	0.066	791
CB2-5	143.46	0.90	130.70	142.18	145.27	90.622	90.619	90.621	145.28	142.14	0.897	90.655	90.657	90.656	0.036	392
CB2-6	165.97	0.85	151.23	163.76	167.05	90.495	90.505	90.500	167.07	163.81	0.853	90.513	90.518	90.516	0.016	171

Table B.5 Moisture wetting, moisture retention, and frost dilatometry for Canada Brick #3

	M_{sat} (g)	S_{target}	M_{dry} (g)	M_{wet} (g)	M_{wrap} (g)	$L_{0,1}$ (mm)	$L_{0,2}$ (mm)	$L_{0,avg}$ (mm)	M_{wrap} (g)	M_{wet} (g)	S_{actual}	$L_{6,1}$ (mm)	$L_{6,2}$ (mm)	$L_{6,avg}$ (mm)	L_6-L_0 (mm)	Strain (x 10^6)
DATE:				**June 10, 2009**							**June 12, 2009**					
CB3-3	128.03	1.00	119.14	128.00	131.08	77.872	77.870	77.871	131.07	127.94	0.990	77.935	77.935	77.935	0.064	822
DATE:				**June 12, 2009**							**June 15, 2009**					
CB3-5	143.09	0.95	132.87	142.52	145.41	86.665	86.665	86.665	145.41	142.45	0.937	86.688	86.700	86.694	0.029	335
CB3-6	162.78	0.90	150.5	161.55	164.50	87.205	87.206	87.206	164.49	161.4	0.888	87.216	87.220	87.218	0.012	143

Table B.6 Summary of Canada Brick #1, 2 & 3 material data

Specimen ID	Dimensions				Dry	Density		Boil Porosity		Vacuum Porosity	
	Length	Height	Thickness	Volume	Mass	Specimen	Average	Specimen	Average	Specimen	Average
	mm	mm	mm	mm^3	g	kg/m^3	kg/m^3	m^3/m^3	m^3/m^3	m^3/m^3	m^3/m^3
CB1-1	87	69	12	72036	161.14	2237		0.191		0.228	
CB1-2	87	69	11	66033	140.29	2125		0.184		0.216	
CB1-3	80	69	11	60720	125.86	2073	2212	0.186	0.192	0.217	0.228
CB1-4	82	70	11	63140	146.46	2320		0.208		0.245	
CB1-5	87	69	11	66033	152.26	2306		0.191		0.232	
CB2-1	88	69	10	60720	147.09	2422		0.192		0.242	
CB2-2	88	69	10	60720	128.75	2120		0.169		0.211	
CB2-3	81	69	12	67068	142.89	2131	2223	0.171	0.182	0.211	0.219
CB2-4	80	69	10	55200	121.17	2195		0.179		0.217	
CB2-5	87	69	10	60030	130.70	2177		0.188		0.213	
CB2-6	87	69	11	66033	151.24	2290		0.195		0.223	
CB3-1	84	67	10	56280	125.90	2237		0.140		0.170	
CB3-2	84	67	11	61908	139.78	2258		0.146		0.174	
CB3-3	76	68	11	56848	119.11	2095	2249	0.132	0.146	0.156	0.172
CB3-4	76	67	11	56012	133.62	2386		0.154		-	
CB3-5	84	68	10	57120	132.87	2326		0.151		0.179	
CB3-6	84	68	12	68544	150.40	2194		0.156		0.179	

Table B.7 Effect of vacuum pressure on moisture content (basis of Figure 5-13)

Pressure	Saturated Moisture Content (% Dry Mass)					
(ATM)	CB1-3	CB1-4	CB2-1	CB2-2	CB3-1	CB3-2
0.265	9.21%	9.12%	8.56%	8.68%	6.26%	6.34%
0.132	9.39%	9.58%	9.06%	8.93%	6.82%	6.91%
0.112	9.72%	9.78%	9.24%	9.28%	6.93%	6.99%
0.001	10.46%	10.56%	9.98%	9.98%	7.58%	7.71%

Appendix C

Material Data: Old Montreal Bricks #1 & 2
Upper Canada College Bricks #6 & 8

Table C.1 Vacuum & boiling saturation of Old Montreal Brick #1

Specimen ID		Mass (g) Dry	Mass (g) Sat_{Boil}	Mass (g) Dry	Mass (g) Sat_{Vac}
OM1-1	Mass (g)	103.35	117.53	103.45	117.57
	% Change	-	13.72%	-	13.65%
OM1-2	Mass (g)	108.64	123.75	108.70	123.93
	% Change	-	13.91%	-	14.01%
OM1-3	Mass (g)	110.35	125.8	110.45	125.94
	% Change	-	14.00%	-	14.02%
OM1-4	Mass (g)	110.83	126.53	110.92	126.53
	% Change	-	14.17%	-	14.07%
OM1-5	Mass (g)	109.90	125.48	109.92	125.55
	% Change	-	14.18%	-	14.22%
OM1-6	Mass (g)	106.58	121.65	106.62	121.70
	% Change	-	14.14%	-	14.14%
OM1-7	Mass (g)	118.80	135.62	118.89	135.82
	% Change	-	14.16%	-	14.24%
OM1-8	Mass (g)	97.96	111.54	97.97	111.70
	% Change	-	13.86%	-	14.01%
OM1-9	Mass (g)	107.12	122.01	107.22	122.18
	% Change	-	13.90%	-	13.95%
OM1-10	Mass (g)	116.17	132.46	116.21	132.56
	% Change	-	14.02%	-	14.07%
OM1-11	Mass (g)	111.53	127.13	111.41	127.11
	% Change	-	13.99%	-	14.09%
OM1-12	Mass (g)	98.54	112.41	98.49	112.41
	% Change	-	14.08%	-	14.13%

Table C.2 Vacuum & boiling saturation of Old Montreal Brick #2

Specimen ID		Mass (g) Dry	Mass (g) Sat_{Boil}	Mass (g) Dry	Mass (g) Sat_{Vac}
OM2-2	Mass (g)	110.76	128.09	110.79	128.41
	% Change	-	15.65%	-	15.90%
OM2-3	Mass (g)	101.54	117.33	101.57	117.54
	% Change	-	15.55%	-	15.72%
OM2-4	Mass (g)	100.48	116.13	100.50	116.22
	% Change	-	15.58%	-	15.64%
OM2-5	Mass (g)	117.01	135.13	117.04	135.38
	% Change	-	15.49%	-	15.67%
OM2-6	Mass (g)	100.50	115.84	100.54	116.13
	% Change	-	15.26%	-	15.51%
OM2-7	Mass (g)	116.75	134.56	116.80	134.86
	% Change	-	15.25%	-	15.46%
OM2-8	Mass (g)	100.73	116.00	100.78	116.27
	% Change	-	15.16%	-	15.37%
OM2-9	Mass (g)	118.35	136.36	118.41	136.60
	% Change	-	15.22%	-	15.36%
OM2-10	Mass (g)	95.45	109.72	95.50	109.91
	% Change	-	14.95%	-	15.09%
OM2-11	Mass (g)	119.09	136.75	119.16	136.89
	% Change	-	14.83%	-	14.88%
OM2-12	Mass (g)	114.47	131.48	-	-
	% Change	-	14.86%	-	-

Table C.3 Vacuum & boiling saturation of Upper Canada College Brick #6

Specimen ID		Mass (g) Dry	Mass (g) Sat_{Boil}	Mass (g) Dry	Mass (g) Sat_{Vac}
UC6-2	Mass (g)	108.17	124.51	108.20	125.25
	% Change	-	15.11%	-	15.76%
UC6-3	Mass (g)	94.61	108.82	94.61	109.52
	% Change	-	15.02%	-	15.76%
UC6-4	Mass (g)	91.77	105.40	91.79	106.08
	% Change	-	14.85%	-	15.57%
UC6-5	Mass (g)	90.09	103.43	90.10	104.05
	% Change	-	14.81%	-	15.48%
UC6-6	Mass (g)	86.92	99.81	86.95	100.33
	% Change	-	14.83%	-	15.39%
UC6-7	Mass (g)	89.33	102.76	89.34	103.34
	% Change	-	15.03%	-	15.67%
UC6-8	Mass (g)	87.64	100.84	87.65	101.34
	% Change	-	15.06%	-	15.62%
UC6-9	Mass (g)	110.16	126.47	110.20	127.23
	% Change	-	14.81%	-	15.45%
UC6-10	Mass (g)	79.55	91.46	110.20	127.23
	% Change	-	14.97%	-	15.45%
UC6-11	Mass (g)	103.08	118.34	-	-
	% Change	-	14.80%	-	-
UC6-12	Mass (g)	96.94	111.30	79.57	91.86
	% Change	-	14.81%	-	15.45%

Table C.4 Vacuum & boiling saturation of Upper Canada College Brick #8

Specimen ID		Mass (g) Dry	Mass (g) Sat_{Boil}	Mass (g) Dry	Mass (g) Sat_{Vac}	Mass (g) Dry	Mass (g) Sat_{Vac}	Mass (g) Dry	Mass (g) Sat_{Vac}
UC8-1	Mass (g)	101.15	119.27	101.07	120.29	101.12	120.44	101.07	120.29
	% Change	-	17.91%	-	19.02%	-	19.11%	-	19.02%
UC8-2	Mass (g)	96.25	113.44	96.17	114.31	96.19	114.47	96.17	114.31
	% Change	-	17.86%	-	18.86%	-	19.00%	-	18.86%
UC8-3	Mass (g)	96.83	113.98	96.74	114.93	96.79	115.00	96.74	114.93
	% Change	-	17.71%	-	18.80%	-	18.81%	-	18.80%
UC8-4	Mass (g)	90.07	105.99	90.01	106.83	90.00	106.87	90.01	106.83
	% Change	-	17.68%	-	18.69%	-	18.74%	-	18.69%
UC8-5	Mass (g)	88.15	103.82	88.13	104.63	88.12	104.75	88.13	104.63
	% Change	-	17.78%	-	18.72%	-	18.87%	-	18.72%
UC8-6	Mass (g)	87.13	102.69	87.08	103.39	87.09	103.48	87.08	103.39
	% Change	-	17.86%	-	18.73%	-	18.82%	-	18.73%
UC8-7	Mass (g)	102.32	120.59	102.27	121.55	102.28	121.59	102.27	121.55
	% Change	-	17.86%	-	18.85%	-	18.88%	-	18.85%
UC8-8	Mass (g)	87.18	102.81	87.09	103.59	87.12	103.63	87.09	103.59
	% Change	-	17.93%	-	18.95%	-	18.95%	-	18.95%
UC8-9	Mass (g)	90.48	106.75	90.42	107.48	90.44	107.69	90.42	107.48
	% Change	-	17.98%	-	18.87%	-	19.07%	-	18.87%
UC8-10	Mass (g)	86.10	101.43	86.01	102.16	86.05	102.33	86.01	102.16
	% Change	-	17.80%	-	18.78%	-	18.92%	-	18.78%
UC8-11	Mass (g)	89.95	105.77	89.88	106.67	89.90	106.77	89.88	106.67
	% Change	-	17.59%	-	18.68%	-	18.77%	-	18.68%
UC8-12	Mass (g)	90.71	106.72	88.67	105.16	90.66	107.61	88.67	105.16
	% Change	-	17.65%	-	18.60%	-	18.70%	-	18.60%

Table C.5 Water uptake test & A-value of Old Montreal Brick #1

Specimen ID		Nominal Time (Mins) 0	1	2	5	10	15	20	30	45	60	180	Length (mm)	Height (mm)	A-Value $kg/m^2\sqrt{s}$
	Mass (g)	103.49	114.04	114.04	113.95	113.92	113.99	114.02	114.17	114.28	114.41	114.50	82	62	
OM1-1	TimeStamp	12:24	12:25	12:26	12:29	12:34	12:39	12:44	12:54	13:09	13:24	15:24			
	Time($s^{1/2}$)	0	8	11	17	24	30	35	42	52	60	104			0.268
	Mass (g)	108.75	120.32	120.32	120.17	120.11	120.18	120.26	120.28	120.48	120.58	120.74	82	62	
OM1-2	TimeStamp	12:27	12:28	12:29	12:32	12:37	12:42	12:47	12:57	13:12	13:27	15:27			
	Time($s^{1/2}$)	0	8	11	17	24	30	35	42	52	60	104			0.294
	Mass (g)	110.47	122.31	122.14	122.09	122.02	122.05	122.14	122.29	122.41	122.50	122.76	82	62	
OM1-3	TimeStamp	12:30	12:31	12:32	12:35	12:40	12:45	12:50	13:00	13:15	13:30	15:30			
	Time($s^{1/2}$)	0	8	11	17	24	30	35	42	52	60	104			0.301
OM1-4	Mass (g)	110.96	122.82	122.75	122.67	122.61	122.65	122.72	122.93	123.01	123.15	123.30	82	62	
	TimeStamp	12:33	12:34	12:35	12:38	12:43	12:48	12:53	13:03	13:18	13:33	15:33			
	Time($s^{1/2}$)	0	8	11	17	24	30	35	42	52	60	104			0.301
	Mass (g)	110.04	121.88	121.80	121.73	121.70	121.69	121.73	121.87	122.05	122.10	122.24	83	62	
OM1-5	TimeStamp	12:36	12:37	12:38	12:41	12:46	12:51	12:56	13:06	13:21	13:36	15:36			
	Time($s^{1/2}$)	0	8	11	17	24	30	35	42	52	60	104			0.297
	Mass (g)	106.71	118.10	118.08	118.01	118.01	117.96	118.02	118.17	118.37	118.44	118.55	82	62	
OM1-6	TimeStamp	12:39	12:40	12:41	12:44	12:49	12:54	12:59	13:09	13:24	13:39	15:39			
	Time($s^{1/2}$)	0	8	11	17	24	30	35	42	52	60	104			0.289

	Mass (g)	118.94	131.62	131.59	131.58	131.5	131.46	131.62	131.64	131.77	131.92	132.04	82	62	
OM1-7	TimeStamp	12:42	12:43	12:44	12:47	12:52	12:57	13:02	13:12	13:27	13:42	15:41			
	Time($s^{½}$)	0	8	11	17	24	30	35	42	52	60	104			0.322
	Mass (g)	98.07	108.47	108.43	108.41	108.35	108.31	108.32	108.45	108.57	108.61	108.86	85	62	
OM1-8	TimeStamp	10:20	10:21	10:22	10:25	10:30	10:35	10:40	10:50	11:05	11:20	13:30			
	Time($s^{½}$)	0	8	11	17	24	30	35	42	52	60	107			0.255
	Mass (g)	107.25	118.55	118.52	118.42	118.41	118.40	118.39	118.52	118.65	118.73	119.02	80	62	
OM1-9	TimeStamp	10:23	10:24	10:25	10:28	10:33	10:38	10:43	10:53	11:08	11:23	13:30			
	Time($s^{½}$)	0	8	11	17	24	30	35	42	52	60	106			0.294
	Mass (g)	116.31	128.55	128.53	128.53	128.41	128.39	128.41	128.55	128.68	128.78	129.03	82	62	
OM1-10	TimeStamp	10:26	10:27	10:28	10:31	10:36	10:41	10:46	10:56	11:11	11:26	13:31			
	Time($s^{½}$)	0	8	11	17	24	30	35	42	52	60	105			0.311
OM1-11	Mass (g)	111.65	123.47	123.46	123.37	123.31	123.29	123.34	123.48	123.59	123.73	123.93	84	62	
	TimeStamp	10:29	10:30	10:31	10:34	10:39	10:44	10:49	10:59	11:14	11:29	13:31			
	Time($s^{½}$)	0	8	11	17	24	30	35	42	52	60	104			0.293
	Mass (g)	98.63	109.21	109.21	109.15	109.04	109.00	109.11	109.19	109.2	109.42	109.62	83	62	
OM1-12	TimeStamp	10:32	10:33	10:34	10:37	10:42	10:47	10:52	11:02	11:17	11:32	13:32			
	Time($s^{½}$)	0	8	11	17	24	30	35	42	52	60	104			0.265

Table C.6 Water uptake test & A-value of Old Montreal Brick #2

Specimen ID		Nominal Time (Mins) 0	1	2	5	10	15	20	30	45	60	180	Length (mm)	Height (mm)	A-Value $kg/m^2\sqrt{s}$
OM2-2	Mass (g)	110.90	124.24	124.18	124.10	124.03	124.02	124.04	124.08	124.16	124.25	124.51	81	62	
	TimeStamp	10:35	10:36	10:37	10:40	10:45	10:50	10:55	11:05	11:20	11:35	13:32			
	Time($s^{1/2}$)	0	8	11	17	24	30	35	42	52	60	103			0.343
OM2-3	Mass (g)	101.65	114.02	113.96	113.88	113.82	113.80	113.77	113.90	114.00	114.13	114.32	84	61	
	TimeStamp	10:38	10:39	10:40	10:43	10:48	10:53	10:58	11:08	11:23	11:38	13:32			
	Time($s^{1/2}$)	0	8	11	17	24	30	35	42	52	60	102			0.312
OM2-4	Mass (g)	100.59	112.78	112.73	112.59	112.56	112.59	112.59	112.7	112.82	112.94	113.15	83	61	
	TimeStamp	10:41	10:42	10:43	10:46	10:51	10:56	11:01	11:11	11:26	11:41	13:33			
	Time($s^{1/2}$)	0	8	11	17	24	30	35	42	52	60	102			0.311
OM2-5	Mass (g)	117.13	131.03	130.98	130.89	130.86	130.81	130.85	131.02	131.17	131.30	131.50	83	62	
	TimeStamp	10:44	10:45	10:46	10:49	10:54	10:59	11:04	11:14	11:29	11:44	13:33			
	Time($s^{1/2}$)	0	8	11	17	24	30	35	42	52	60	101			0.349
OM2-6	Mass (g)	100.60	112.56	112.50	112.44	112.37	112.39	112.45	112.54	112.73	112.75	112.94	84	62	
	TimeStamp	10:47	10:48	10:49	10:52	10:57	11:02	11:07	11:17	11:32	11:47	13:33			
	Time($s^{1/2}$)	0	8	11	17	24	30	35	42	52	60	100			0.296
OM2-7	Mass (g)	116.86	130.7	130.64	130.67	130.56	130.51	130.58	130.54	130.67	130.80	131.05	83	62	
	TimeStamp	9:25	9:26	9:27	9:30	9:35	9:40	9:45	9:55	10:10	10:25	12:36			
	Time($s^{1/2}$)	0	8	11	17	24	30	35	42	52	60	107			0.347
OM2-8	Mass (g)	100.79	112.79	112.76	112.73	112.66	112.63	112.65	112.67	112.86	112.92	113.12	82	62	
	TimeStamp	9:28	9:29	9:30	9:33	9:38	9:43	9:48	9:58	10:13	10:28	12:37			
	Time($s^{1/2}$)	0	8	11	17	24	30	35	42	52	60	106			0.305

OM2-9	Mass (g)	118.46	132.46	132.44	132.38	132.36	132.37	132.28	132.42	132.57	132.65	132.95	85	62	
	TimeStamp	9:31	9:32	9:33	9:36	9:41	9:46	9:51	10:01	10:16	10:31	12:37			
	Time($s^{½}$)	0	8	11	17	24	30	35	42	52	60	106			0.343
OM2-10	Mass (g)	95.54	106.76	106.72	106.74	106.67	106.60	106.65	106.77	106.84	106.98	107.20	83	62	
	TimeStamp	9:34	9:35	9:36	9:39	9:44	9:49	9:54	10:04	10:19	10:34	12:38			
	Time($s^{½}$)	0	8	11	17	24	30	35	42	52	60	105			0.281
OM2-11	Mass (g)	119.22	132.92	132.90	132.87	132.80	132.85	132.84	132.99	132.99	133.20	133.49	84	62	
	TimeStamp	9:37	9:38	9:39	9:42	9:47	9:52	9:57	10:07	10:22	10:37	12:38			
	Time($s^{½}$)	0	8	11	17	24	30	35	42	52	60	104			0.340
OM2-12	Mass (g)	114.60	127.82	127.81	127.76	127.72	127.72	127.71	127.84	128	128.06	128.37	85	62	
	TimeStamp	9:40	9:41	9:42	9:45	9:50	9:55	10:00	10:10	10:25	10:40	12:39			
	Time($s^{½}$)	0	8	11	17	24	30	35	42	52	60	104			0.324

Table C.7 Water uptake test & A-value of Upper Canada College Brick #6

		Nominal Time (Mins)											Length	Height	Frog	A-Value
Specimen ID		0	1	2	5	10	15	20	30	45	60	180	(mm)	(mm)	(mm^2)	$kg/m^2\sqrt{s}$
UC6-2	Mass (g)	108.20	116.78	-	117.93	117.98	118.02	117.99	117.98	118.00	118.03	118.12	84	60		
	TimeStamp	14:25	14:26	-	14:30	14:35	14:40	14:45	14:55	15:10	15:25	17:21			0	
	Time($s^{½}$)	0	8	-	17	24	30	35	42	52	60	103				0.220
UC6-3	Mass (g)	94.64	102.45	-	103.01	103.07	103.03	103.04	103.05	103.07	103.14	103.20	83	60		
	TimeStamp	14:28	14:29	-	14:33	14:38	14:43	14:48	14:58	15:13	15:28	17:21			480	
	Time($s^{½}$)	0	8	-	17	24	30	35	42	52	60	102				0.224
UC6-4	Mass (g)	91.81	99.35	-	99.84	99.83	99.91	99.87	99.91	99.95	99.99	100.05	83	60		
	TimeStamp	14:31	14:32	-	14:36	14:41	14:46	14:51	15:01	15:16	15:31	17:22			644	
	Time($s^{½}$)	0	8	-	17	24	30	35	42	52	60	101				0.224

UC6-5	Mass (g)	90.11	97.3	-	97.97	98.05	98.06	98.1	98.1	98.12	98.16	98.19	83	60			
	TimeStamp	14:37	14:38	-	14:42	14:47	14:52	15:00	15:10	15:25	15:40	17:22			644		
	Time($s^{½}$)	0	8	-	17	24	30	37	44	54	61	99					0.214
UC6-6	Mass (g)	86.94	94.22	-	94.52	94.62	94.63	94.62	94.68	94.70	94.67	94.79	82	60			
	TimeStamp	14:40	14:41	-	14:45	14:50	14:55	15:00	15:10	15:25	15:40	17:23			644		
	Time($s^{½}$)	0	8	-	17	24	30	35	42	52	60	99					0.220
UC6-7	Mass (g)	89.35	96.93	-	97.21	97.26	97.30	97.31	97.34	97.38	97.39	97.40	83	60			
	TimeStamp	14:43	14:44	-	14:48	14:53	14:58	15:03	15:15	15:28	15:43	17:22			644		
	Time($s^{½}$)	0	8	-	17	24	30	35	44	52	60	98					0.226
UC6-8	Mass (g)	87.68	95.23	95.45	95.51	95.48	95.50	95.46	95.52	95.53	95.55	95.58	84	60			
	TimeStamp	15:33	15:34	15:35	15:38	15:42	15:47	15:52	16:02	16:17	16:32	18:23			644		
	Time($s^{½}$)	0	8	11	17	23	29	34	42	51	59	101					0.222
UC6-9	Mass (g)	110.22	117.85	119.55	119.73	119.86	119.82	119.86	119.90	119.97	119.96	120.01	83	60			
	TimeStamp	15:35	15:36	15:37	15:40	15:45	15:50	15:55	16:05	16:20	16:35	18:23			644		
	Time($s^{½}$)	0	8	11	17	24	30	35	42	52	60	100					0.227
UC6-10	Mass (g)	79.57	86.49	86.56	86.60	86.66	86.63	86.63	86.63	86.69	86.7	86.74	84	60			
	TimeStamp	15:38	15:39	15:40	15:43	15:48	15:53	15:58	16:08	16:23	16:38	18:24			644		
	Time($s^{½}$)	0	8	11	17	24	30	35	42	52	60	100					0.203
UC6-11	Mass (g)	103.10	111.14	111.96	112.07	112.10	112.14	112.13	112.19	112.18	112.21	112.27	84	60			
	TimeStamp	15:41	15:42	15:43	15:46	15:51	15:56	16:01	16:11	16:26	16:41	18:24			644		
	Time($s^{½}$)	0	8	11	17	24	30	35	42	52	60	99					0.236
UC6-12	Mass (g)	96.96	104.85	105.44	105.59	105.61	105.52	105.66	105.65	105.57	105.66	105.68	82	60			
	TimeStamp	9:05	9:06	9:07	9:10	9:15	9:20	9:25	9:35	9:50	10:05	12:05			0		
	Time($s^{½}$)	0	8	11	17	24	30	35	42	52	60	104					0.207

Table C.8 Water uptake test & A-value of Upper Canada College Brick #8

Specimen ID		Nominal Time (Mins) 0	1	2	5	10	15	20	30	45	60	180	Length (mm)	Height (mm)	Frog (mm^2)	A-Value $kg/m^2\sqrt{s}$
UC8-1	Mass (g)	101.18	109.45	112.20	113.45	113.58	113.62	113.62	113.66	113.68	113.67	113.80	83	59		
	TimeStamp	9:08	9:09	9:10	9:13	9:18	9:23	9:28	9:38	9:53	10:08	12:08			0	
	Time($s^{1/2}$)	0	8	11	17	24	30	35	42	52	60	104				0.218
UC8-2	Mass (g)	96.28	104.86	107.34	107.97	107.99	108.07	108.08	108.10	108.13	108.10	108.23	84	60		
	TimeStamp	9:11	9:12	9:13	9:16	9:21	9:26	9:31	9:41	9:56	10:11	12:10			0	
	Time($s^{1/2}$)	0	8	11	17	24	30	35	42	52	60	104				0.220
UC8-3	Mass (g)	96.85	105.78	108.11	108.49	108.58	108.66	108.66	108.67	108.68	108.7	108.78	84	60		
	TimeStamp	9:14	9:15	9:16	9:19	9:24	9:29	9:34	9:44	9:59	10:14	12:10			150	
	Time($s^{1/2}$)	0	8	11	17	24	30	35	42	52	60	103				0.236
UC8-4	Mass (g)	90.11	98.85	100.73	100.96	101.02	101.09	101.08	101.09	101.14	101.21	101.29	82	60		
	TimeStamp	9:17	9:18	9:19	9:22	9:27	9:32	9:37	9:47	10:02	10:17	12:11			656	
	Time($s^{1/2}$)	0	8	11	17	24	30	35	42	52	60	102				0.265
UC8-5	Mass (g)	88.19	97.21	98.59	98.80	98.87	98.90	98.93	98.96	98.98	99.05	99.15	82	60		
	TimeStamp	9:20	9:21	9:22	9:25	9:30	9:35	9:40	9:50	10:05	10:20	12:11			656	
	Time($s^{1/2}$)	0	8	11	17	24	30	35	42	52	60	101				0.273
UC8-6	Mass (g)	87.16	96.07	97.52	97.75	97.8	97.83	97.85	97.87	97.91	97.98	98.06	83	60		
	TimeStamp	9:23	9:24	9:25	9:28	9:33	9:38	9:43	9:53	10:08	10:21	12:12			624	
	Time($s^{1/2}$)	0	8	11	17	24	30	35	42	52	59	101				0.264
UC8-7	Mass (g)	102.36	111.9	114.44	114.94	114.97	114.97	114.97	115.03	115.05	115.16	115.19	84	60		
	TimeStamp	9:26	9:27	9:28	9:31	9:36	9:41	9:46	9:56	10:11	10:26	12:12			624	
	Time($s^{1/2}$)	0	8	11	17	24	30	35	42	52	60	100				0.279

UC8-9	Mass (g)	90.50	99.7	101.32	101.51	101.56	101.64	101.66	101.67	101.72	101.74	101.90	82	60		
	TimeStamp	9:32	9:33	9:34	9:37	9:42	9:47	9:52	10:02	10:17	10:32	12:13			624	
	Time($s^{1/2}$)	0	8	11	17	24	30	35	42	52	60	98				0.276
UC8-10	Mass (g)	86.12	95.31	96.35	96.51	96.54	96.58	96.62	96.61	96.64	96.70	96.82	83	60		
	TimeStamp	12:15	12:16	12:17	12:20	12:25	12:30	12:35	12:45	13:00	13:15	15:15			624	
	Time($s^{1/2}$)	0	8	11	17	24	30	35	42	52	60	104				0.272
UC8-11	Mass (g)	89.98	99.1	100.54	100.75	100.80	100.79	100.79	100.85	101.03	100.92	100.99	84	60		
	TimeStamp	12:18	12:19	12:20	12:23	12:28	12:33	12:38	12:48	13:03	13:18	15:18			656	
	Time($s^{1/2}$)	0	8	11	17	24	30	35	42	52	60	104				0.269
UC8-12	Mass (g)	90.75	99.43	101.33	101.48	101.51	101.55	101.60	101.64	101.64	101.69	101.78	83	60		
	TimeStamp	12:21	12:22	12:23	12:26	12:31	12:36	12:41	12:51	13:06	13:21	15:21			624	
	Time($s^{1/2}$)	0	8	11	17	24	30	35	42	52	60	104				0.257

Table C.9 Moisture wetting, moisture retention, and frost dilatometry for Old Montreal Brick #1

	$M_{vac,sat}$ (g)	$M_{boil,sat}$ (g)	S_{target} (Boil)	M_{dry} (g)	M_{wet} (g)	M_{wrap} (g)	$L_{0,1}$ (mm)	$L_{0,2}$ (mm)	$L_{0,avg}$ (mm)	M_{wrap} (g)	M_{wet} (g)	S_{actual} (Vac)	$L_{6,1}$ (mm)	$L_{6,2}$ (mm)	$L_{6,avg}$ (mm)	L_6-L_0 (mm)	Strain ($x10^6$)
DATE:					**March 31, 2009**									**April 3, 2009**			
OM1-1	117.57	117.53	0.60	103.35	111.85	114.61	84.088	84.100	84.094	114.62	111.80	0.594	84.131	84.130	84.131	0.037	434
OM1-2	123.93	123.75	0.60	108.64	117.69	120.57	84.120	84.123	84.122	120.59	117.65	0.589	84.154	84.156	84.155	0.034	398
OM1-3	125.94	125.80	0.70	110.35	121.26	124.04	83.797	83.799	83.798	124.06	121.23	0.698	83.838	83.830	83.834	0.036	430
OM1-4	126.53	126.53	0.70	110.83	121.79	124.69	83.066	83.069	83.068	124.70	121.75	0.696	83.073	83.077	83.075	0.007	90
OM1-5	125.55	125.48	0.80	109.90	122.34	125.19	84.859	84.859	84.859	125.24	122.32	0.794	84.905	84.904	84.905	0.046	536
OM1-6	121.70	121.65	0.80	106.58	118.58	121.43	83.897	83.899	83.898	121.47	118.53	0.790	83.950	83.942	83.946	0.048	572
OM1-7	135.82	135.62	0.85	118.80	133.15	135.97	84.180	84.181	84.181	135.99	133.09	0.840	84.236	84.234	84.235	0.055	647
OM1-8	111.70	111.54	0.85	97.96	109.51	112.21	86.360	86.364	86.362	112.21	109.47	0.838	86.421	86.422	86.422	0.060	689
OM1-9	122.18	122.01	0.90	107.12	120.50	123.30	81.901	81.901	81.901	123.30	120.44	0.884	81.956	81.961	81.959	0.058	702
OM1-10	132.56	132.46	0.90	116.17	130.84	133.68	83.972	83.974	83.973	133.67	130.78	0.891	84.025	84.028	84.027	0.053	637
DATE:					**March 24, 2009**									**March 30, 2009**			
OM1-11	127.11	127.13	0.00	111.34	111.34	114.31	86.348	86.344	86.346	114.34	111.37	0.002	86.337	86.338	86.338	-0.008	-98
OM1-12	112.41	112.41	1.00	98.54	111.95	114.64	85.185	85.181	85.183	114.61	111.83	0.958	85.208	85.223	85.216	0.032	382

Table C.10 Moisture wetting, moisture retention, and frost dilatometry for Old Montreal Brick #2

	$M_{vac,sat}$ (g)	$M_{boil,sat}$ (g)	S_{target} (Boil)	M_{dry} (g)	M_{wet} (g)	M_{wrap} (g)	$L_{0,1}$ (mm)	$L_{0,2}$ (mm)	$L_{0,avg}$ (mm)	M_{wrap} (g)	M_{wet} (g)	S_{actual} (Vac)	$L_{6,1}$ (mm)	$L_{6,2}$ (mm)	$L_{6,avg}$ (mm)	L_6-L_0 (mm)	Strain ($x10^6$)
DATE:					**April 3, 2009**								**April 9, 2009**				
OM2-2	128.41	128.09	0.90	110.76	126.38	129.01	82.198	82.196	82.197	129.01	126.27	0.879	82.217	82.219	82.218	0.021	255
OM2-3	117.54	117.33	0.70	101.54	112.56	115.41	85.985	85.989	85.987	115.39	112.49	0.684	86.007	86.003	86.005	0.018	209
OM2-4	116.22	116.13	0.50	100.48	108.31	111.14	84.924	84.917	84.921	111.14	108.21	0.491	84.936	84.928	84.932	0.011	135
OM2-5	135.38	135.13	0.30	117.01	122.44	125.21	85.281	85.278	85.280	125.21	122.37	0.292	85.279	85.281	85.280	0.000	6
DATE:					**April 9, 2009**								**April 13, 2009**				
OM2-6	116.13	115.84	0.35	100.50	105.86	108.56	86.500	86.506	86.503	108.56	105.77	0.337	86.525	86.526	86.526	0.022	260
OM2-7	134.86	134.56	0.35	116.75	122.97	125.61	85.386	85.388	85.387	125.59	122.87	0.338	85.399	85.396	85.398	0.011	123
OM2-8	116.27	116.00	0.40	100.73	106.81	109.30	84.124	84.118	84.121	109.26	106.72	0.385	84.143	84.141	84.142	0.021	250
OM2-9	136.60	136.36	0.40	118.35	125.57	128.16	86.939	86.939	86.939	128.12	125.48	0.391	86.955	86.954	86.955	0.016	178
OM2-10	109.91	109.72	0.45	95.45	101.89	104.56	85.856	85.861	85.859	104.53	101.81	0.440	85.881	85.878	85.880	0.021	245
OM2-11	136.89	136.75	0.45	118.96	127.03	129.80	85.732	85.732	85.732	129.74	126.95	0.446	85.745	85.745	85.745	0.013	152
DATE:					**March 24, 2009**								**March 30, 2009**				
OM2-11	136.89	136.75	0.00	118.96	118.96	122.13	85.728	85.732	85.730	122.17	118.99	0.002	85.732	85.733	85.733	0.003	29
OM2-12	-	131.48	1.00	114.47	114.37	134.26	87.364	87.372	87.368	134.22	131.13	0.979*	87.387	87.391	87.389	0.021	240

*Actual saturation of OM2-12 based on boil saturation as vacuum saturation data was not available.

Table C.11 Moisture wetting, moisture retention, and frost dilatometry for Upper Canada College Brick #6

	$M_{vac,sat}$ (g)	$M_{boil,sat}$ (g)	S_{target} (Boil)	M_{dry} (g)	M_{wet} (g)	M_{wrap} (g)	$L_{0,1}$ (mm)	$L_{0,2}$ (mm)	$L_{0,avg}$ (mm)	M_{wrap} (g)	M_{wet} (g)	S_{actual} (Vac)	$L_{6,1}$ (mm)	$L_{6,2}$ (mm)	$L_{6,avg}$ (mm)	L_6-L_0 (mm)	Strain ($x10^6$)
DATE:					**April 23, 2009**							**April 27, 2009**					
UC6-2	125.25	124.51	50%	108.17	116.37	119.51	85.809	85.815	85.812	119.49	116.30	47.6%	85.838	85.833	85.836	0.023	274
UC6-3	109.52	108.82	40%	94.61	100.29	103.54	84.792	84.789	84.791	103.51	100.19	37.4%	84.801	84.798	84.800	0.009	106
UC6-4	106.08	105.4	30%	91.77	95.88	98.95	84.982	84.981	84.982	98.97	95.85	28.5%	85.015	85.018	85.017	0.035	412
UC6-5	104.05	103.43	20%	90.09	92.80	95.9	85.459	85.457	85.458	95.90	92.78	19.3%	85.462	85.457	85.460	0.001	18
DATE:					**April 27, 2009**							**April 30, 2009**					
UC6-5	104.05	103.43	20%	90.09	92.80	96.18	85.462	85.463	85.463	96.19	92.77	19.2%	85.466	85.461	85.464	0.001	12
UC6-6	100.33	99.81	25%	86.92	90.15	93.33	83.952	83.948	83.950	93.33	90.12	23.9%	83.961	83.964	83.963	0.013	149
UC6-7	103.34	102.76	25%	89.33	92.68	95.81	84.973	84.971	84.972	95.81	92.65	23.7%	84.972	84.969	84.971	-0.002	-18
UC6-8	101.34	100.84	30%	87.64	91.65	94.76	86.211	86.210	86.211	94.73	91.62	29.1%	86.234	86.232	86.233	0.023	261
UC6-9	127.23	126.47	30%	110.16	115.06	118.29	84.554	84.554	84.554	118.29	114.98	28.2%	84.575	84.574	84.575	0.020	242
UC6-10	91.86	91.46	35%	79.55	83.73	86.98	85.429	85.426	85.428	86.97	83.70	33.7%	85.453	85.449	85.451	0.023	275
DATE:					**March 24, 2009**							**March 30, 2009**					
UC6-11	-	118.34	0%	103.08	103.09	106.03	85.255		85.255								
UC6-12	-	111.30	100%	96.94	110.89	113.83	84.338		84.338	* Bag in chilled bath was punctured and brick samples were wet with glycol/water mixture.							

Table C.12 Moisture wetting, moisture retention, and frost dilatometry for Upper Canada College Brick #8

	$M_{vac,sat}$ (g)	$M_{boil,sat}$ (g)	S_{target} (Boil)	M_{dry} (g)	M_{wet} (g)	M_{wrap} (g)	$L_{0,1}$ (mm)	$L_{0,2}$ (mm)	$L_{0,avg}$ (mm)	M_{wrap} (g)	M_{wet} (g)	S_{actual} (Vac)	$L_{6,1}$ (mm)	$L_{6,2}$ (mm)	$L_{6,avg}$ (mm)	L_6-L_0 (mm)	Strain ($x10^6$)
DATE:					**April 3, 2009**								**April 9, 2009**				
UC8-1	120.44	119.27	90%	101.15	117.44	120.11	85.015	85.013	85.014	120.10	117.34	83.9%	85.007	85.010	85.009	-0.006	-65
UC8-2	114.47	113.44	70%	96.25	108.27	111.12	85.628	85.638	85.633	111.12	108.19	65.5%	85.654	85.665	85.660	0.026	309
UC8-3	115.00	113.98	50%	96.83	105.42	108.16	85.661	85.659	85.660	108.14	105.35	46.9%	85.682	85.684	85.683	0.023	269
UC8-4	106.87	105.99	30%	90.07	94.88	97.88	84.148	84.154	84.151	97.84	94.77	28.0%	84.158	84.159	84.159	0.008	89
DATE:					**April 15, 2009**								**April 20, 2009**				
UC8-5	104.75	103.82	35%	88.15	93.64	96.65	84.743	84.745	84.744	96.60	93.52	32.3%	84.765	84.761	84.763	0.019	224
UC8-6	103.48	102.69	40%	87.13	93.32	96.43	85.462	85.460	85.461	96.42	93.23	37.3%	85.476	85.475	85.476	0.014	170
UC8-7	121.59	120.59	45%	102.32	110.55	-	86.190	86.194	86.192	113.76	110.43	42.1%	86.205	86.204	86.205	0.012	145
DATE:					**April 20, 2009**								**April 23, 2009**				
UC8-8	103.63	102.81	25%	87.18	91.07	94.15	85.801	85.803	85.802	94.14	91.01	23.3%	85.798	85.804	85.801	-0.001	-12
UC8-9	107.69	106.75	20%	90.48	93.71	96.76	84.052	84.052	84.052	96.75	93.66	18.5%	84.057	84.056	84.057	0.004	54
UC8-10	102.33	101.43	15%	86.10	88.41	91.94	85.690	85.687	85.689	91.91	88.37	14.0%	85.690	85.689	85.690	0.001	12
DATE:					**April 23, 2009**								**April 27, 2009**				
UC8-8	103.63	102.81	30%	87.18	91.87	95.04	85.798	85.802	85.800	95.04	91.84	28.3%	85.810	85.810	85.810	0.010	117
UC8-9	107.69	106.75	30%	90.48	95.36	98.46	84.059	84.059	84.059	98.43	95.33	28.2%	84.065	84.070	84.068	0.008	101
UC8-10	102.33	101.43	35%	86.10	91.48	94.47	85.686	85.685	85.686	94.43	91.40	32.7%	85.694	85.691	85.693	0.007	82
UC8-11	106.77	105.77	35%	89.95	95.55	99.07	86.376	86.374	86.375	99.09	95.5	33.0%	86.393	86.393	86.393	0.018	208
DATE:					**March 24, 2009**								**March 30, 2009**				
UC8-11	106.77	105.77	0%	89.95	90.05	93.74	86.369	86.380	86.375	93.78	90.04	0.5%	86.366	86.382	86.374	-0.001	-6
UC8-12	107.61	106.72	100%	90.71	106.46	109.28	84.755	84.755	84.755	109.24	106.32	92.4%	84.774	84.770	84.772	0.017	201

Table C.13 Summary of Old Montreal Bricks #1 &2 and Upper Canada College Bricks #6 & 8 material data

Specimen ID	Dimensions					Dry Mass	Boil Sat Mass	Vac Sat Mass	Density		Boil Porosity		Vacuum Porosity	
	Length mm	Height mm	Frog mm^2	Thickness mm	Volume mm^3	g	g	g	Specimen kg/m^3	Average kg/m^3	Specimen m^3/m^3	Average m^3/m^3	Specimen m^3/m^3	Average m^3/m^3
OM1-1	82	62	0	10	50840	103.35	117.53	117.57	2033		0.279		0.280	
OM1-2	82	62	0	10	50840	108.64	123.75	123.93	2137		0.297		0.301	
OM1-3	82	62	0	11	55924	110.35	125.80	125.94	1973		0.276		0.279	
OM1-4	82	62	0	11	55924	110.83	126.53	126.53	1982		0.281		0.281	
OM1-5	83	62	0	11	56606	109.90	125.48	125.55	1941		0.275		0.276	
OM1-6	82	62	0	10.5	53382	106.58	121.65	121.70	1997	2021	0.282	0.283	0.283	0.285
OM1-7	82	62	0	11.5	58466	118.80	135.62	135.82	2032		0.288		0.291	
OM1-8	85	62	0	9	47430	97.96	111.54	111.70	2065		0.286		0.290	
OM1-9	80	62	0	10.5	52080	107.12	122.01	122.18	2057		0.286		0.289	
OM1-10	82	62	0	11	55924	116.17	132.46	132.56	2077		0.291		0.293	
OM1-11	84	62	0	11	57288	111.53	127.13	127.11	1947		0.272		0.272	
OM1-12	83	62	0	9.5	48887	98.54	112.41	112.41	2016		0.284		0.284	
OM2-2	81	62	0	11	55242	110.76	128.09	128.41	2005		0.314		0.320	
OM2-3	84	61	0	10	51240	101.54	117.33	117.54	1982		0.308		0.312	
OM2-4	83	61	0	10.5	53162	100.48	116.13	116.22	1890		0.294		0.296	
OM2-5	83	62	0	11	56606	117.01	135.13	135.38	2067		0.320		0.325	
OM2-6	84	62	0	10	52080	100.50	115.84	116.13	1930		0.295		0.300	
OM2-7	83	62	0	11.5	59179	116.75	134.56	134.86	1973	1980	0.301	0.302	0.306	0.307
OM2-8	82	62	0	10	50840	100.73	116.00	116.27	1981		0.300		0.306	
OM2-9	85	62	0	11	57970	118.35	136.36	136.60	2042		0.311		0.315	
OM2-10	83	62	0	10	51460	95.45	109.72	109.91	1855		0.277		0.281	
OM2-11	84	62	0	11	57288	119.09	136.75	136.89	2079		0.308		0.311	
OM2-12	85	62	0	11	57970	114.47	131.48	-	1975		0.293		-	

UC6-2	84	60	0	11	55440	108.17	124.51	125.25	1951		0.295		0.308	
UC6-3	83	60	600	11	48180	94.61	108.82	109.52	1964		0.295		0.309	
UC6-4	83	60	644	11	47096	91.77	105.40	106.08	1949		0.289		0.304	
UC6-5	83	60	644	11	47696	90.09	103.43	104.05	1889		0.280		0.293	
UC6-6	82	60	644	10	42760	86.92	99.81	100.33	2033		0.301		0.314	
UC6-7	83	60	644	10	43360	89.33	102.76	103.34	2060	1957	0.310	0.292	0.323	0.394
UC6-8	84	60	644	10	43960	87.64	100.84	101.34	1994		0.300		0.312	
UC6-9	83	60	644	13	56368	110.16	126.47	127.23	1954		0.289		0.303	
UC6-10	84	60	644	10	43960	79.55	91.46	127.23	1810		0.271		1.085	
UC6-11	84	60	644	11	48356	103.08	118.34	-	2132		0.316		-	
UC6-12	82	60	0	11	54120	96.94	111.30	-	1791		0.265		-	
UC8-1	83	59	0	11	53867	101.15	119.27	120.44	1878		0.336		0.358	
UC8-2	84	60	0	10	50280	96.25	113.44	114.47	1914		0.342		0.362	
UC8-3	84	60	150	11	53090	96.83	113.98	115.00	1824		0.323		0.342	
UC8-4	82	60	656	11	46904	90.07	105.99	106.87	1920		0.339		0.358	
UC8-5	82	60	656	10.5	44772	88.15	103.82	104.75	1969		0.350		0.371	
UC8-6	83	60	624	10	43560	87.13	102.69	103.48	2000	1934	0.357	0.344	0.375	0.364
UC8-7	84	60	624	11.5	50784	102.32	120.59	121.59	2015		0.360		0.379	
UC8-8	83	60	624	10	43560	87.18	102.81	103.63	2001		0.359		0.378	
UC8-9	82	60	624	11	47256	90.48	106.75	107.69	1915		0.344		0.364	
UC8-10	83	60	624	10	43560	86.10	101.43	102.33	1977		0.352		0.373	
UC8-11	84	60	656	10.5	46032	89.95	105.77	106.77	1954		0.344		0.365	
UC8-12	83	60	500	11	49280	90.71	106.72	107.61	1841		0.325		0.343	